Master Thesis

Design of Microstrip Patch Antennas at 5.8 GHz

Kapsch TrafficComm AB, Jönkoping, Sweden

Prepared By: **Asad ullah Noor**

Supervisor: **Hans Johansson**

Senior Radio Engineer, R & D Department.

Examiner: **Per-Simon Kildal**

Professor at Chalmers University of Technology

Table of Contents

Acknowledgement

I would like to express my sincere gratitude to both CHALMERS and Kapsch TrafficCom AB Jönköping for the effective contribution in carrying out this thesis work. It has been a great learning, and the experiences which I have achieved during these months have proven to be valuable when designing antennas.

My deepest appreciation is due to my supervisor Hans Johansson for his guidance and encouragement throughout the thesis work. I would like to thank my examiner Per-Simon Kildal who let me work in the Antenna Group with an HFSS License.

I would also like to mention the significant help I have got from

- AWR Technical Support
- CHALMERS Antenna Group
- Cogra Pro AB

Finally, I would like to thank my family and friends for their support during this thesis work.

Abstract

The purpose of this thesis work was to design microstrip antennas at 5.8 GHz dedicated short-range communication (DSRC) band. This frequency band includes road transport and traffic telematics (RTTT) applications, which impose severe cost and size limitations on microwave RTTT devices.

Initially extensive literature study at dedicated short-range communication (DSRC) band was done for the selection of antenna, feasible for our interested band which can meet the specification. Later on the selected antennas were designed both in Microwave Office and HFSS.

The dielectric substrates used are FR4 and Nelco 4350-RF13. Different thicknesses of these dielectrics were used for different antennas.

Chapter 1

Overview

1.1 Kapsch TrafficCom

Kapsch TrafficCom is an international supplier of innovative traffic telematic solutions. The company develops and delivers primarily electronic toll collection systems, especially for multi-lane free-flow traffic and offers technical and commercial operation of these systems. In addition Kapsch TrafficCom offers traffic management solutions focusing on traffic safety and control, electronic access systems and parking management systems.

With references in 41 countries on five continents, and with about 64 million delivered on-board units (OBUs),Kapsch TrafficCom has positioned itself among the leading suppliers of ETC systems worldwide. Kapsch TrafficCom is headquartered in Vienna, Austria, and has subsidiaries and representative offices in 25 countries [15].

1.2 Products and Components

Kapsch TrafficCom designs, develops and manufactures its core technology components in its eight engineering competence centers on 4 continents. The product design philosophy is based on cornerstones of creating high product configurability, standards-based interfaces, user-friendliness, esthetic, yet robust design. In software and hardware design the company utilizes state of the art technologies [15].

1.2.1 Multi-Lane Transceivers

The Kapsch CEN DSRC Multi-Lane transceivers are based on the latest processor technology and are designed for maximum lifetime and reliability. The Kapsch multi-lane transceivers consist of the following product families:

- **Kapsch TRX-1220 CEN DSRC Multi-Lane Transceivers**
  This transceiver platform is optimized for Multi-Lane applications on highways. The TRX-1220 transceivers are the smallest CEN DSRC transceivers on the market [15].

- **Kapsch TRX-1230 CEN-DSRC Low Power Multi-Lane Transceiver**
  The Kapsch TRX-1230 Multi-Lane transceiver has been designed especially for multi-lane applications on the secondary street network, where no data connection and power connection is available. The TRX-1230 has very low power consumption which allows for a power supply via independent power sources (e.g. solar power panels). Data connection to the central system can be done via a GSM/GPRS connection [15].
- **Kapsch TS-3252 CEN-DSRC Multi-Lane Transceiver**
  The TS-3252 Multi-Lane transceiver is equipped with a unique functionality that is able to report the direction to a communicating on-board unit (localization

functionality). This localization functionality is independent of signal strength and it is essential in a Multi-Lane or urban enforcement system to be able to match an on-board unit to a vehicle that is detected by a vehicle detection system [15].

- **Kapsch 1430 CEN-DSRC Multi-Lane Transceiver**
  The 1430 transceiver is the newest Kapsch CEN Multi-Lane transceiver. As TS-3253 it has a localization functionality. In a long term this transceiver will replace the TS-3252 Transceiver [15].

1.2.2 Single-Lane Transceivers

The Kapsch TS3200/06 Roadside System comprises a family of equipment for Dedicated Short-Range Communication (DSRC) intended for Electronic Fee Collection (EFC) applications in a single-lane environment. The high performance of the system makes it suitable for high speed implementations as well as for conventional low speed lanes equipped with a barrier. The combination of full compliance with the CEN TC278 DSRCstandards, and to other harmonized specifications such as A1, CARDME and CESARE/PISTA, secures interoperability with other EFC systems.

The basic transceiver platform of the TS3200/06 Roadside System is the single-lane transceiver TRX1320-E that in one compact unit handles both the DSRC and the EFC functionality. The transceiver can be configured at commissioning to handle several different EFC applications to allow on board units from several issuers to be accepted by the system [15].

1.2.3 Access Systems

The Access Transceivers TRX-1321-A and TRX-1221-A are devices for communication with on-board units and transponders to control parking areas, restricted areas, payment applications and generate traffic statistics. Full compliance with DSRC standards according to CEN TC278 secures interoperability with other systems.

Access Transceivers act as the stationary communication device between DSRC vehicle on-board units and an Access Control System. Their main purpose is to automatically identify and report the identity and the content of the on-board unit to the host computer. The host computer is part of the Access Control System and controls all peripherals like barriers, vehicle detection sensors as well as the Access Transceiver [15].

1.2.4 On-Board Units (OBU)

Kapsch offers a variety of CEN-compliant DSRC on-board units suitable for any kind of EFC application:

- Kapsch TS3203 mini tag for passenger cars
- Kapsch OBU 3021/4021 for heavy goods vehicles with integrated MMI
- Kapsch TS3209 hybrid DSRC/GPS on-board unit suitable for passenger cars as well as heavy goods vehicles.

The On-Board Units above provide CEN TC278 5.8 GHz based DSRC functionality enabling interoperability with CEN-compliant DSRC systems from other vendors.

- Kapsch TS3304 tolling tag
- Kapsch TS3306 intellidrive tag

The On-Board Units above provide IEEE 802.11p 5.9 GHz WLAN based DSRC functionality designed for the US market.

All on-board units are designed for windscreen mounting and are self-installable within a few minutes. Due to a very simple MMI all on-board units are designed for easy use. The OBUs can be easily distributed via a broad spectrum of point-of-sales such as gas stations, kiosks, etc [15].

1.2.5 OBU Programming Station (OPS)

The Kapsch OBU Programming Station OPS is designed for personalization of the on-board unit. Prior to issuance to a user and first use, an on-board unit requires "personalization" with specific vehicle data (e.g. license plate number, nationality, type of contract etc.). For this purpose, Kapsch provides an easy-to-use OBU Programming Station which can be operated at any point-of-sale [15].

1.2.6 OBU Mobile Reader (OMR)

The Kapsch OBU Mobile Reader OMR allows reading out on-board unit data via a handheld terminal to control parking fees, access authorizations etc. The OBU Mobile Reader OMR consists of a ruggedized PDA with color touch screen and a DSRC modem for communication with the OBU. Add-on modules (WLAN, GPRS, GPS) transmit the data and additional information to a central system. The OMR can be used for manual enforcement of vehicles in on-street parking applications and for payment purposes (e.g. payment of fares on ferries) [15].

1.3 Research Work

As mentioned in the Products and Components section, the On-Board Unit or transponder as shown in the figure 1.1 is one of the most important components in Road tolling system. The transponder is normally mounted on the inside of the vehicle windscreen. Kapsch TrafficCom delivers each year approx. 3 million transponders all over the world.

Figure 1.1 A transponder

The transponders are based on a European short range communication standard, using the 5.8 GHz frequency band. The antenna in the transponder is very important for the system performance and has a high influence of the production cost efficiency [15].

The task is to investigate the concept of antennas and design a cost and space effective antenna. The new antenna concept should have the possibility to replace the existing antennas and must be possible to produce in volume production. The following tasks are included in the Research/Thesis work :

- Literature study
- Patent review
- Construction of the antenna
- Development of prototypes
- Testing and verification
- Cost estimate

Some basic requirements for the antennas are as under

- Return Loss better than -10 dB.
- Left hand circularly polarized.
- Good peak gain as well as within $\pm 35^{o}$ for both azimuth and elevation.
- As small as possible (around 20mm x 20mm).
- Low cost production.

Chapter 2

Introduction to Microstrip Patch Antennas

2.1 Introduction

A microstrip patch antenna is a narrowband, wide-beam antenna fabricated by etching the antenna element pattern in metal trace bonded to an insulating dielectric substrate, such as a printed circuit board, with a continuous metal layer bonded to the opposite side of the substrate which forms a ground plane as shown in the figure 2.1. Low dielectric constant substrates are generally preferred for maximum radiation. The conducting patch can take any shape but rectangular and circular configurations are the most commonly used configurations. Other configurations are complex to analyze and require heavy numerical computations. A microstrip antenna is characterized by its Length, Width, Input impedance, polarization, Gain and radiation patterns [16].

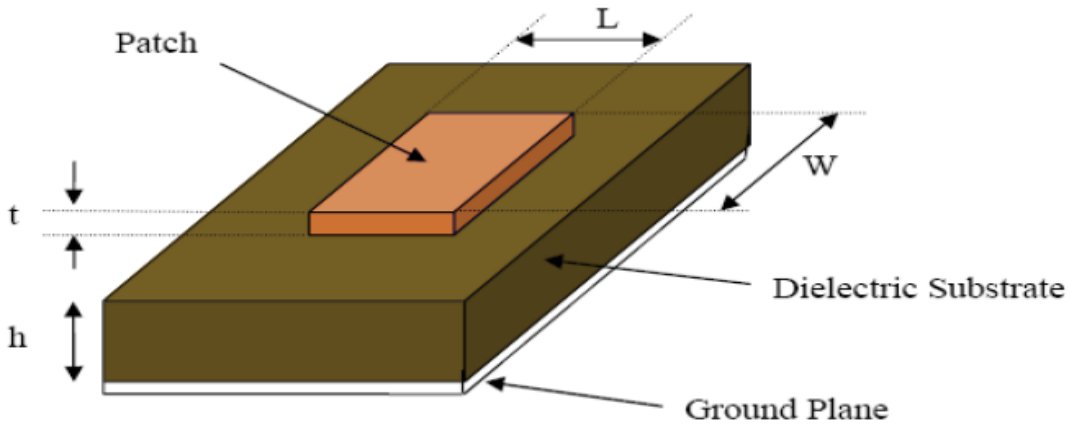

Figure 2.1 A Microstrip Patch Antenna

2.2 Advantages and Disadvantages

Microstrip patch antennas are increasing in popularity for use in wireless applications due to their low-profile structure. Therefore they are extremely compatible for embedded antennas in handheld wireless devices such as cellular phones, pagers (used for messaging only) etc... The telemetry and communication antennas on missiles need to be thin and conformal and are often in the form of Microstrip patch antennas. Another area where they have been used successfully is in Satellite communication [18]. Some of the major advantages are

- Light weight and low volume.
- Low profile planar configuration which can be easily made conformal to host surface.
- Low fabrication cost, hence can be manufactured in large quantities.
- Supports both, linear as well as circular polarization.

- Can be easily integrated with microwave integrated circuits (MICs).
- Capable of multiple frequency operations.
- Mechanically robust when mounted on rigid surfaces.

Microstrip patch antennas suffer from drawbacks compared to conventional antennas. Some of their major disadvantages are given below:

- Narrow bandwidth
- Low efficiency
- Low Gain
- Extraneous radiation from feeds and junctions
- Low power handling capacity.
- Surface wave excitation

2.3 Basic Principles of Operation

The figure 2.2 shows a patch antenna in its basic form: a flat plate over a ground plane (usually a PC board). The center conductor of a coax serves as the feed probe to couple electromagnetic energy in and/or out of the patch. The electric field distribution of a rectangular patch excited in its fundamental mode is also indicated [6].

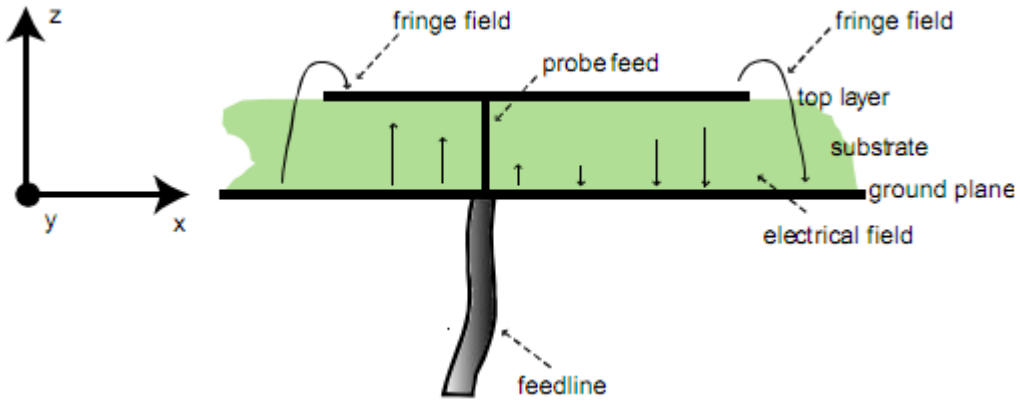

Figure 2.2 A Side view of Microstrip Patch Antenna

The electric field is zero at the center of the patch, maximum (positive) at one side, and minimum (negative) on the opposite side. It should be mentioned that the minimum and maximum continuously change side according to the instantaneous phase of the applied signal.

The electric field does not stop abruptly at the patch's periphery as in a cavity; Rather, the fields extend the outer periphery to some degree. These field extensions are known as fringing fields and cause the patch to radiate. Some popular analytic modeling techniques for patch antennas are based on this leaky-cavity concept. Therefore, the fundamental mode of a rectangular patch is often denoted using cavity theory as the TM10 mode.

Since this notation frequently causes confusion, we will briefly explain it. TM stands for transversal magnetic field distribution. This means that only three field components are considered instead of six. The field components of interest are: the electric field in the z direction and the magnetic field components in x and y direction using a Cartesian coordinate system, where the x and y axes are parallel with the ground-plane and the z-axis is perpendicular.

In general, the modes are designated as TM_{nmz}. The z value is mostly omitted since the electric field variation is considered negligible in the z-axis. Hence TM_{nm} remains with n and m the field variations in x and y direction. The field variation in the y direction (impedance width direction) is negligible; Thus m is 0. And the field has one minimum-to--maximum variation in the x direction (resonance length direction) ; Thus n is 1 in the case of the fundamental. Hence the notation TM10 [6].

2.4 Feeding Techniques

There are several feeding techniques for micro-strip patch antennas:

- Coaxial probe feed
- Micro-strip transmission line feed
  - Edge feed
  - Inset feed
- Aperture coupled feed
- Proximity coupled feed

However, only those techniques will be discussed which are used in this research work.

2.4.1 Coaxial Probe Feed

The Coaxial feed or probe feed is a very common technique used for feeding Microstrip Patch antennas. The inner conductor of the coaxial connector extends through the dielectric up to the patch, while the outer conductor is connected to the ground plane. Figure 2.3 shows a microstrip antenna with coaxial feeding [18].

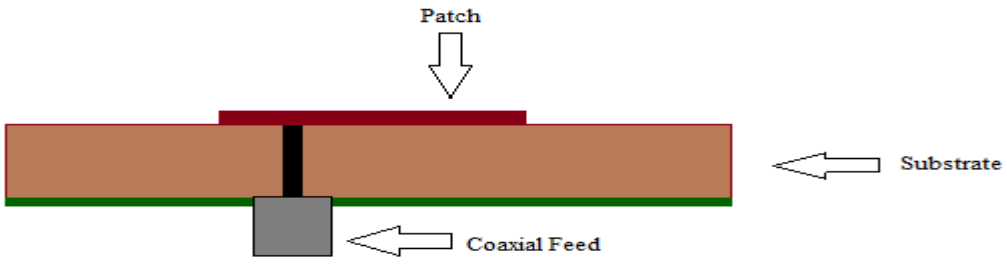

Figure 2.3 Coaxial Feeding of Microstrip Antenna

The main advantage of this type of feeding scheme is that the feed can be placed at any location inside the patch in order to match with its input impedance. This feed method is

easy to fabricate and has low spurious radiation. However, a major disadvantage is that it provides narrow bandwidth and is difficult to model since a hole has to be drilled in the substrate and the connector protrudes outside the ground plane [18].

2.4.2 Microstrip line feed

There are two methods in which this type of feeding can be used however in the thesis work only Inset feed method is used. Since the current is low at the ends of a patch and increases in magnitude toward the center, the input impedance (Z=V/I) could be reduced if the patch is fed closer to the center as shown in the figure 2.4. The distance y_o is optimized to get the best return loss.

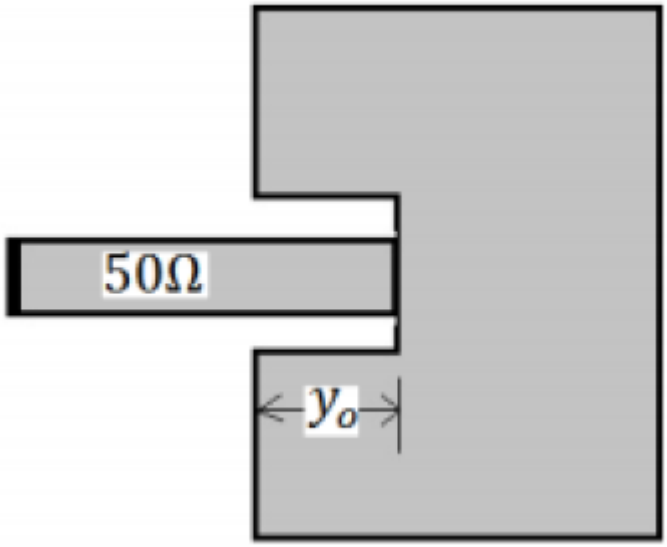

Figure 2.4 Micro-strip transmission line Inset feeding

2.4.3 Aperture coupled feed

In this type of feed technique, the radiating patch and the microstrip feed line are separated by the ground plan. Coupling between the patch and the feed line is made through an aperture in the ground plane as shown in the figure 2.5. The upper substrate is normally made with a lower permittivity to produce loosely bound fringing fields, yielding better radiation. The lower substrate can be independently made with a high value of permittivity for tightly coupled fields that don't produce spurious radiation. The major disadvantage of this feed technique is that it is difficult to fabricate due to multiple layers, which also increases the antenna thickness. This feeding scheme also provides narrow bandwidth [18].

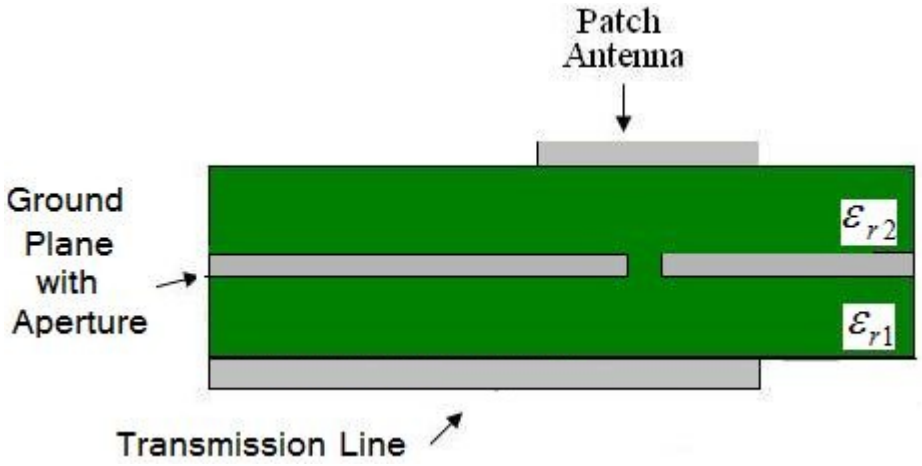

Figure 2.5 Aperture Coupled Feeding of Microstrip Antenna

2.5 Antenna Parameters

Antenna parameters are used to characterize performance of an antenna when designing and measuring antennas. In this Section, terms like bandwidth, radiation pattern, gain, polarization, input impedance are explained.

2.5.1 Bandwidth

Bandwidth is a fundamental antenna parameter. It describes the range of frequencies over where the antenna parameters, such as input impedance, radiation pattern, polarization, side-lobe level and gain is within an acceptable value from those at the center frequency. Often, the desired bandwidth is one of the determining parameters used to decide upon an antenna. For instance, many antenna types have very narrow bandwidths and cannot be used for wideband operation [16].

However the bandwidth requirements for the thesis work was not very strict. That's why many antennas with a narrow bandwidth were selected to be studied in this work.

2.5.2 Polarization

The polarization of an electromagnetic field is defined in terms of the direction of its electric field vector. If the electric field vector is always in one plane, then it is said to be linearly-polarized. Special cases are vertical polarization for the electric field vector in a vertical plane, and horizontal polarization for the electric field vector in a horizontal plane (typically with reference to the surface of the earth).

In general, the electric field vector rotates about a line parallel to the direction of propagation and its tip traces out an ellipse. This is known as elliptical polarization. Circular polarization (CP) is a special case of elliptical polarization in which the trace of the electric field vector is a circle. Because the electric field vector travels as a wave, the actual pattern is that of a spiral with an elliptical or circular cross section. The polarization of the receiving

antenna must be matched to the polarization of the transmit antenna in order to extract maximum power from the field. If the antenna polarization is perpendicular to the field polarization (such as vertical vs. horizontal or right hand vs. left hand circular) the antenna will not extract any power from the incident wave [16]. As all the antenna designs in this thesis work are circularly polarized it will be discussed in detail in the next section

Circular Polarization

In general, circularly polarized microstrip antennas can be categorized into two types according to the number of feed points: namely single-fed and dual-fed antennas. The basic configurations of a dual-fed CP antenna are illustrated in figure 2.6 (a). Figure 2.6 (a) shows the antennas that are fed with an external polarizer, such as a 3 dB hybrid or offset feedline. In such an antenna system, the polarizer excites two linearly polarized orthogonal waves. The fields due to these orthogonal waves have equal amplitude and are 90° out of phase. Therefore, an antenna excited by an external polarizer acts as a CP wave radiator. Both the impedance and axial ratio characteristics of dual-fed antennas are broader than those of single-fed antennas because the 3-dB hybrid is typically broadband.

On the other hand, single-fed circularly polarized patches are very attractive, because they can be arrayed and fed like any linearly polarized patch. The basic configurations of a single-fed antenna are shown in figure 2.6 (b). Dual-fed CP patches require an additional circuit, which makes the overall size of the radiating element quite large, thus limiting the frequency performance of the array because of grating lobes. Single-fed CP patches have been extensively evaluated in the literature, where they are shown to be extremely narrowband antennas (1% bandwidth or less). The most frequently used types of single-fed circularly polarized patches are the slotted patch, the notched patch and the “almost square” patch.

In figure 2.6 (b), Δs represents the size of the perturbation segment as shown at the edges of single-fed circularly-polarized Microstrip Antennas and S denotes the area of the antenna. The two orthogonal (“degenerate”) modes are separated into two modes by the effect of the perturbation segment Δs. The radiated fields caused by these two modes are perpendicular to each other and have equal amplitude, but are 90° out of phase if the size of the perturbation segment for an antenna is adjusted to the optimum. Therefore, a single-fed antenna with an optimum perturbation segment acts as a CP-wave radiator without using an external polarizer. Due to the perturbation, the patch surface currents in the x and y directions are simultaneously affected, which makes the manufacturing tolerance critical for CP operation. To avoid the need for fine tolerance, in this study the simple CP design technique was applied to single probe-feed elliptical microstrip antennas. In an elliptical microstrip patch antenna, the feed position is located along the 45º line between the long and short axis of the elliptical patch, in order to simultaneously excite the two nearly degenerate modes corresponding to the long and short axes of the elliptical patch. The impedance matching is achieved by varying the feed position that is by moving the feed along the 45º line between the patch edge and the patch center [16].

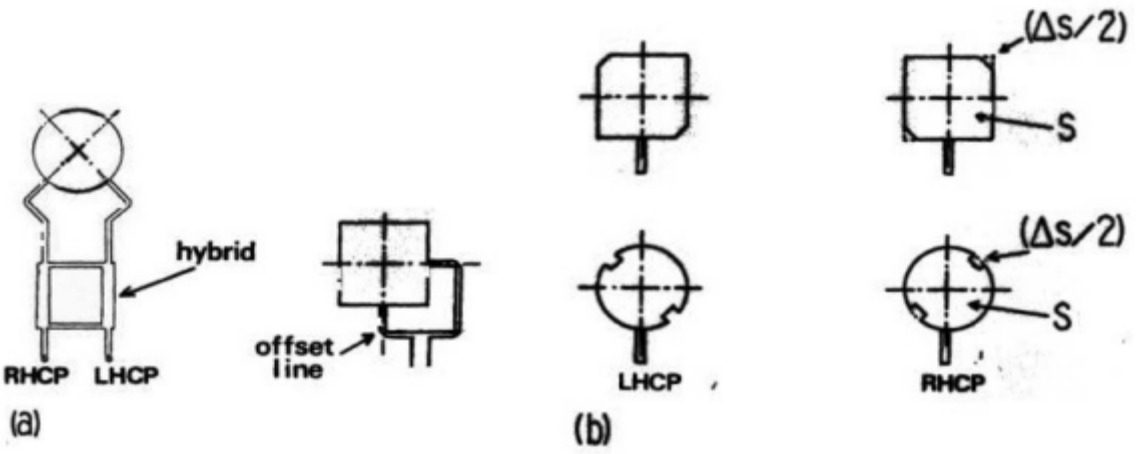

Figure 2.6 Various Type of Circularly Polarized Microstrip Patch Antennas: (a) Dual-Fed CP-Wave Patches; (b) Single Fed CP-Wave Patches (From [Ref. 2])

2.5.3 Return Loss

Return loss is an important parameter when connecting an antenna. It is related to impedance matching and the maximum transfer of power theory. It is also a measure of the effectiveness of an antenna to deliver power from the source to the antenna. The return loss (RL) is defined by the ratio of the incident power of the antenna P_{in} to the power reflected back from the antenna of the source P_{ref} [1] the mathematical expression is:

$$RL = 10\log_{10}\frac{P_{in}}{P_{ref}} \quad (dB)$$

For good power transfer, the ratio P_{in}/ P_{ref} shall be high. If we have low RL there is a risk that there will occur standing wave phenomena's (resonances) and it will end up in a frequency ripple of gain etc. In most practical circuits a RL value of -10 dB is good enough.

2.5.4 Radiation Pattern

Radiation pattern is defined as "the spatial distribution of a quantity that characterizes the electromagnetic field generated by antenna" (IEEE, 1993). Radiation pattern can be a two- or three-dimensional spatial distribution of power flux density, radiation intensity, field strength, directivity, phase or polarization. Radiation pattern is a function of the observer's position along a path or surface of constant radius (Balanis, 1997) and goes through a direction at which maximum radiation occurs. Usually, the spherical coordinate system is used to visualize the radiation pattern. A two-dimensional pattern can be a function of the elevation angle, θ, at constant azimuth angle, ϕ, or a function of ϕ at constant θ-value [1]. The spherical coordinate system is shown in figure 2.7.

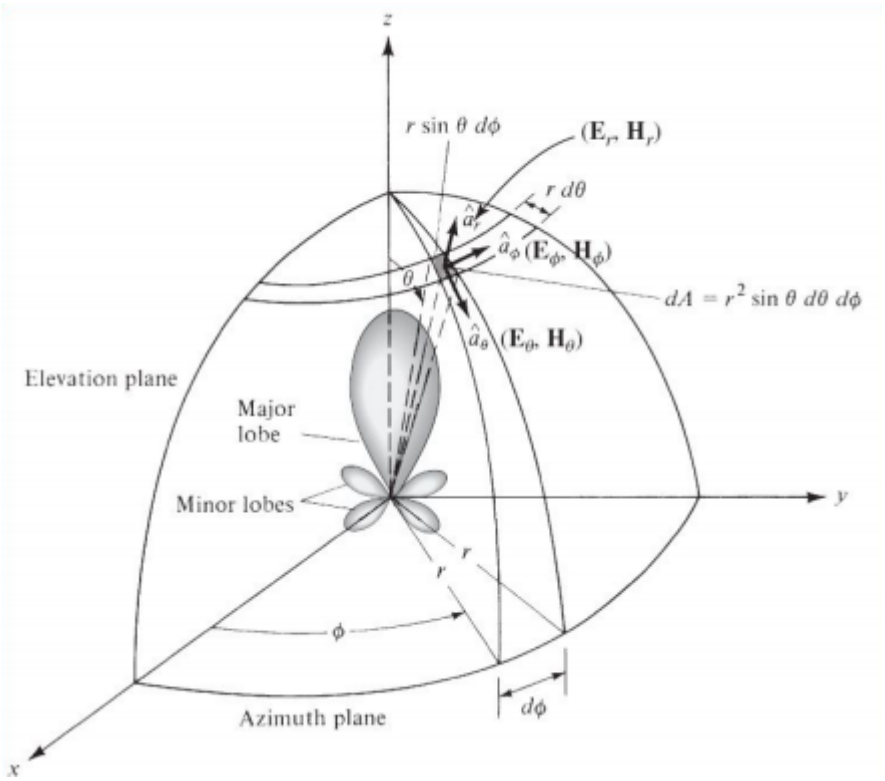

Figure 2.7 Spherical Coordinate Systems for Antenna Analysis

2.5.5 Directivity

Directivity is "the ratio of the radiation intensity in a given direction from the antenna to the radiation intensity averaged over all directions" (IEEE, 1993). It is a function of direction but it is often defined only to the direction of the major lobe Directivity can be expressed as

$$D = \frac{\omega}{pt/4\pi} = \frac{4\pi|E(r)|^2}{\int|E(r)|^2\, d\Omega}$$

Where ω is the radiation density per solid angle and p_t is the total power transmitted by the antenna and is the solid angle (Lindell & Nikoskinen, 1995).

2.5.6 Gain

The directivity was defined from the radiation intensity in the main beam direction and the total radiated power. The antenna gain has the same definition, except that the total radiated power is replaced by the total power delivered to the antenna port [1]. This may be expressed by using the directivity as

$$G = e_{rad} e_{pol} D$$

Where e_{rad} is the total radiation efficiency and e_{pol} is the polarization efficiency.

2.5.7 Conversion Gain

The conversion gain, CG, quantifies the ratio between incident power and returned power in a CEN DSRC OBU. It is called 'conversion' gain because it indicates the relative level of an output which has been converted to a frequency which differs from that of the input. In an OBU the conversion gain (dB) can be calculated as the sum of the input antenna gain, the output antenna gain and the modulator gain. According to the CEN DSRC standard the conversion gain must have a value between 1 and 10 dB within $\pm 35^{o}$ for both azimuth and elevation.

2.5.8 Axial Ratio

The polarization ellipse is the curve which the peak of the E-field describes when the time varies in a plane normal to the propagation direction of the wave. The ellipse can be characterized by its maximum and minimum field values, $|E_{max}|$ and $|E_{min}|$, respectively [1]. The **axial ratio** (AR) of the ellipse is defined by

$$(AR)_{dB} = 10\log\left|\frac{E_{max}}{E_{min}}\right|^2 dB.$$

For a desired circular polarization the axial ratio AR in *dB* and the amplitudes of the co- and cross-polar fields are related by

$$(AR)_{dB} = 10\log\left[\frac{|E_{co}| + |E_{xp}|}{|E_{co}| - |E_{xp}|}\right]^2 dB.$$

Chapter 3

X Antenna

3.1 Introduction

Many wireless application systems use microstrip patch antennas due to their compact, conformal, and low-cost designs. The X Antenna is also designed on the basics of microstrip technology. We call it X Antenna because there are two diagonal slots in the patch which makes an X shape in the patch. The slots are used to achieve circular polarization. Circularly polarized antennas are particularly of interest to radio communication. Enabling the space orientation, such antennas also reduce considerably the multipath fading and thus increase the spectral efficiency of RF systems. In addition, the use of receive and transmit antennas with circular polarization can maximize the isolation between the two antennas [3].

3.2 Design

Figure 3.1 shows the top and side view of the optimized single-feed patch antenna operating at 5.8 GHz and having a circular polarization. This antenna is designed using both Microwave Office and HFSS-Ansoft software.

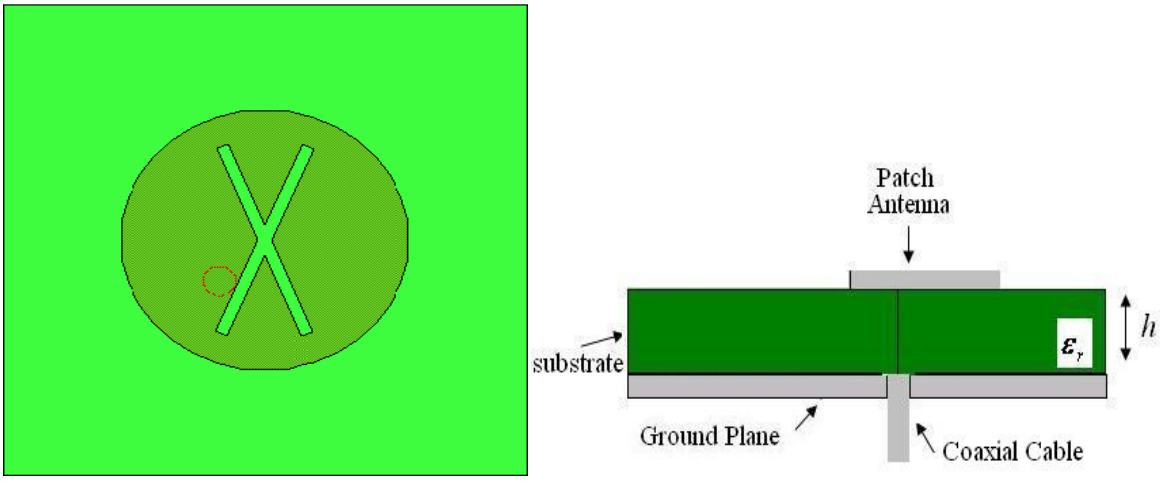

(a) (b)

Figure 3.1 Top (a) and Side (b) view of X Antenna

Firstly it was required to determine the resonant length of the antenna, which in circular antenna can be called the diameter. So the diameter of the patch for a frequency of 5.8 GHz and dielectric of 4.3 was calculated as

$$L \approx 0.49\ \lambda_d = 0.49\ \frac{\lambda_0}{\sqrt{\varepsilon_r}}.$$

⇨ L =12.2 mm

However when the design was optimized the diameter was found to be 11.6 mm. So the antenna is composed of a circular patch with a radius of 5.8 mm printed on a FR4 substrate with ε_r =4.3 and thickness of 3.2mm. The two diagonal slots have length of 9mm and width of 0.5mm. The antenna is fed by a probe with a radius of 1.3 mm. The feed location and the slots were optimized to give good impedance matching and circular polarization. The size of the ground plane is 21 mm 21 mm. The hole in the ground plane for the SMA connection is 4 mm.

3.3 Results

The results are obtained from both HFSS and Microwave Office and are quite similar. In the following chapter the simulated results on both tools are presented.

3.3.1 Simulated Results

Return Loss

The simulated return loss of the optimized antenna from MWO is shown in figure 3.2. At 5.8 GHz a return loss of -11 dB is achieved.

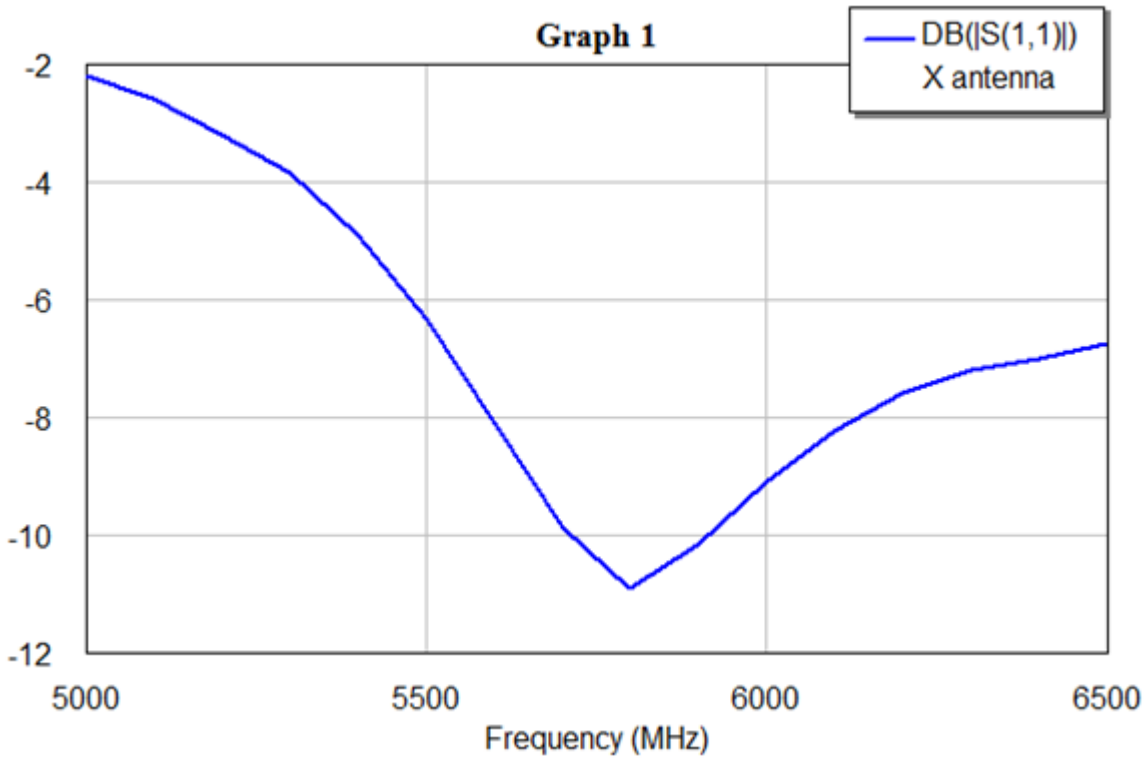

Figure 3.2 Return Loss of X Antenna in Microwave Office

In comparison to MWO the return loss in HFSS showed slightly better matching. The figure 3.3 shows the return loss from HFSS. At 5.8 GHz a return loss of -14 dB is achieved.

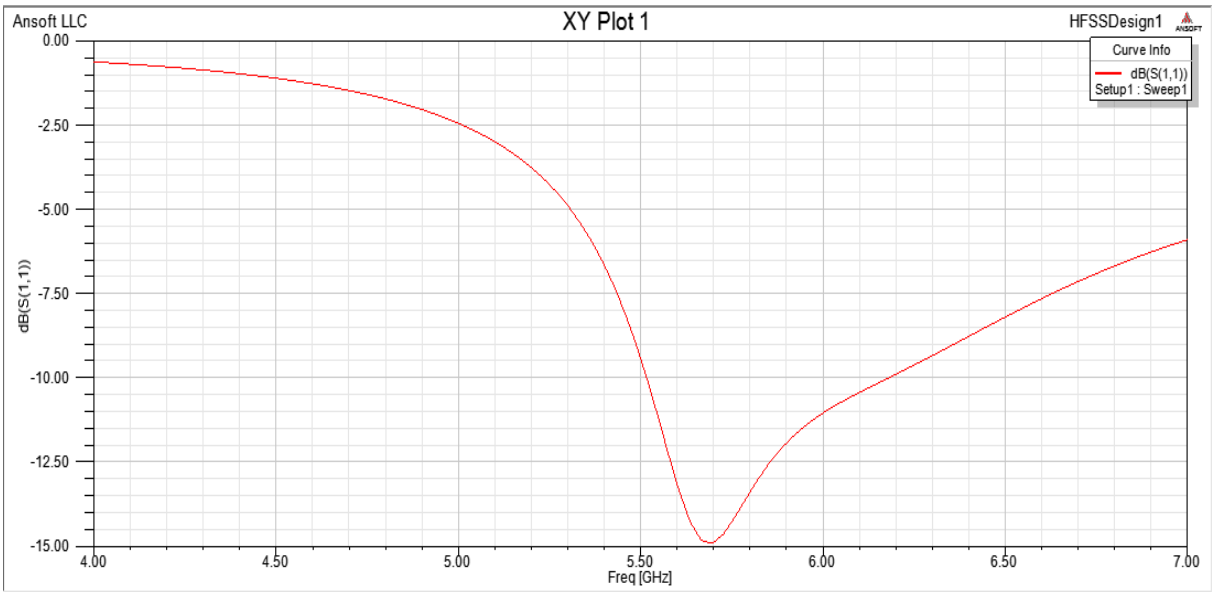

Figure 3.3 Return Loss of X Antenna in HFSS

Radiation Pattern

Since a microstrip patch antenna radiates normal to its patch surface, the radiation pattern for $\phi=0^{o}$ and $\phi=90^{o}$ are important. Figure 3.4 shows the radiation pattern from MWO both at $\phi=0^{o}$ and $\phi=90^{o}$.

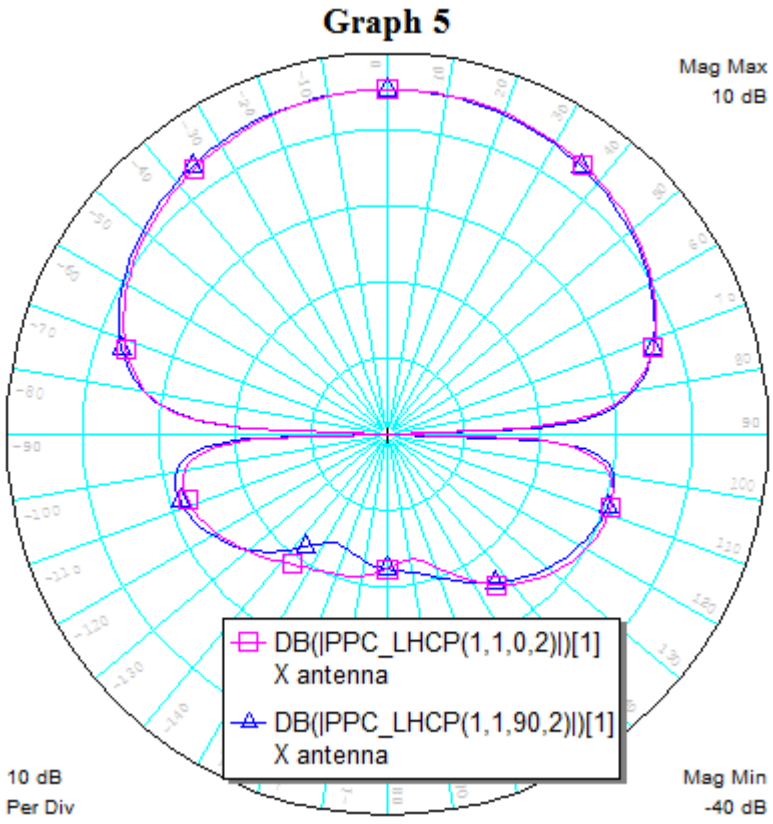

Figure 3.4 Radiation Pattern for $\phi=0^{o}$ and $\phi=90^{o}$ in Microwave office

It can be seen that radiation pattern is almost same for both $\phi=0^{o}$ and $\phi=90^{o}$. Similarly the radiation pattern for $\phi=0^{o}$ and $\phi=90^{o}$ from HFSS is also shown in figure 3.5

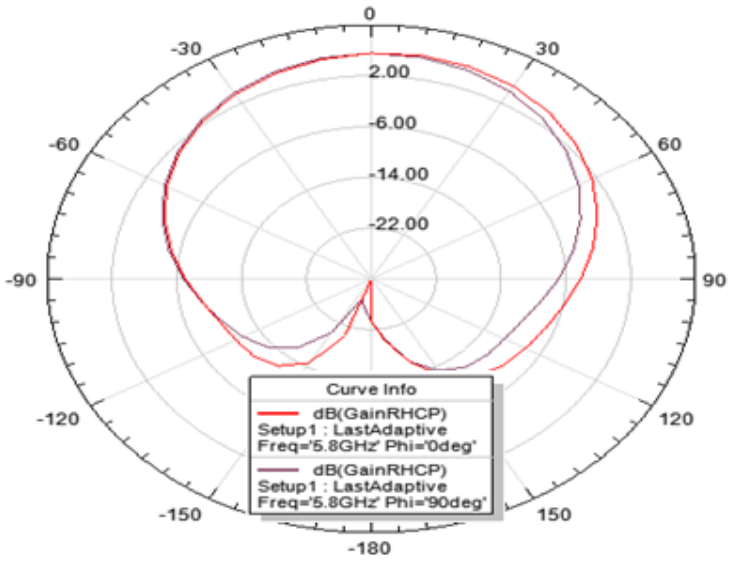

Figure 3.5 Radiation Pattern for $\phi=0^{o}$ and $\phi=90^{o}$ in HFSS

Both simulators show almost similar radiation patterns. There may be a slight difference in the back lobe however the radiated power backwards shows low values and small variations in power is magnified in the diagrams because they are presented in dB. Because of the low power radiated backwards is small, the differences are not very important.

Gain

The Gain for LHCP (Left Hand Circular Polarization) is very important considering the fact that microstrip antennas always yield low gain. The peak gain and the gain at $\theta=\pm35^{o}$ are for this application really important to consider. The Gain curve from MWO is shown in figure 3.6. A peak gain of 5.5 dB is achieved. At $\theta=+35^{o}$ a gain of 4.6 dB and at $\theta=-35^{o}$ a gain of 3 dB is achieved. A good separation between the co and cross polarization is also visible which will guarantee a good circular polarization.

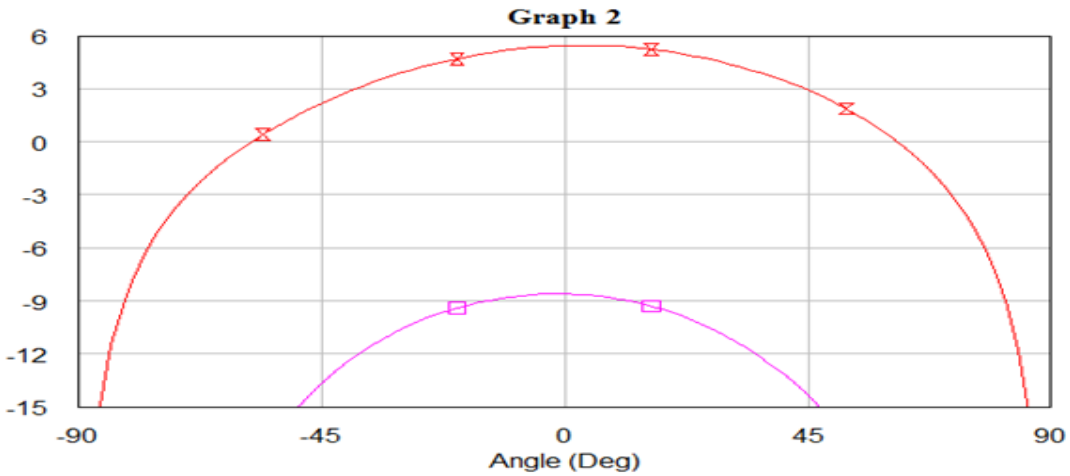

Figure 3.6 Gain (RHCP (pink) and LHCP(red)) in Microwave Office

Similarly the Gain from HFSS is shown in figure 3.7. A peak gain of 5.6 dB is achieved at $\theta=10^{o}$. A gain of 4.5 dB and 3 db are achieved at $\theta=+35^{o}$ and $\theta=-35^{o}$. However the separation between the co and cross polarization is not as much as it was in MWO. Both MWO and HFSS have shown that the peak gain is slightly tilted towards positive θ.

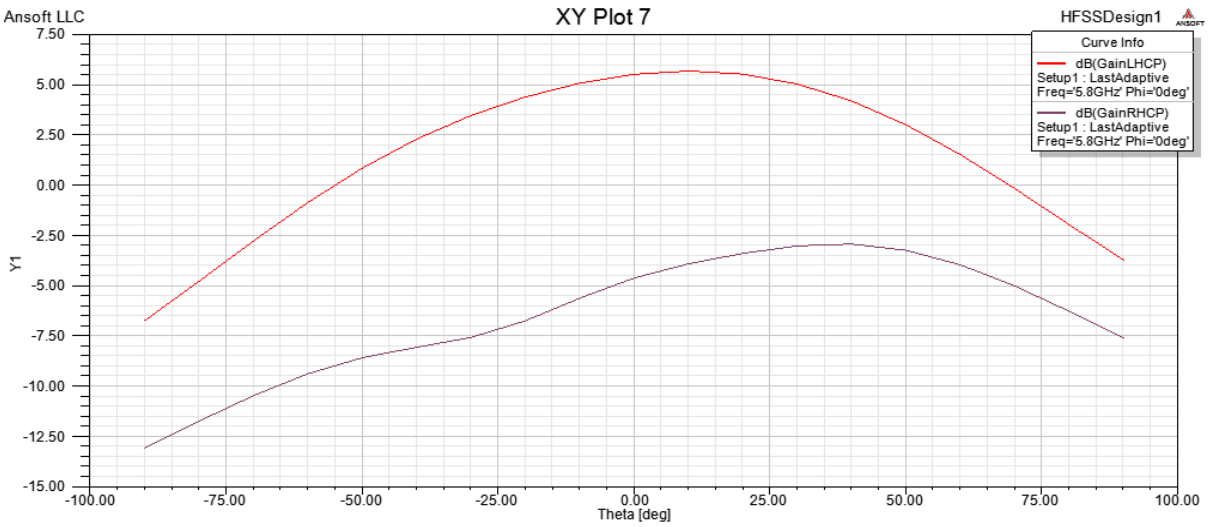

Figure 3.7 Gain (RHCP(red) and LHCP(gray)) in HFSS

Axial Ratio

Axial ratio is an important factor to check the circular polarization. To have good circular polarization an axial ratio below 3 dB is expected. The axial ratio plot from MWO is shown in figure 3.8. The most part of the curve is less than 3 dB. The peak value however is 3.5 dB

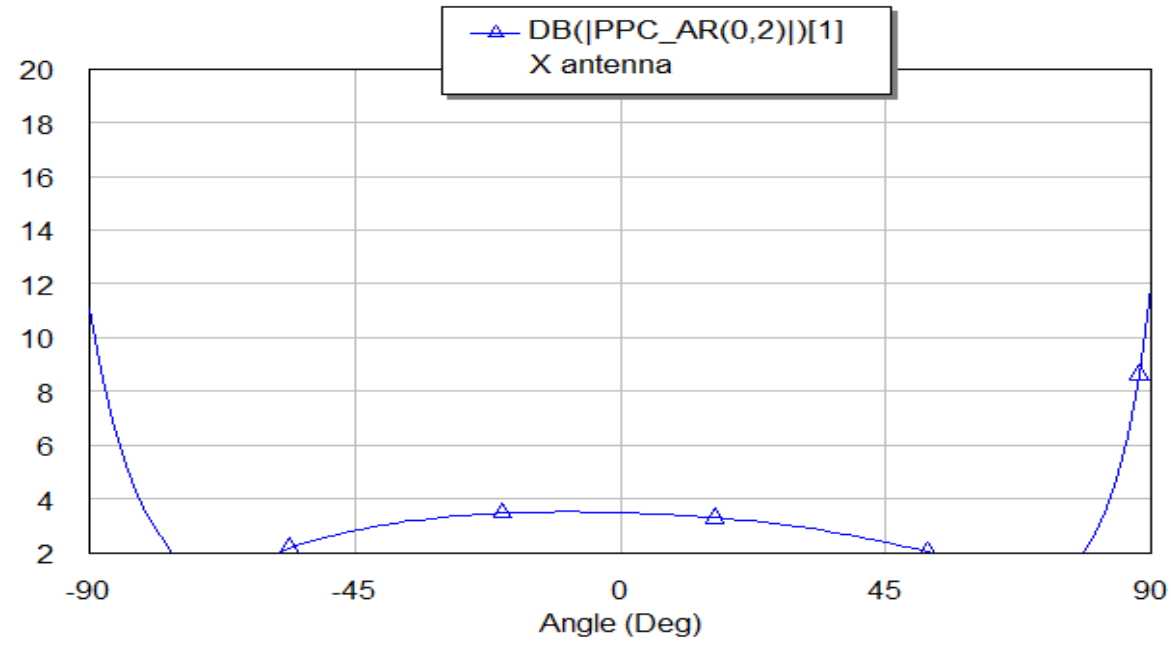

Figure 3.8 Axial Ratio in Microwave Office

Similarly, the axial ratio from HFSS is also shown in Figure 3.9. It can be seen that axial ratio was a lot better in Microwave Office than it is in HFSS which is because of the high cross polarization curve in HFSS.

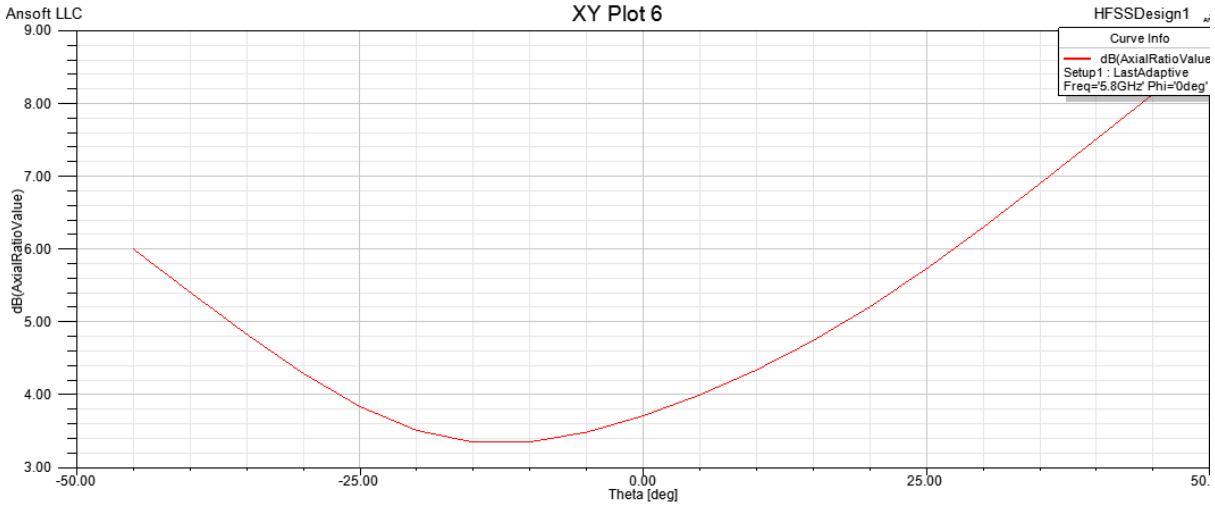

Figure 3.9 Axial Ratio in HFSS

3.3.2 Measured Results

The measured results for the different antenna parameters are shown below.

Return Loss

Both simulators showed a return loss better than -10 dB and the same values were expected in the measurements. The return loss measured in the network analyzer for the X Antenna is shown in the figure 11 which is -10 dB for 5.8 GHz. Comparing simulations and measurements shows almost identical shapes and values.

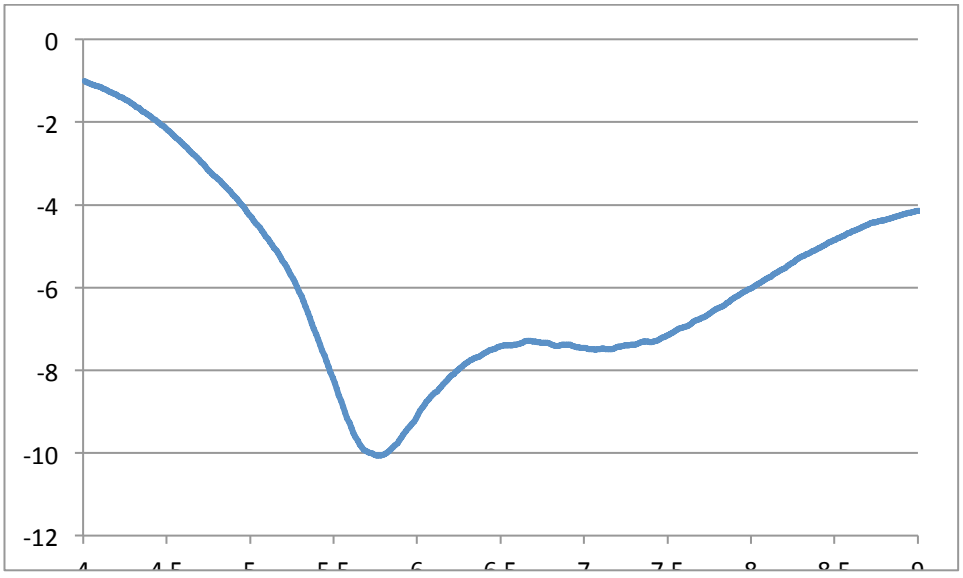

Figure 3.10 Measured Return Loss

Gain

During the gain measurements it was noticed that the antenna is delivering the peak gain at 5.75 GHz and because of this the gain measurements were done at 5.75 GHz. The gain in azimuth is shown in the figure 12 below. Compared with simulations the measurements are not as symetrical, also the peak gain is not in bore sight but at 20 deg offset. A peak gain of 5.9 dB is achieved which is more than the simulated results. At $+35^{o}$ a gain of 4.5 dB and at -35^{o} a gain of 4 dB is achieved which is quite impressive considering the size of the antenna.

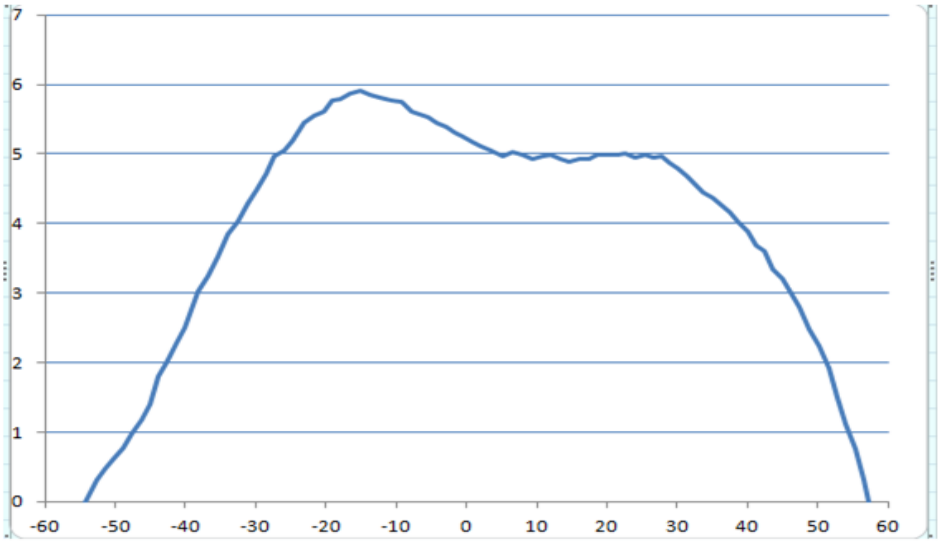

Figure 3.11 Measured Gain in Azimuth

Similarly the gain in the elevation which is shown in figure 3.12 is equally important. The curve is almost identical to the previous one which proves that the antenna delivers good gain both in azimuth and elevation.

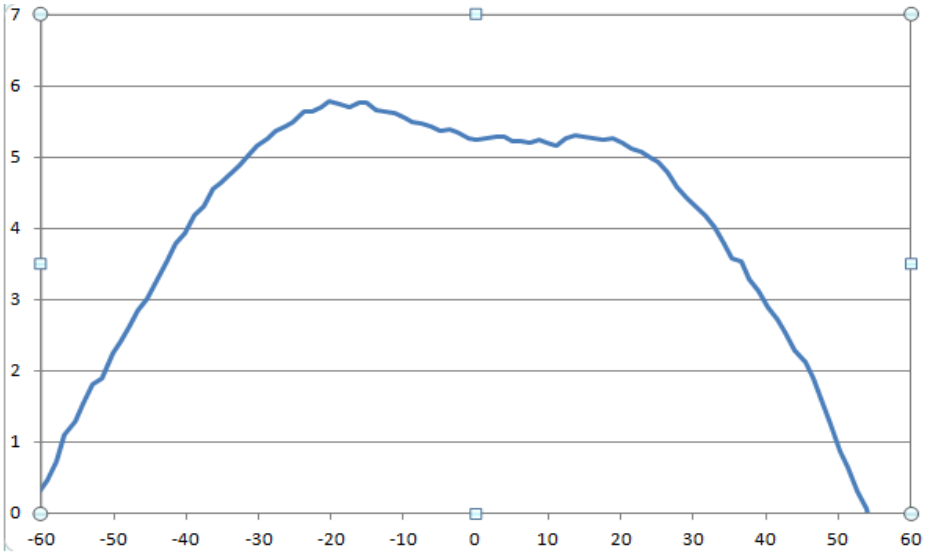

Figure 3.12 Gain in Elevation

Cross Polarization

The cross polarization of both azimuth and elevation is shown in the figure 3.13. The major region of both the curves are below -10 dB which ensures excellent circular polarization.

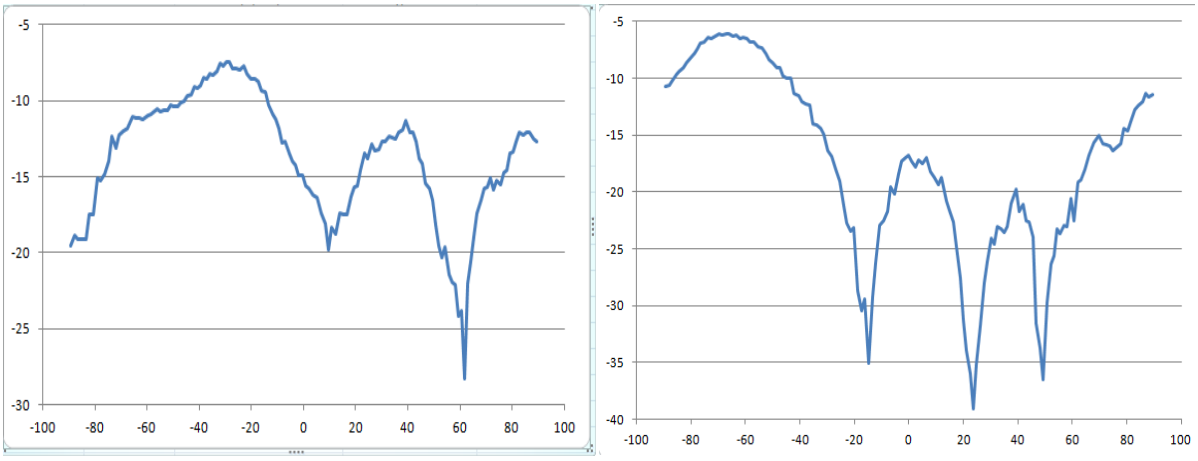

(a) (b)

Figure 3.13 Cross Polarization in Azimuth (a) and Elevation (b)

3.4 Conclusion

The X antenna shows good results for all the major requirements. Firstly it has a good return loss secondly it has shown nice gain and thirdly it has excellent circular polarization. And also the beam width of the antenna is very wide which helps to achieve good gain within $\pm 35^{o}$. The major question mark about this antenna is that it uses a substrate thickness of 3.2mm which makes it a little more expensive however it is fabricated with a standard FR4 substrate which is significantly cheaper than substrates made especially for microwave applications.

Chapter 4

Circular Patch Antenna with Aperture Coupling

4.1 Introduction

As described earlier in the feeding technique section, the aperture coupling is a very common method for feeding a microstrip antenna. It has some disadvantages like narrow bandwidth and increased thickness because of multiple layers however bandwidth is never an issue in the requirements of this research work and also the thickness of a few mm isn't a big problem because there is enough space inside the transponder to place the antenna. On the other hand the advantage of using this technique is that firstly no drilling for via holes is needed and secondly the spurious radiation is minimized due to the reason that ground plane lies between patch and the feed line.

4.2 Design

A power divider with one arm extended by λ/4 distance (to get 90^{o} phase shift) as compared to the other arm is used to feed the antenna in order to achieve circular polarization. An FR4 substrate with ε_r =4.3 and thickness of 0.8mm is used below the power divider. Two rectangular slots with optimized size of 8.1mm x 2.7mm are made in the ground plane of 33mm x 33mm for the aperture coupling. The complete design is shown in the figure 4.1

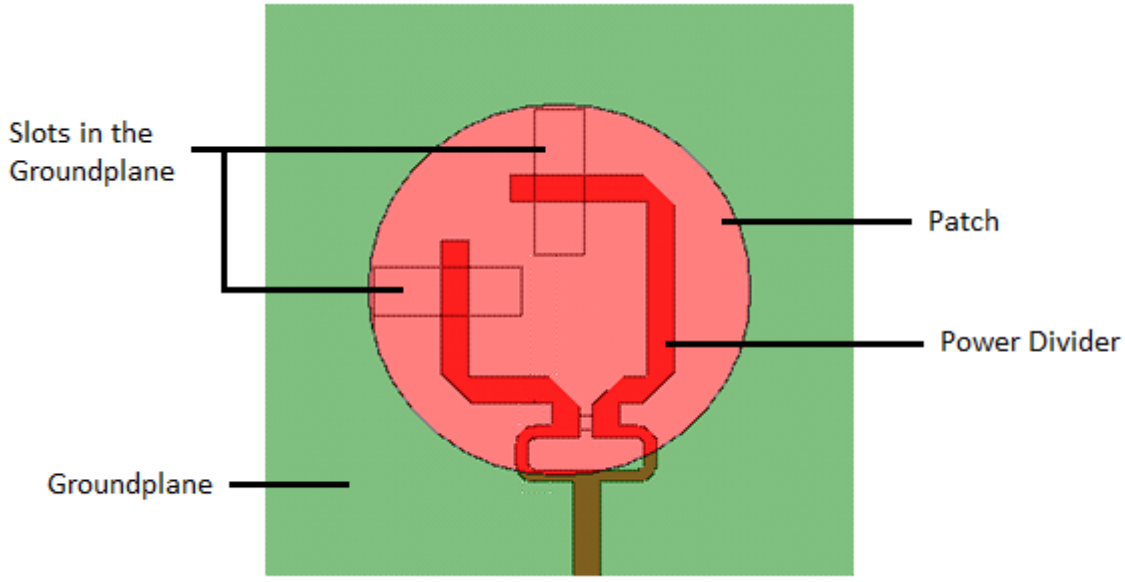

Figure 4.1(a) Circular Patch Antenna with Aperture Coupling

Similarly the side view of the antenna is also shown in the figure 4.1 (b)

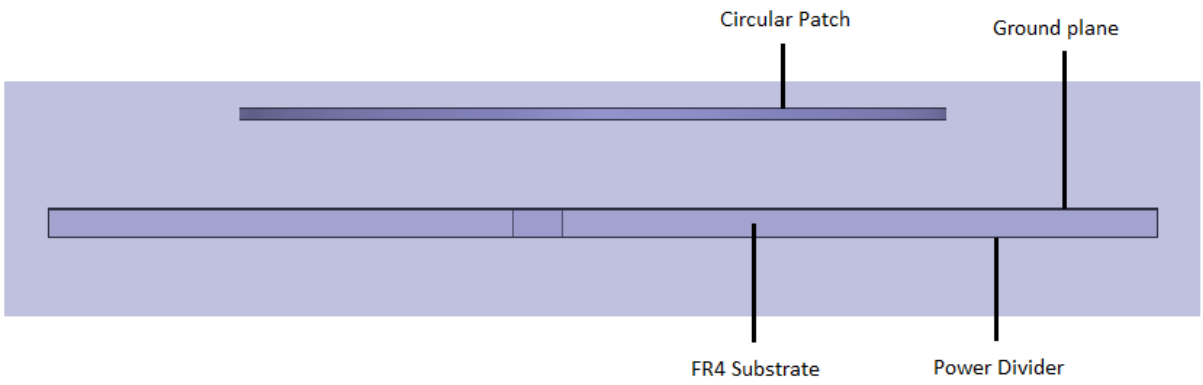

Figure 4.1 (b) Side view of the antenna design

The patch of a radius 10.5 mm is placed at optimized distance from the ground plane. This distance or air spacing is adjusted in both tools. In Microwave Office an air spacing of 5.2 mm is set between ground plane and the patch to achieve the best gain however in HFSS an air spacing of 2.7 mm is set to get the optimized gain.

4.3 Results

Both Simulation and Measured Results are shown in the following section.

4.3.1 Simulated Results

Simulation results with both simulators are shown below.

Return Loss

The return loss calculated from Microwave Office is shown in the figure 4.2 below. A return loss of -15 dB is achieved at 5.8 GHz. An impedance bandwidth (S11<-10dB) is calculated to be 33%.

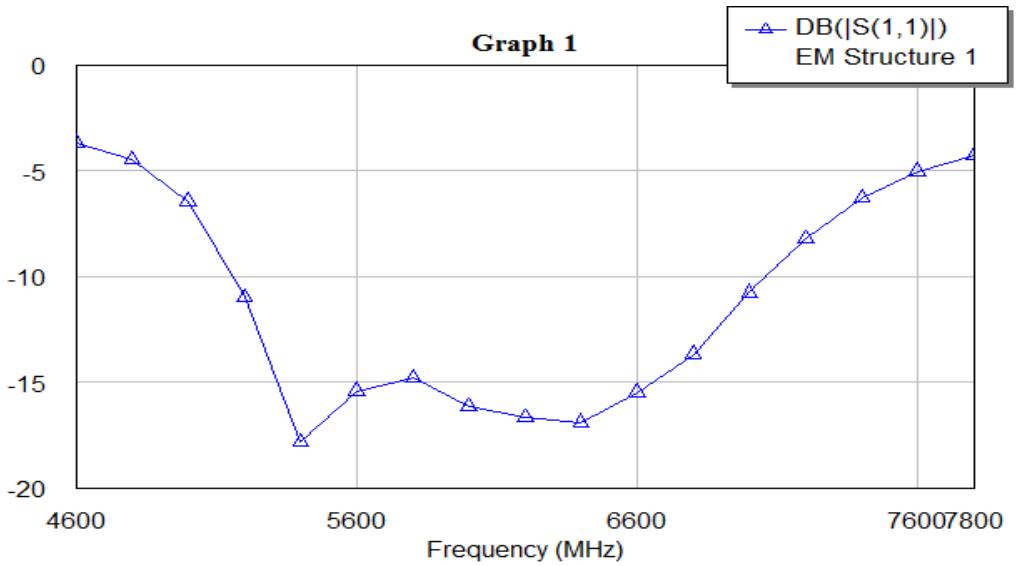

Figure 4.2 Return Loss in Microwave Office

Similarly the return loss from HFSS is also displayed in the figure 4.3 which is very similar to the one from MWO. A return loss of -14 dB is achieved at 5.8 GHz with an impedance bandwidth of 38 %.

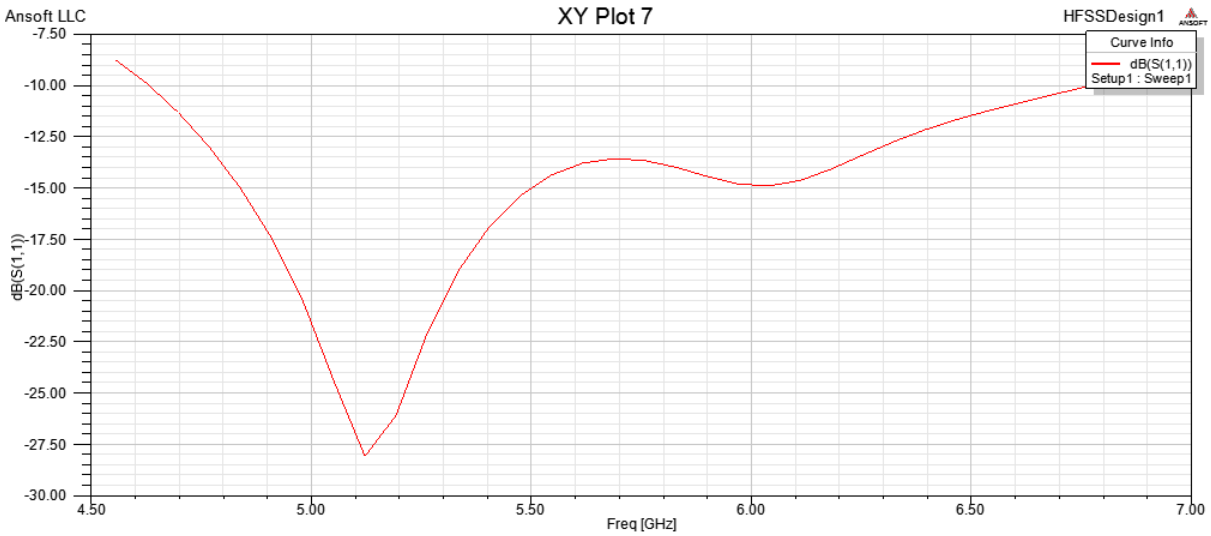

Figure 4.3 Return Loss in HFSS

Radiation Pattern

The elevation pattern for ϕ=0° and ϕ=90° is really important. Figure 4.4 shows the radiation pattern from MWO both for ϕ=0° and ϕ=90°.

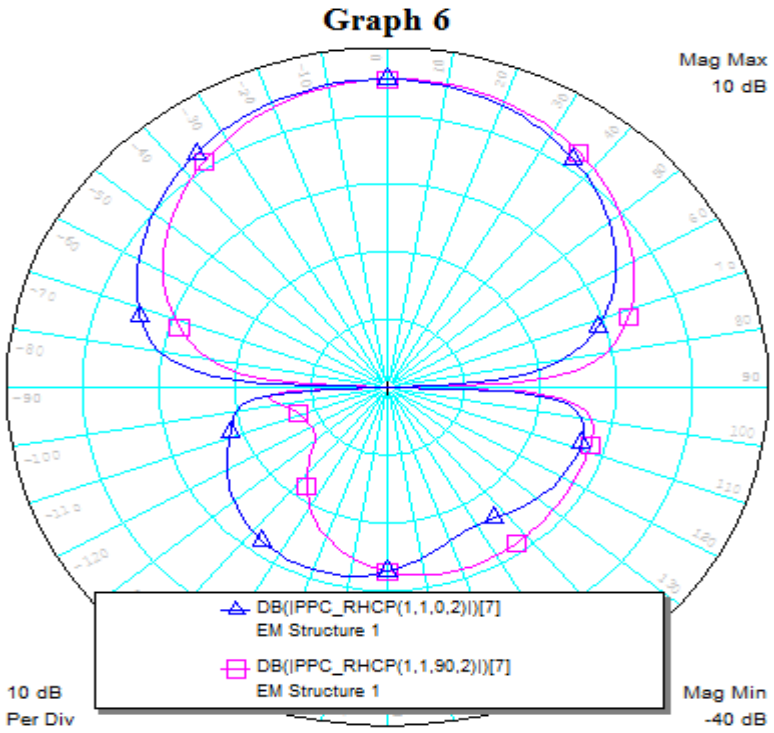

Figure 4.4 Radiation Pattern for ϕ=0° and ϕ=90° in Microwave Office

Similarly radiation pattern for ϕ=0° and ϕ=90° from HFSS is shown in the figure 4.5

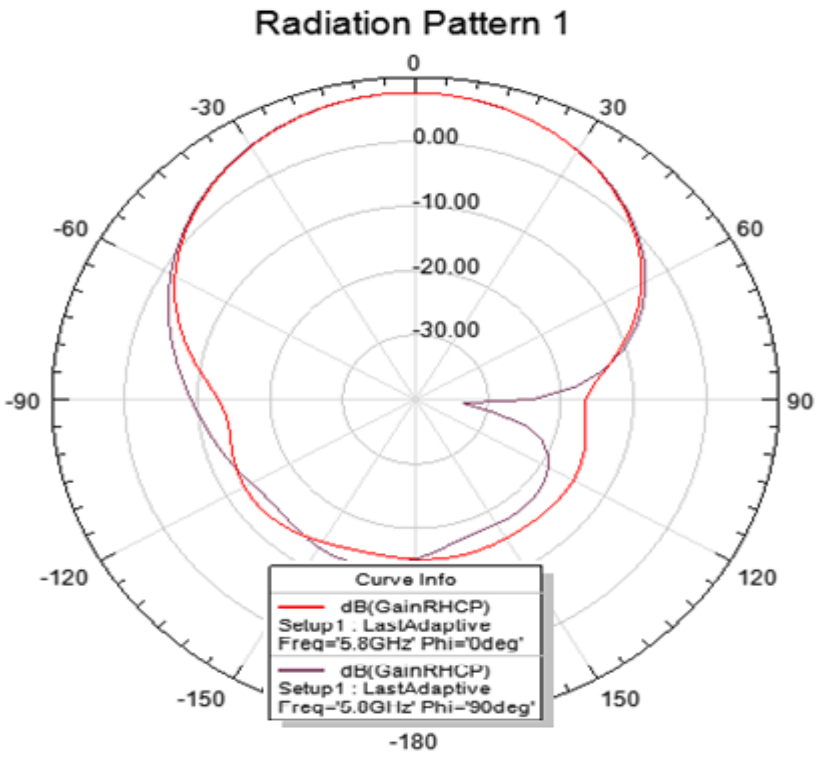

Figure 4.5 Radiation Pattern for $\phi=0^{o}$ and $\phi=90^{o}$ from HFSS

Gain

The gain curve from MWO is shown in the figure 4.6 below. A peak gain of 5.5 dB is achieved at around 0^{o} and a gain of 2.3 dB at $\pm 35^{o}$. A good separation between co and cross polarization is also confirmed which ensures good circular polarization.

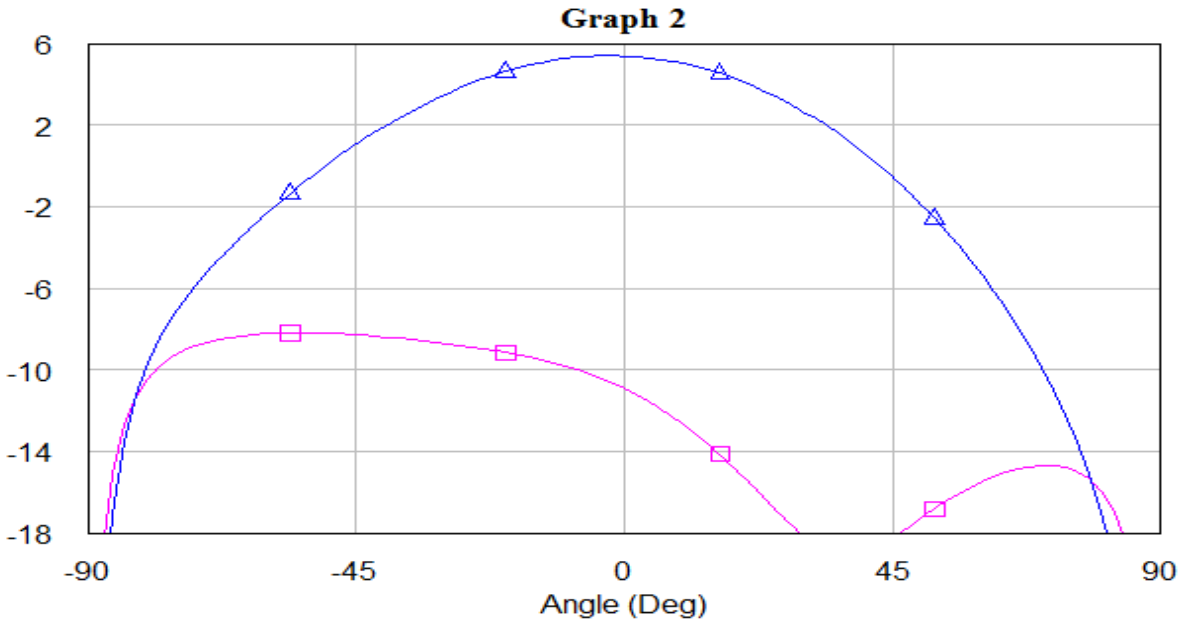

Figure 4.6 Gain (RHCP and LHCP) from Microwave Office

On the other hand the gain calculated from HFSS is higher as compared to MWO as shown in the figure 4.7. A peak gain of 7.5 dB at -5^{o} and a gain of 4 dB at ±35^{o} is achieved. The cross polarization results are also better in HFSS

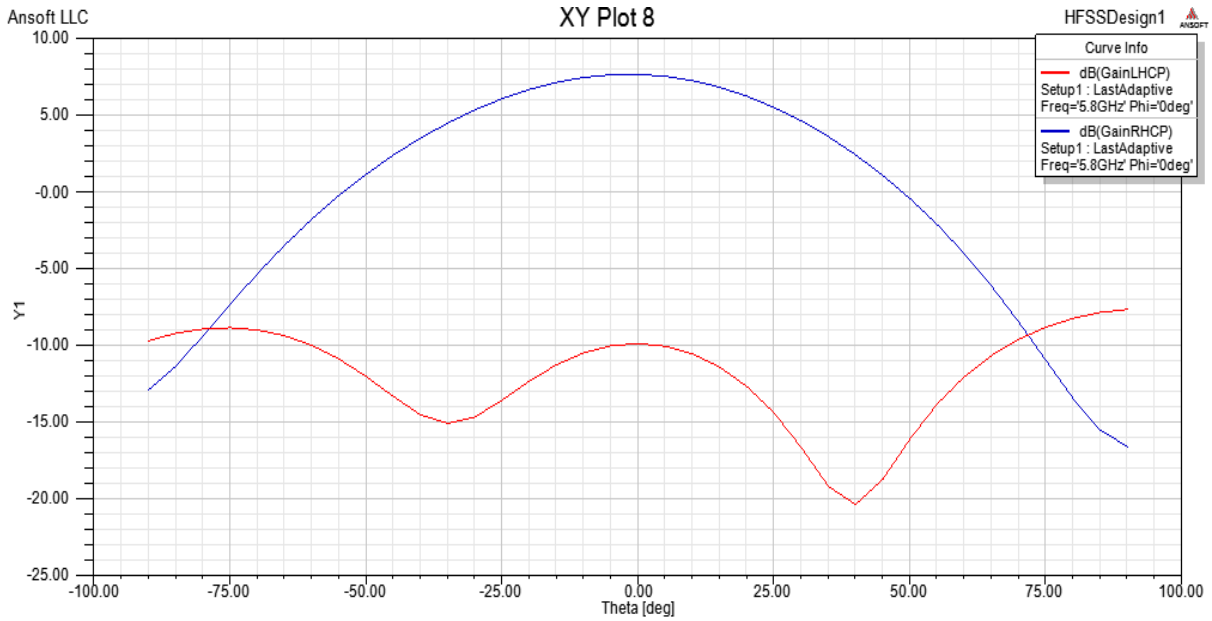

Figure 4.7 Gain (RHCP and LHCP) from HFSS

Axial Ratio

Axial ratio from both tools is also calculated. The figure 4.8 below shows the Axial ratio from MWO. A good part of the desired region (0 to ±35^{o}) is under -3 dB.

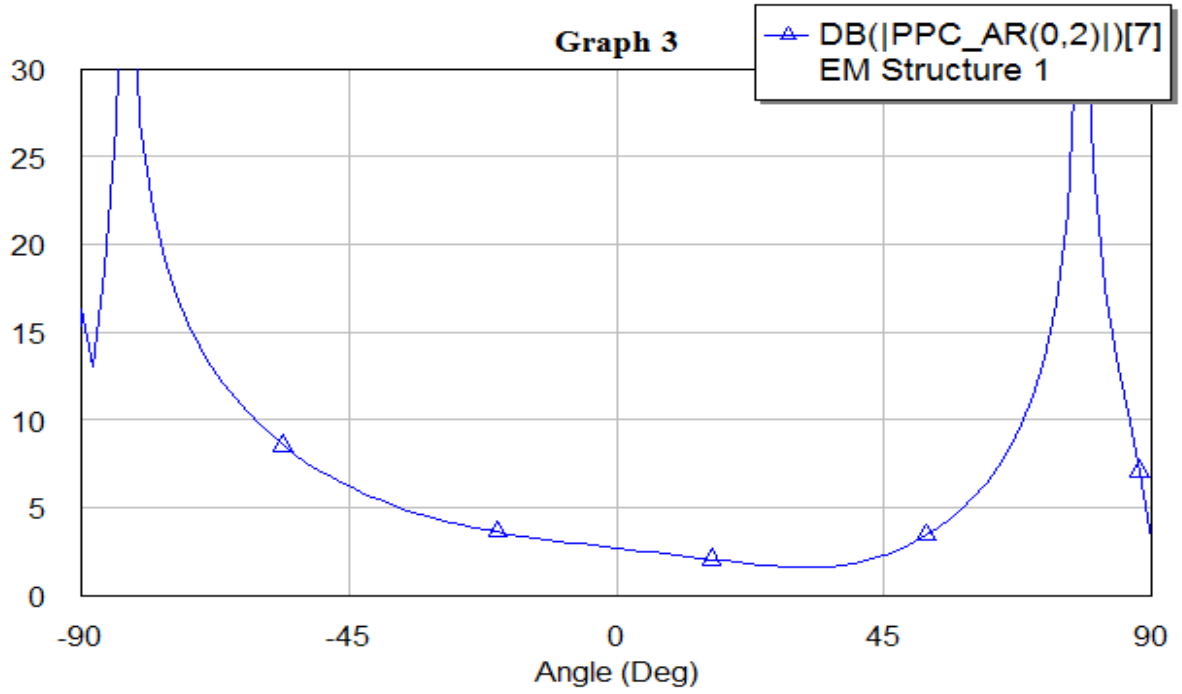

Figure 4.8 Axial Ratio from Microwave Office

Similarly axial ratio from HFSS is also displayed in the figure 4.9. The result is even better due to the fact that a better cross polarization was observed in HFSS. The entire region from (0 to ±35^{o}) is below -3 dB level.

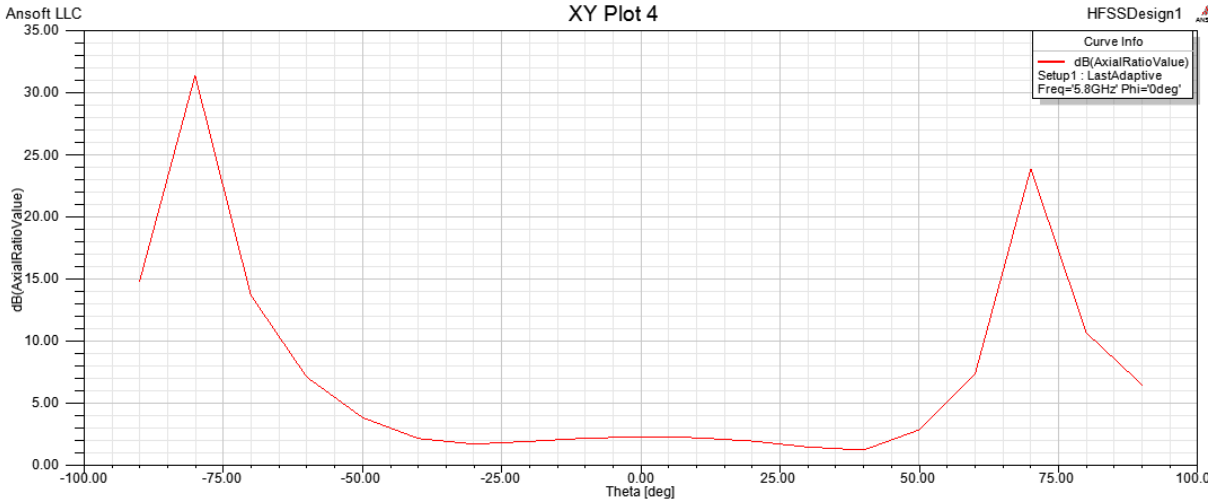

Figure 4.9 Axial Ratio from HFSS

4.3.2 Measured Results

The measured results for the antenna are shown below

Return Loss

Both Simulators showed a return loss in the region of -15 dB and the measurement results are no different. A return loss of -15 dB is achieved at 5.8 GHz in the measurement in Network Analyzer as shown in the figure 4.10

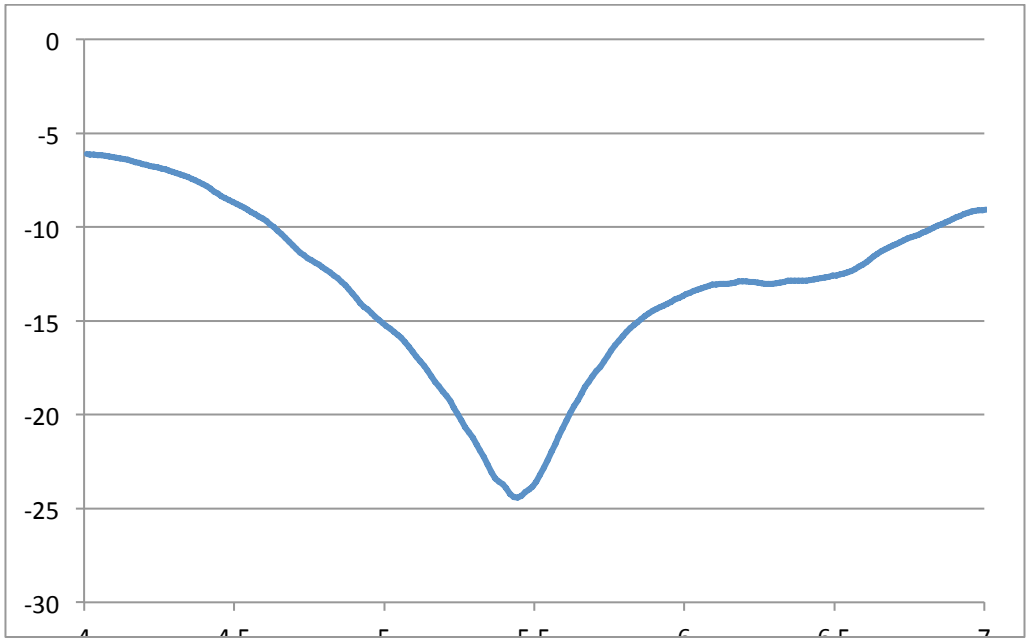

Figure 4.10 Measured Return Loss

Gain

Both simulators have shown different gain as it was shown in the simulation results. In MWO a gain of 5.5 dB and in HFSS a gain of 7.5 dB was recorded. The measured results of the gain are closer to the HFSS results. A peak gain of 7 dB is achieved both in azimuth and elevation. At ±35^{o} a gain of around 3.5 dB is achieved.

The air spacing between ground plane and the patch is 2.7mm. The measured gain in azimuth plane is shown in the figure 4.11.

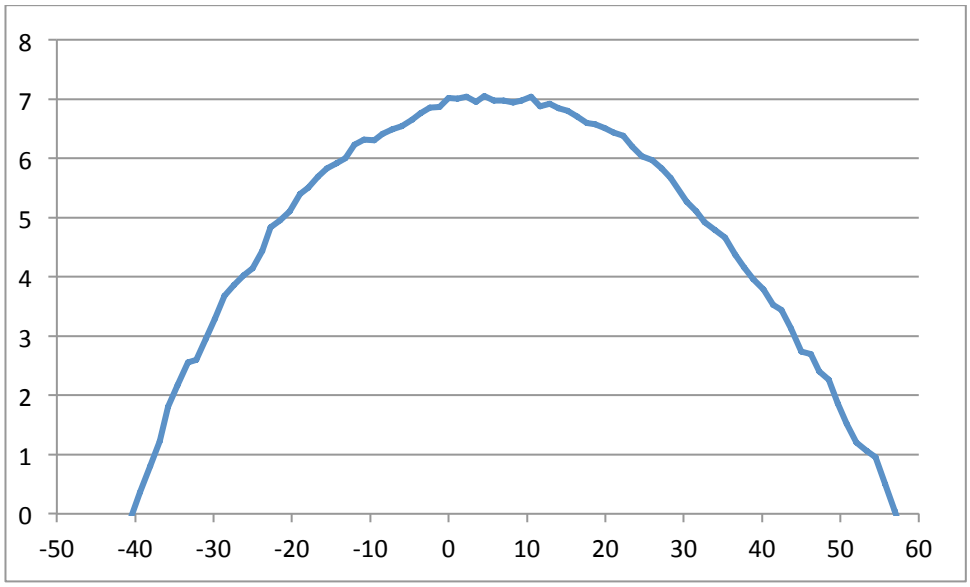

Figure 4.11 Gain in Azimuth

Similarly the measured gain in elevation plane is shown in the figure 4.12 which is very much identical to the gain in azimuth

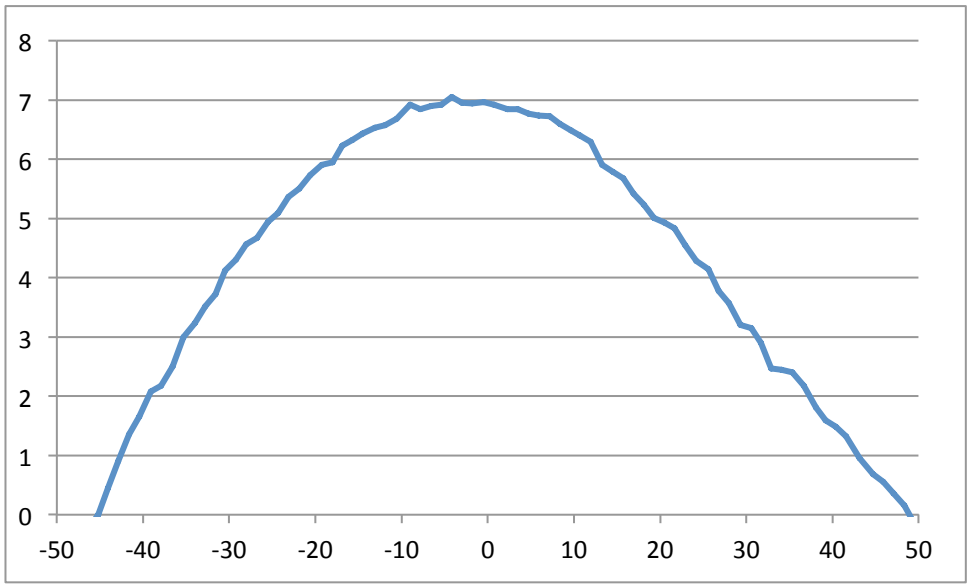

Figure 4.12 Gain in Elevation

Cross polarization

Cross polarization results have also been measured to confirm the good circular polarization. The cross polarization in azimuth plane is shown in the figure 4.13

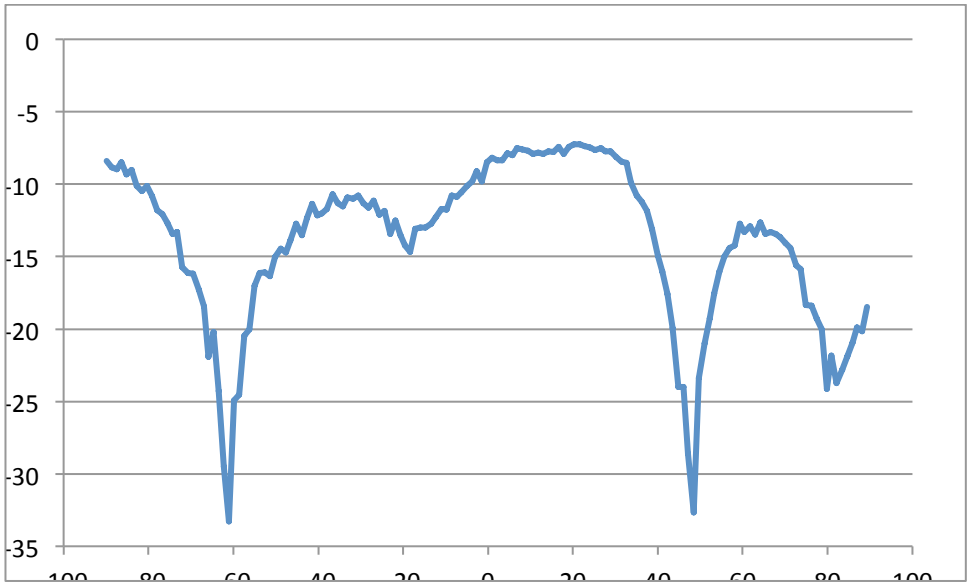

Figure 4.13 Cross polarization in Azimuth

Similarly the cross polarization result in Elevation Plane is shown in figure 4.14

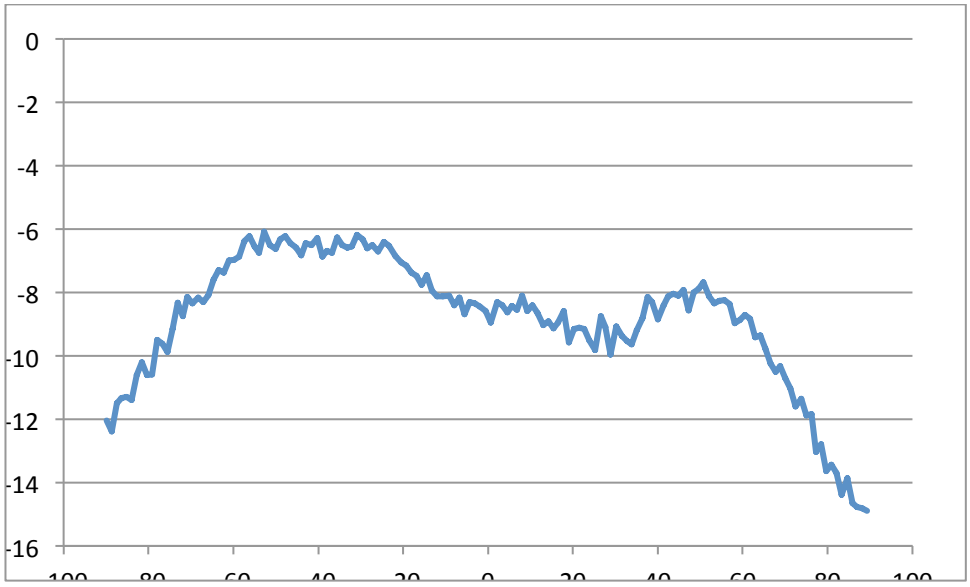

Figure 4.14 Cross Polarization in Elevation

It can be seen from the previous four graphs that there exists a good separation between co and cross polarization which proves a good circular polarization.

4.4 Conclusion

The antenna has a nice performance overall. It has a desired return loss, high gain and a good circular polarization. Size is also small, even if the ground plane is bigger than with the X antenna. Especially when high gain is needed it can be a good choice.

Chapter 5

Patch Antenna with probe feeding

5.1 Introduction

This antenna is similar to the one discussed in the previous chapter. The difference is the feeding technique being used. The geometry of transponder allows us to use air as a substrate for the antenna as some vacant air space is available on either side of the ground plane. It is known that the gain can be enhanced using air as a substrate. For that reason air is used as the substrate in this design.

5.2 Design

The same power divider used in chapter 4 is used with this antenna with the same 0.8 mm FR4 substrate however instead of using an aperture coupling, probe feeding is used. So the probe which starts from the power divider goes into the 0.8 mm FR4 substrate and is than continued in the air up to the patch as shown in the figure 5.1

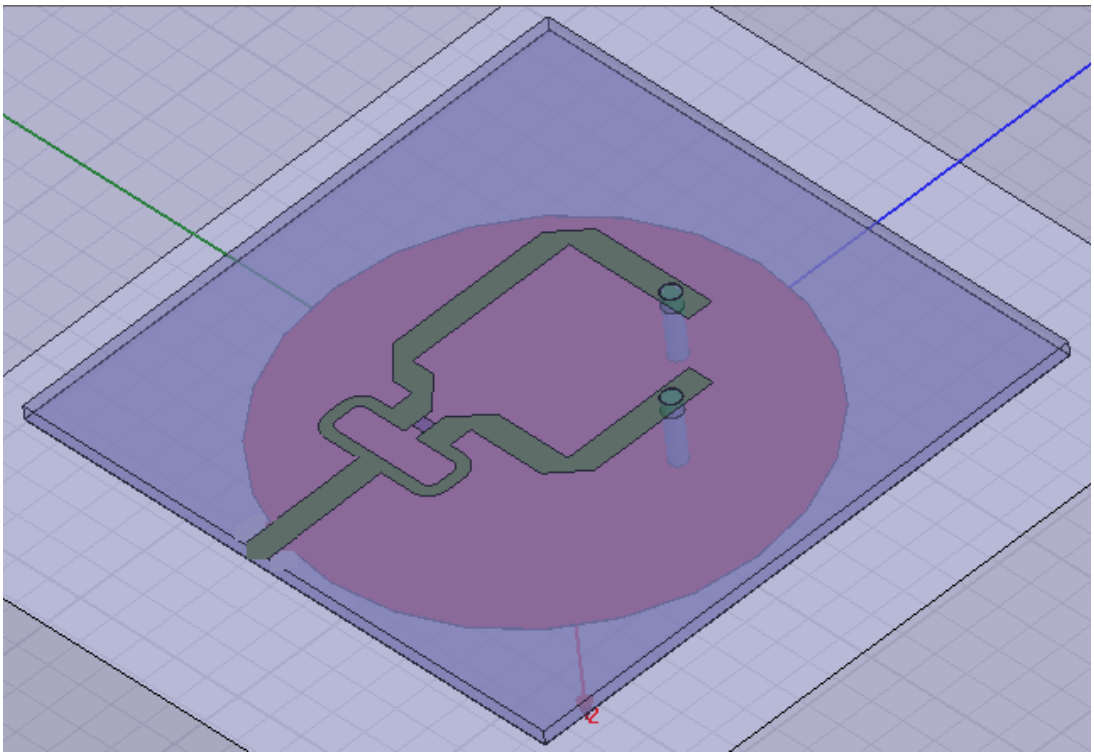

Figure 5.1 Patch Antenna with probe feeding

Similarly a side view of the antenna is shown in the figure 5.2 to get a clear idea of the antenna feeding.

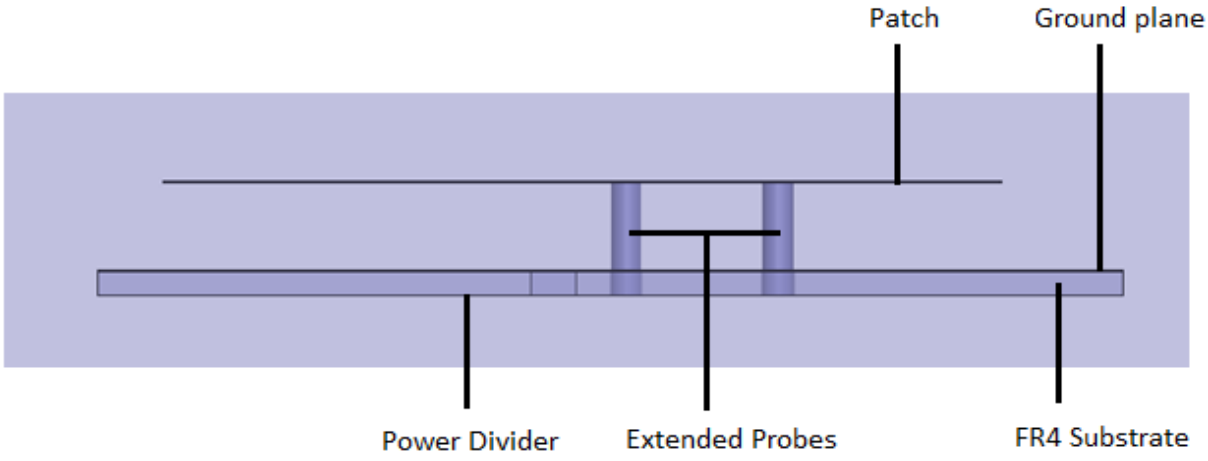

Figure 5.2 Side view of the antenna

The radius of the circular patch is 13.5 mm and of the two probes is 0.5 mm. The ground is 33mm x 33mm and the air spacing between the ground and the patch is set 3mm in both MWO and HFSS.

5.3 Results

Both Simulated and measured results will be shown here.

5.3.1 Simulated Results

Simulation results are shown in the following section.

Return Loss

The return loss from MWO is shown in the figure 5.3. A S11 of -12 dB is achieved at 5.8 GHz

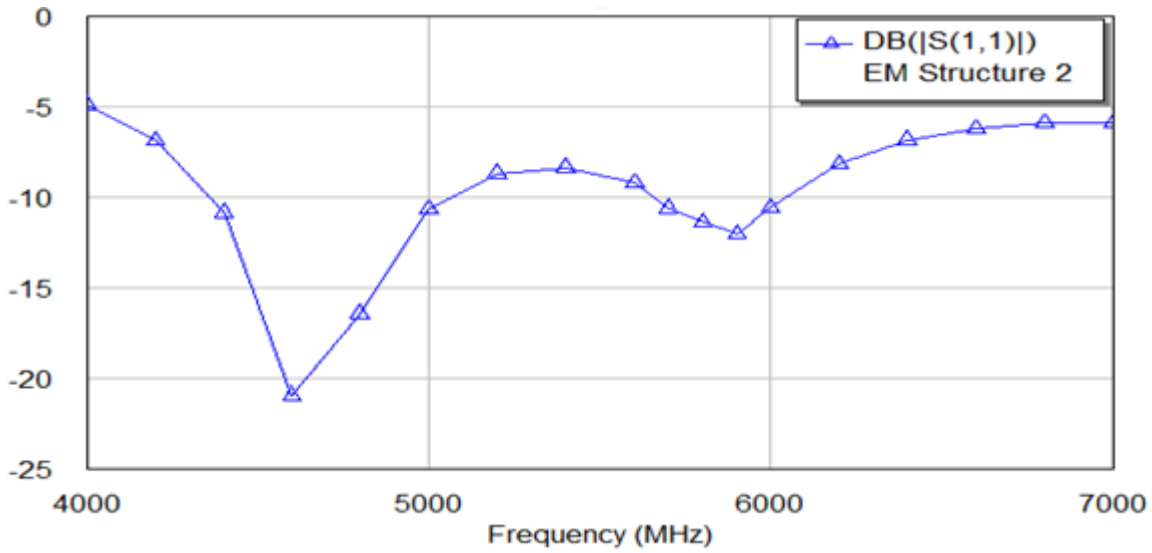

Figure 5.3 Return Loss in Microwave Office

Similarly return loss in HFSS is shown in the figure 5.4 which shows an S11 of -10 dB at 5.8 GHz.

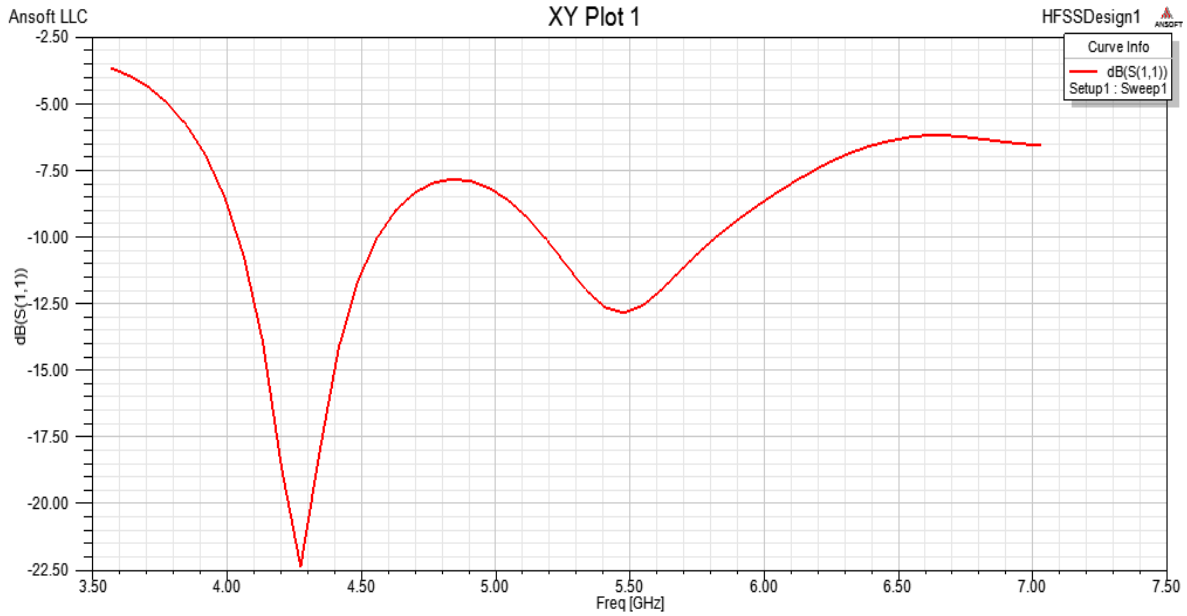

Figure 5.4 Return Loss in HFSS

Radiation Pattern

The radiation pattern for $\phi=0^{o}$ and $\phi=90^{o}$ gives a good measure of the radiation pattern. Figure 5.5 shows the radiation pattern from MWO both for $\phi=0^{o}$ and $\phi=90^{o}$.

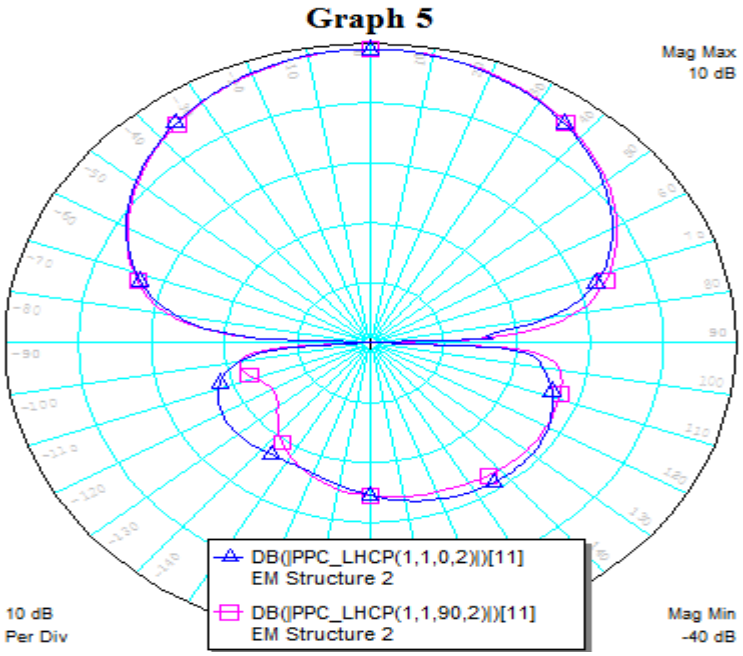

Figure 5.5 Radiation Pattern for $\phi=0^{o}$ and $\phi=90^{o}$ in Microwave Office

Similarly the radiation pattern from HFSS is also shown in the figure 5.6 for for $\phi=0^{o}$ and $\phi=90^{o}$

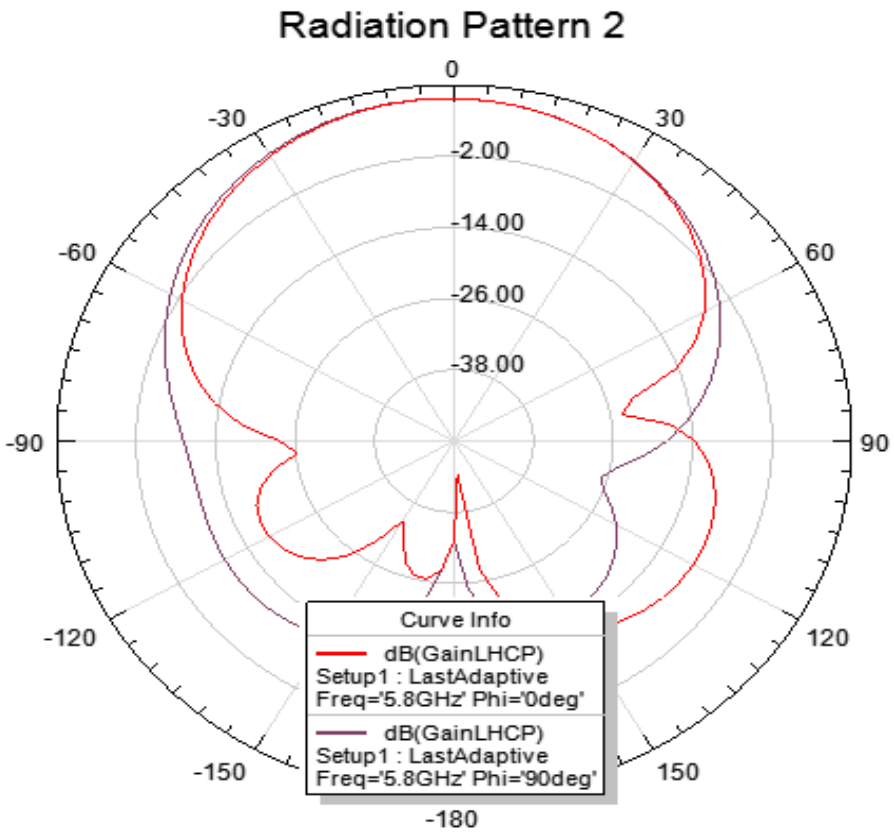

Figure 5.6 Radiation Pattern for $\phi=0^{o}$ and $\phi=90^{o}$ from HFSS

Gain

A high gain was expected as compared to the previous designs. The peak gain from MWO is 8.5 dB which was desired. A gain of 5 dB was achieved at $\pm35^{o}$. A very good isolation is also achieved between co and cross polarization as shown in the figure 5.7.

Similarly the gain result in HFSS is also shown in the figure 5.8. A peak gain of 7.5 dB is achieved which is slightly low as compared to MWO. At $\pm35^{o}$ the gain is found to be 4 dB which is still very good however the cross polarization is a bit higher in HFSS.

Hence both the tools have proved that the gain is enhanced with the air substrate. It is interesting to compare these simulated results with the measured results.

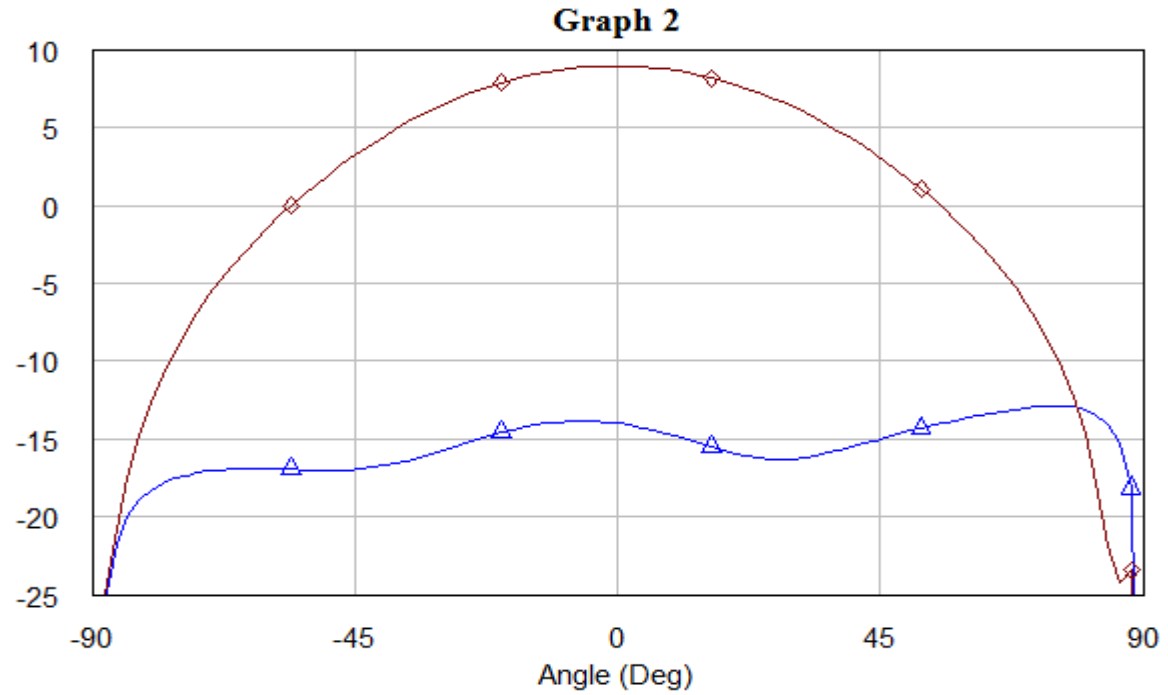

Figure 5.7 Gain (RHCP and LHCP) in Microwave Office

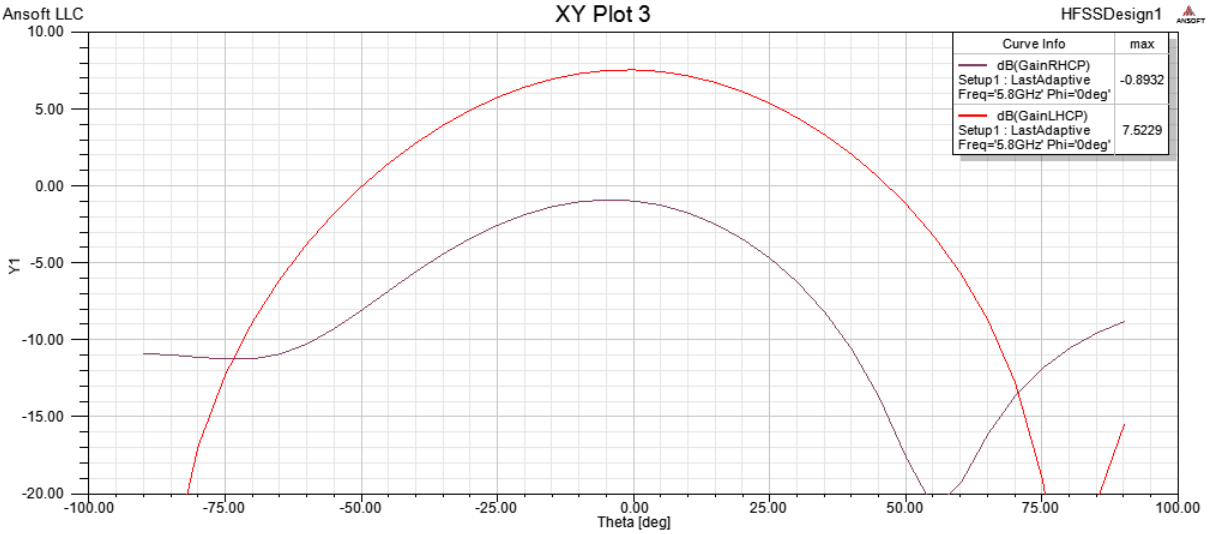

Figure 5.8 Gain (RHCP and LHCP) in HFSS

Axial Ratio

The axial ratio in MWO is shown in the figure 5.9. It is even lower than the 2 dB level for the range 0 to ±35^{o}.

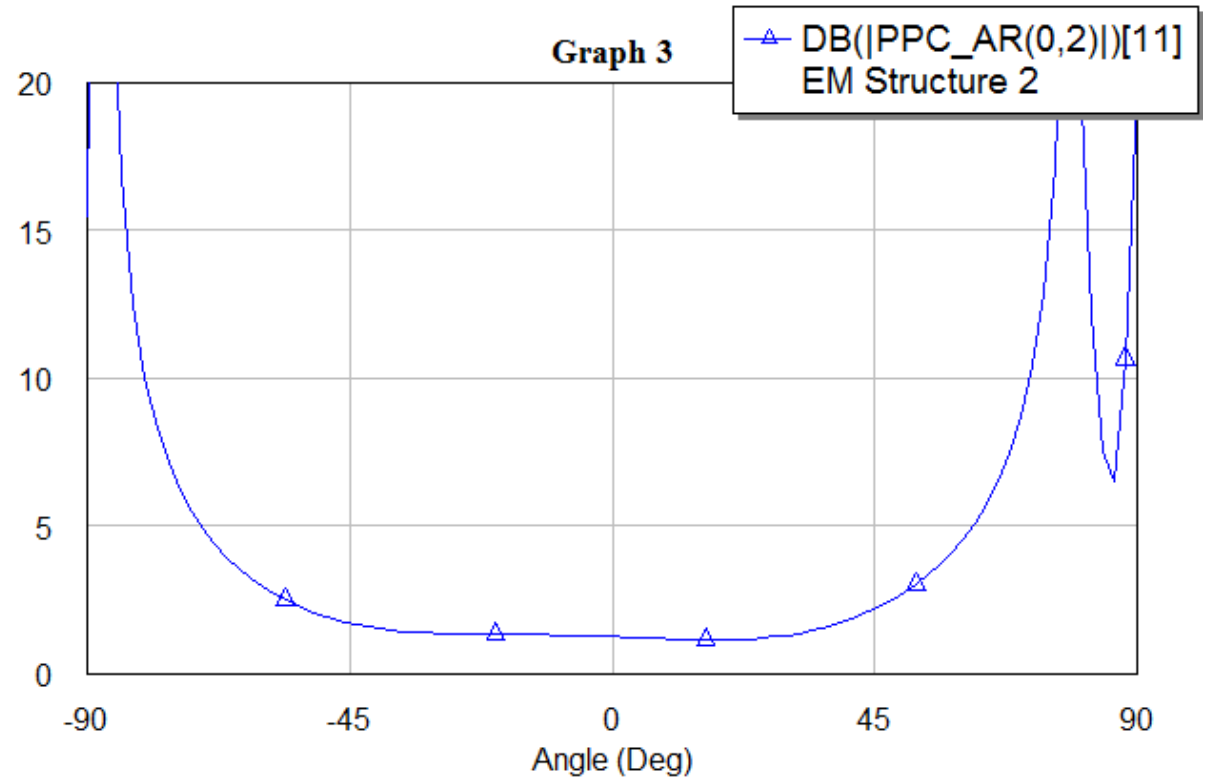

Figure 5.9 Axial Ratio in MWO

The axial ratio in HFSS is also shown in the figure 5.10. It is a bit higher as compared to MWO which was expected because cross polarization level in HFSS was higher compared to MWO.

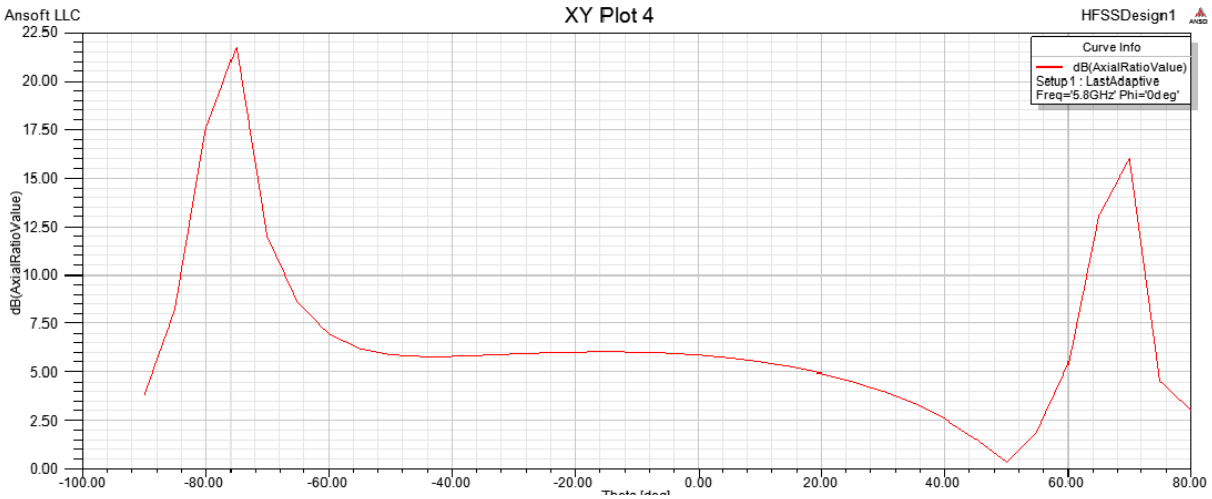

Figure 5.10 Axial Ratio in HFSS

5.3.2 Measured Results

Different measured results are shown in this section.

Return Loss

The measured return loss of the antenna is shown in the figure. A return loss of -30 dB is achieved at 5.8 dB.

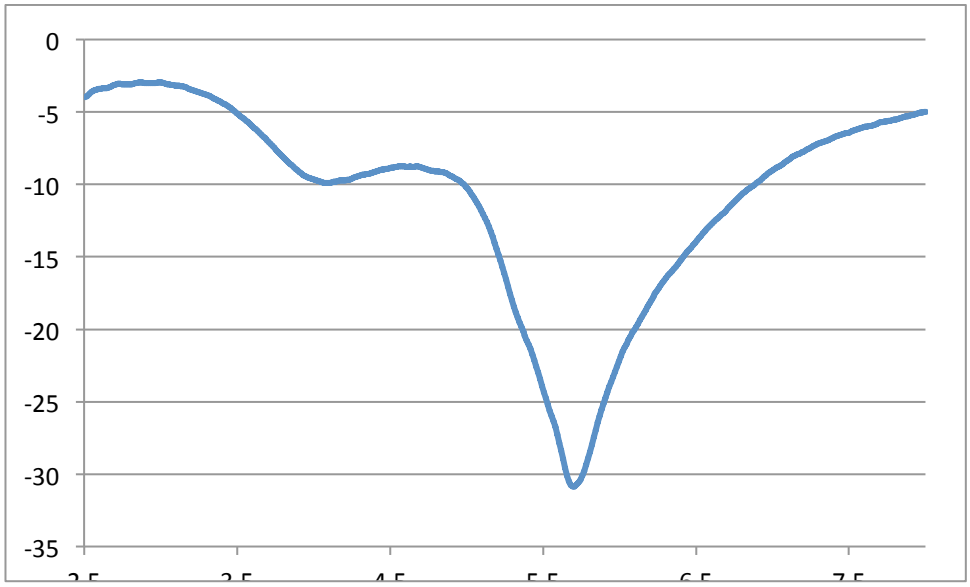

Figure 5.11 Measured Return Loss

Gain

The gain curve in azimuth plane is shown in the figure below. A peak gain of around 8 dB in bore sight and 4.5 dB at ±35^{o} is achieved.

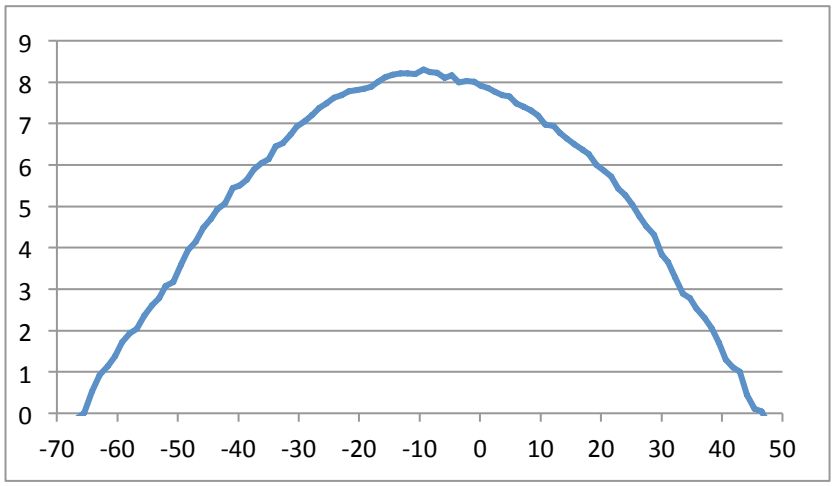

Figure 5.12 Gain in Azimuth

Similarly the gain plot in elevation plane is shown in the figure below. It shows a peak gain of 7.7 dB and around 4.5 at ±35°.

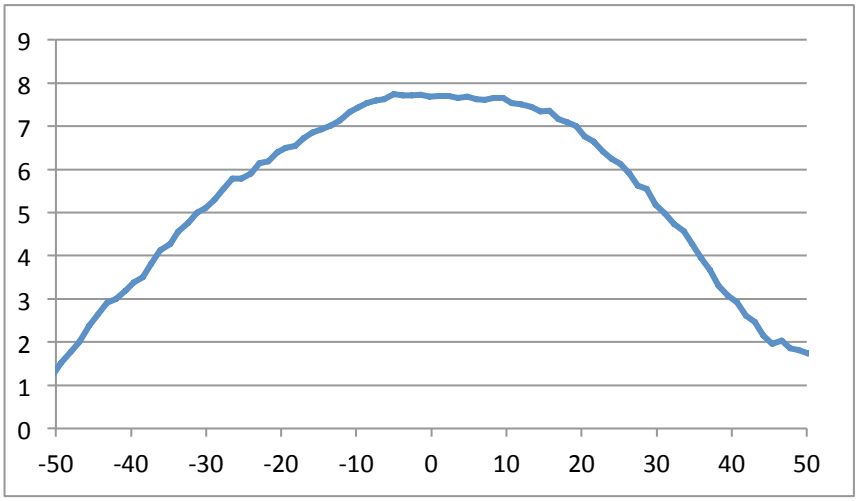

Figure 5.13 Gain in Elevation

Cross Polarization

The cross polarization is shown in the figure below for both azimuth and elevation planes, which proves good circular polarization.

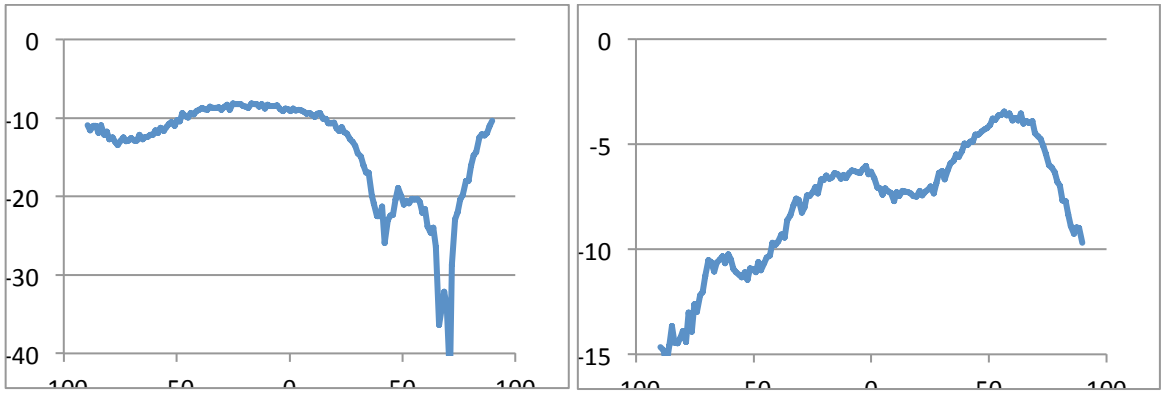

(a) (b)

Figure 5.14 Cross Polarization in azimuth (a) and Elevation (b) plane

5.4 Conclusion

The antenna has shown very nice results i.e. high gain, good return loss and circular polarization. Also the gain within ±35° is very nice. The drawback is that the size is slightly large and also to achieve probe feeding in volume production. Both this antenna and the antenna in chapter 4 are very similar, there is just the difference in the feeding technique, however this antenna has shown better gain results. The beam width is more wide which helps to achieve better gain within ±35°.

Chapter 6

Truncated Patch Antenna

6.1 Introduction

The truncated patch antenna is a simple microstrip patch antenna with a rectangular patch over a substrate and a ground plane at the bottom. This antenna was the last antenna designed in the thesis work and was designed in a limited time. There were six antennas designed of this particular type which although used a same geometry but had different substrates, feeding techniques and substrate thicknesses.

6.2 Design

The design of the truncated patch antenna is shown in the figure. The figure shows the antenna with coaxial probe feeding and the figure shows the antenna with Microstrip line feeding.

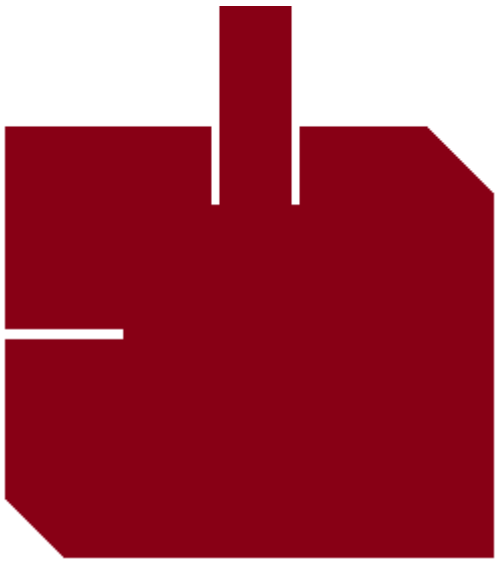

Figure 6.1(a) Truncated Patch antenna with Microstrip Feeding

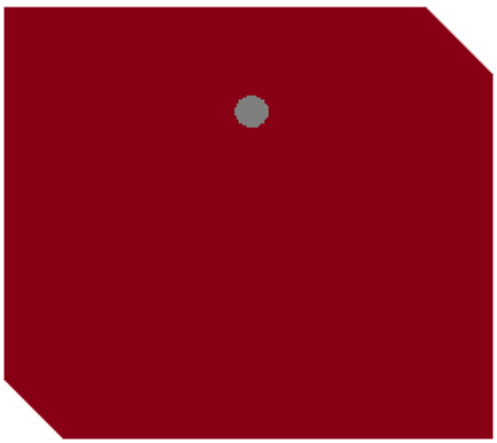

Figure 6.1(b) Truncated Patch antenna with Coaxial Probe Feeding

The edges are truncated to achieve circular polarization and the slit used in the figure 6.1(a) is also used to get better circular polarization.

Two different substrates were used in this antenna i.e. FR4 with a dielectric of 4.3 (with a thickness of 0.8mm and 1.6mm) and Nelco with a dielectric of 3.48 (and thickness of 0.51mm). The six antennas designed with different substrate and feeding technique are shown in the table 6.1 below

Antenna Number	Feeding technique	FR4 (1.6mm thick)	FR4 (0.8mm thick)	Nelko 4350-RF13
1	Coaxial Probe	Yes	-	-
2	Coaxial Probe	-	Yes	-
3	Coaxial Probe	-	-	Yes
4	Microstrip Line	Yes	-	-
5	Microstrip Line	-	Yes	-
6	Microstrip Line	-	-	Yes

Table 6.1

However all of these designs showed not acceptable degradation of measured performance compared with the simulated. The designs which worked to some extent have been mentioned here and the rest are presented in the Appendix.

6.3 Results

6.3.1 Simulated Results for Antennas with Nelco Substrate

Return Loss

The return loss of the antenna with both feeding techniques is shown below. So at 5.8 GHz the antenna with microstrip line feeding shows a return loss of 5.8 dB. On the other hand the antenna with probe feeding has a return loss of -10 dB.

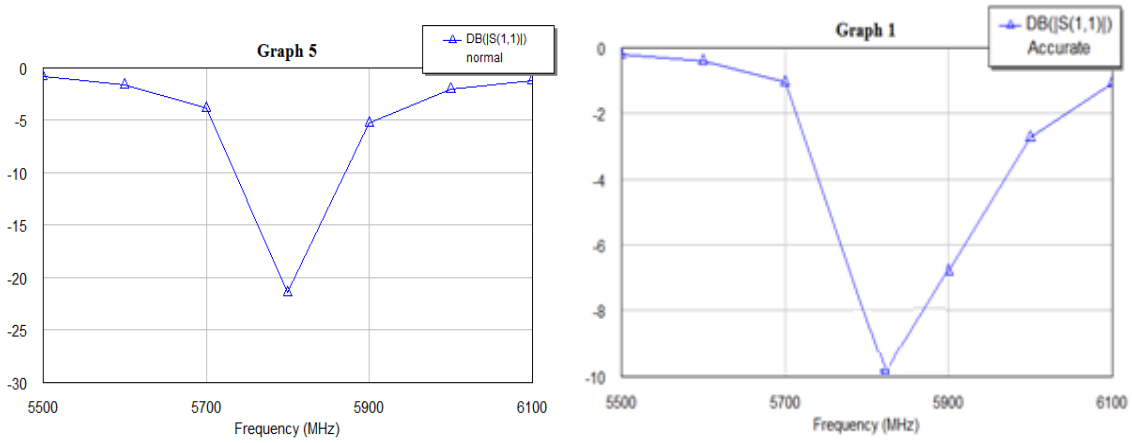

(a) (b)

Figure 6.2 Return Loss of the antenna with Microstrip (a) and Probe (b) feeding

Gain

The gain measurements for both the antennas are shown in the figure 6.3. The antenna with microstrip line feeding has shown a gain of 6 dB and the probe fed antenna showed a gain of 4.2 dB.

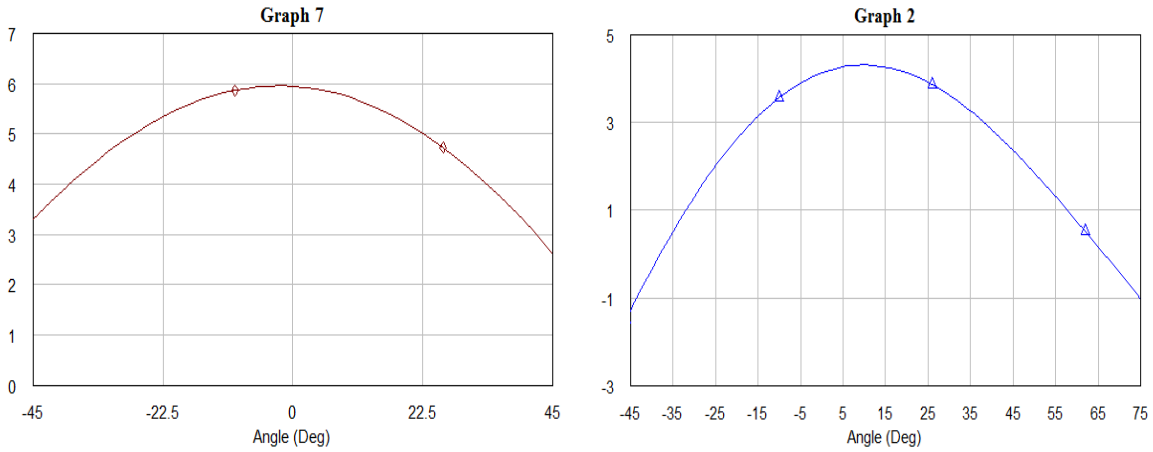

(a) (b)

Figure 6.3 Gain of the antenna with Microstrip (a) and Probe (b) feeding

Cross polarization

The cross polarization curves for the two antennas are shown in the figure 6.4

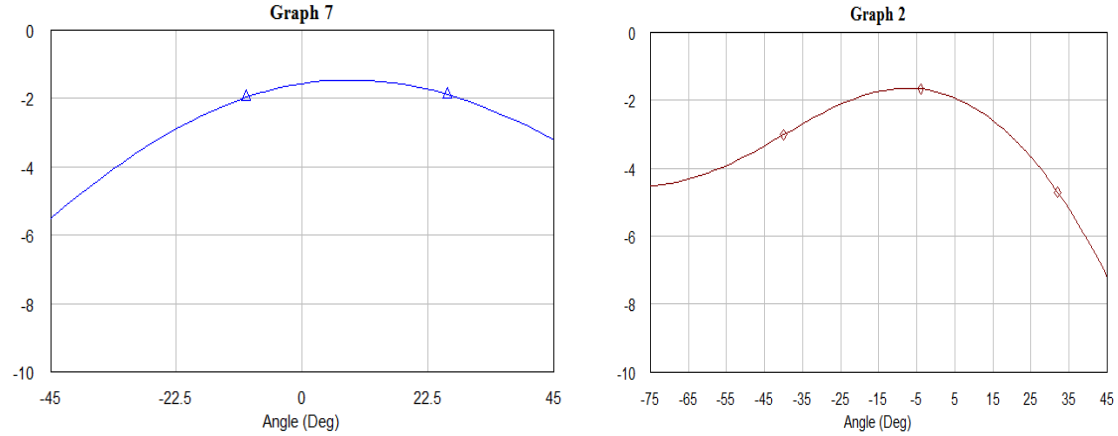

(a) (b)

Figure 6.4 Cross Polarization of the antenna with Microstrip (a) and Probe (b) feeding

The cross polarization values are a little high. These antennas were not designed in HFSS due to the time shortage at the end of the thesis work and they were manually optimized which became a little tricky.

Radiation Pattern

The radiation pattern for azimuth and elevation for both antennas is shown in the figure 6.5 below. The antenna with probe feeding shows a little difference in radiation for azimuth and elevation planes

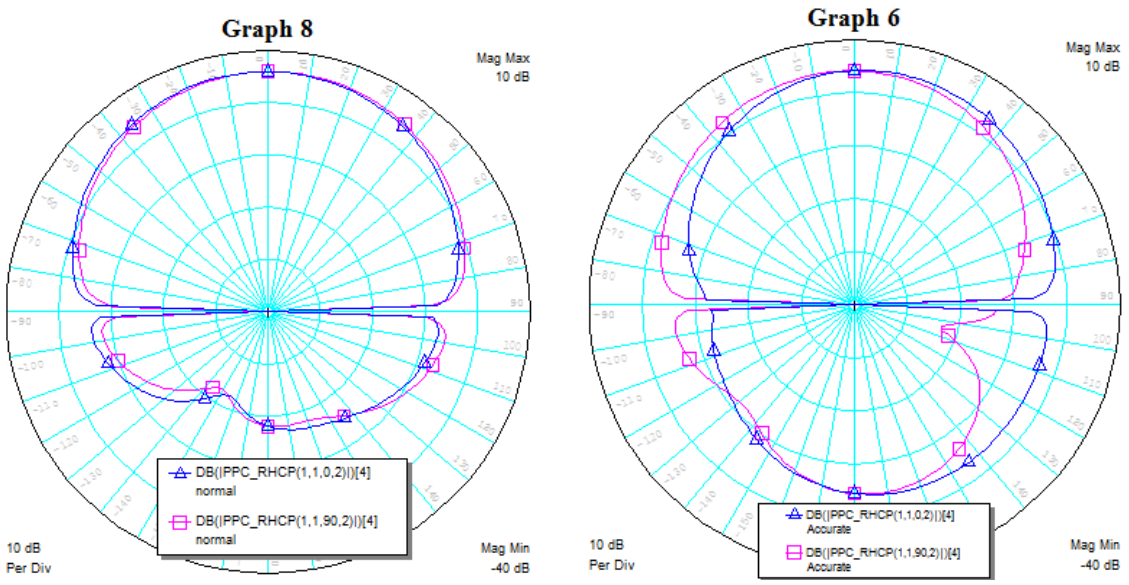

(a) (b)

Figure 6.5 Radiation Pattern of the antenna with Microstrip (a) and Probe (b) feeding

6.3.2 Measured Results for Antennas with Nelco Substrate

The measured results for the antenna with Nelco Substrate are shown below. These results have not followed the simulation results and hence are below the expectations

Return Loss

The return losses of the antenna with both feeding techniques are shown in the figure 6.6

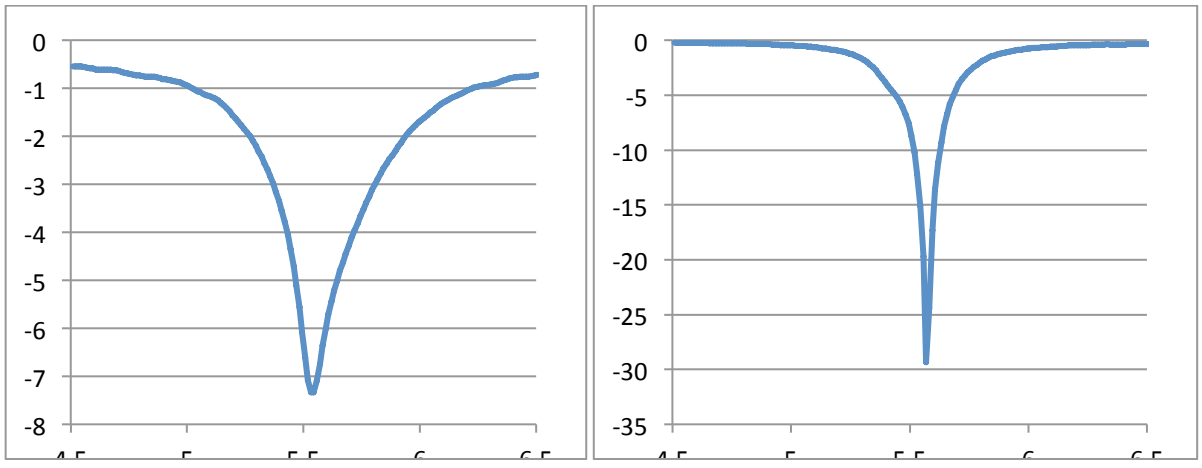

(a) (b)

Figure 6.6 The Return Loss of the antenna with Microstrip Line (a) and Coaxial (b) Feeding

If these results are compared with the simulation results they look entirely different. For the antenna design with Microstrip Line Feeding the return loss was -22 dB in the simulation

results and was centered at 5.8 GHz however, in the measured results the return loss is around -7 dB and centered at 5.5 GHz.

Similarly for the antenna with coaxial probe feeding, the simulated return loss at 5.8 GHz was around -10 dB which changed to -29 dB at 5.52 GHz.

Gain

The gain measurements are also very different from the simulated ones. The gain curves for the antenna with microstrip feeding line technique in both azimuth and elevation plane are shown in the figure 6.7. These measurements are taken on frequencies with minimum return loss value.

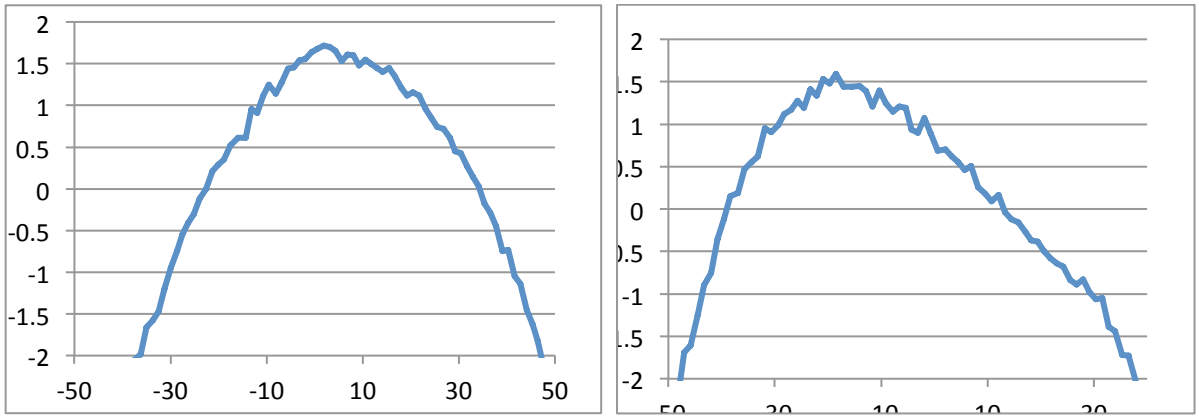

(a) (b)

Figure 6.7 Gain in both azimuth (a) and Elevation (b) plane

Similarly the gain curves for the antenna with probe feeding are shown in the figure 6.8

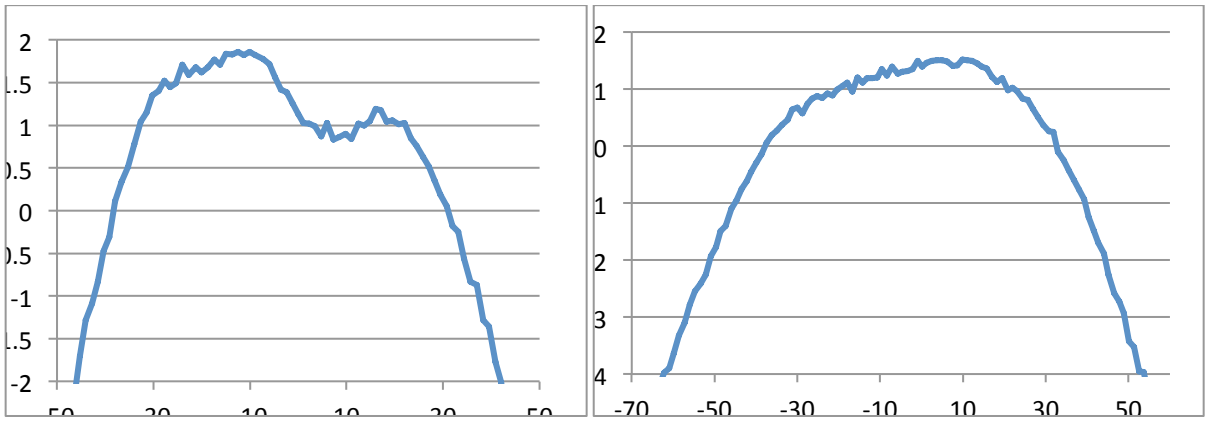

(a) (b)

Figure 6.8 Gain in both azimuth (a) and Elevation (b) plane

There is a vast difference between the measurement and simulation results for the gain curves. Both antennas have shown a 3-4 dB gain reduction from the simulated results.

Cross Polarization

The cross polarization results for the microstrip line feeding antenna are however nice. The measured results for the cross polarization in both azimuth and elevation plane are shown in the figure 6.9

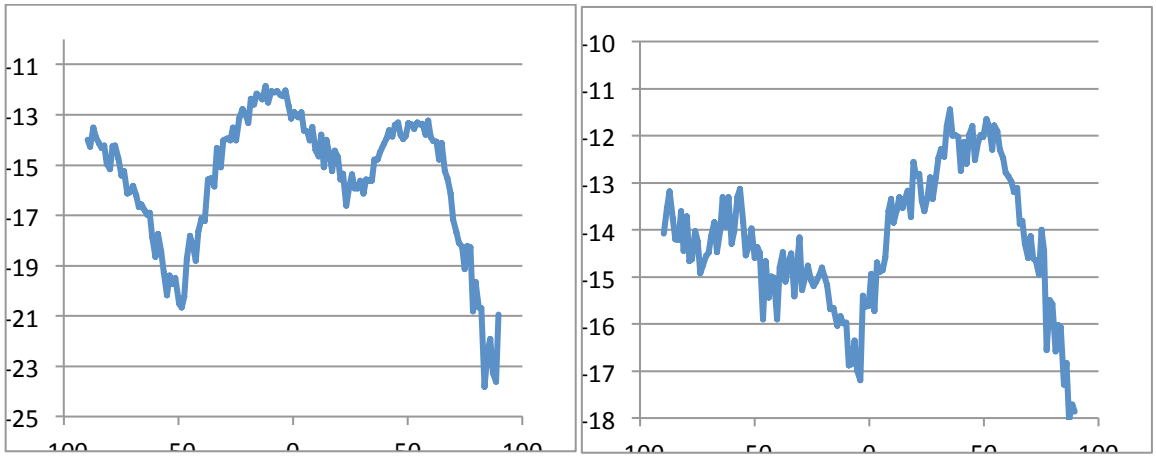

(a) (b)

Figure 6.9 Cross Polarization in both azimuth (a) and Elevation (b) plane

Similarly the measured cross polarization for probe fed antenna in both azimuth and elevation plane are shown in the figure 6.10 which are again below then the expectation level.

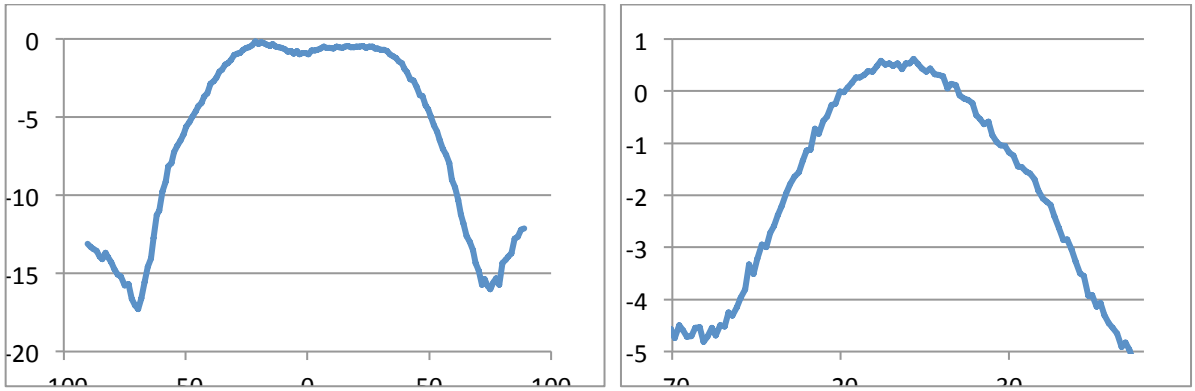

(a) (b)

Figure 6.10 Cross Polarization in both azimuth (a) and Elevation (b) plane

6.3.3 Simulated Results for Antennas with FR4 (0.8mm) Substrate

The same two antennas were designed with FR4 substrate however only the one with coaxial probe feeding will be discussed here as the other one didn't yield any result at all, however there are more information in the appendix of the report.

Return Loss

The return loss for this antenna is shown in the figure 6.11 which is around -11 dB for 5.8 GHz.

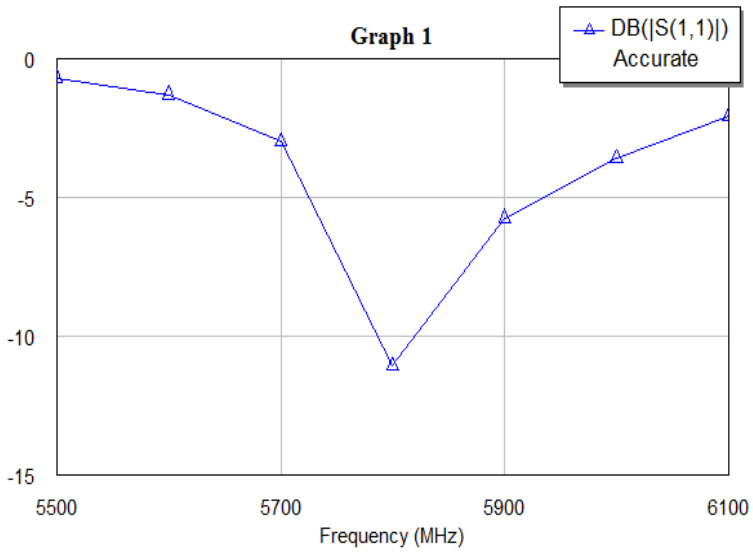

Figure 6.11 Return Loss of the antenna

Gain

The simulated gain for the antenna is shown in the figure below. A peak gain of 6 dB at 2^{o} and a gain around 3.7 dB at $\pm 35^{o}$ is achieved. The gain curve is shown in the figure 6.12 below.

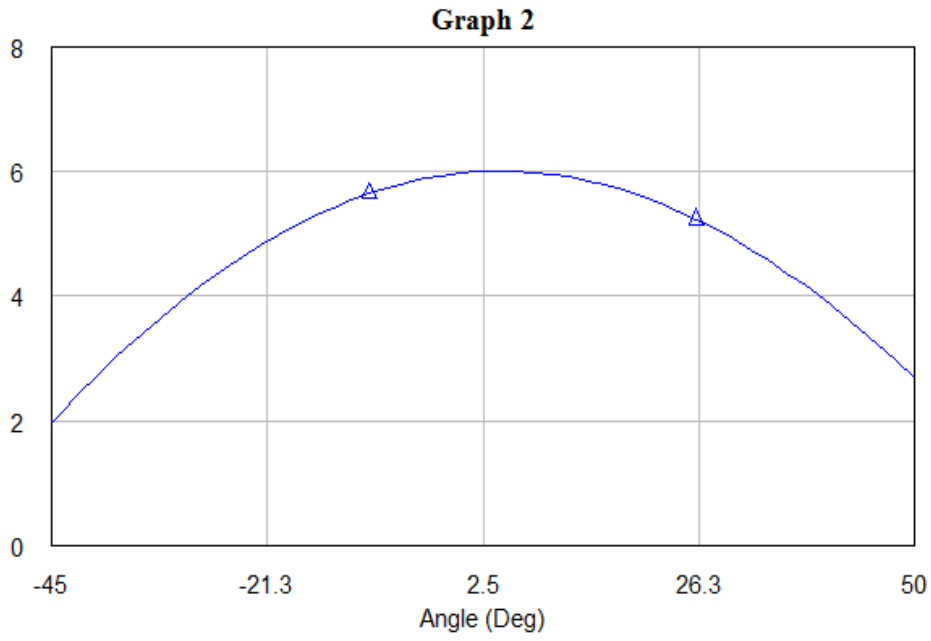

Figure 6.12 Gain of the antenna

Cross Polarization

The cross polarization level is an important factor to check the circular polarization. The cross polarization curve is shown in the figure below which shows a good separation from the co polarization of the above figure 6.13.

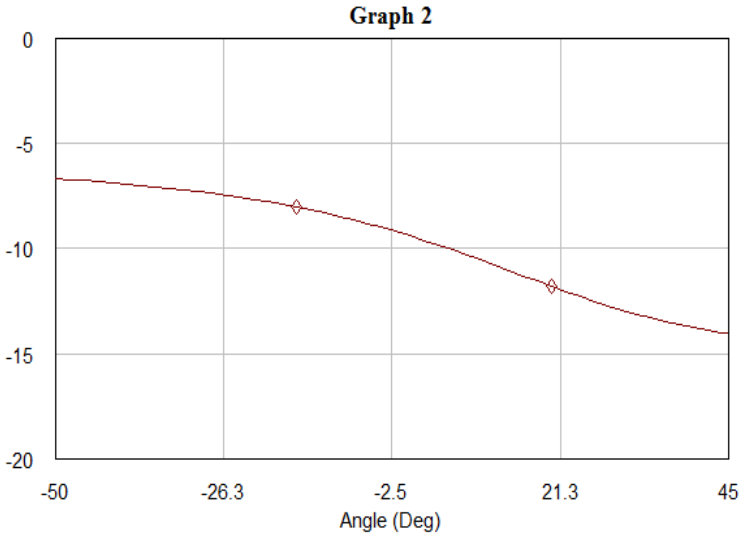

Figure 6.13 Cross Polarization of the antenna

Radiation Pattern

The radiation pattern of the antenna is another important factor. The radiation pattern for both azimuth and elevation pattern is shown in the figure 6.14 below

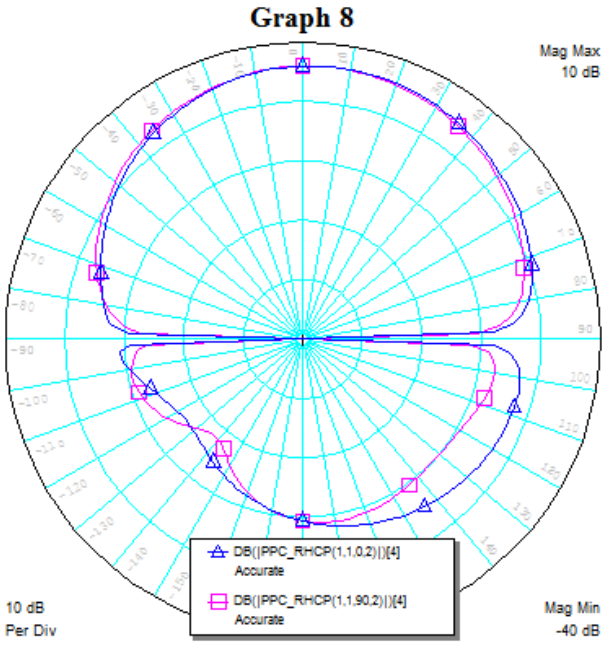

Figure 6.14 Radiation Pattern for both azimuth and elevation

Axial Ratio

Axial ratio gives an idea about how good the circular polarization is for an antenna. The Axial ratio simulation result is shown in the figure 6.15 below. The result shows a little higher axial ratio value for the negative angle values.

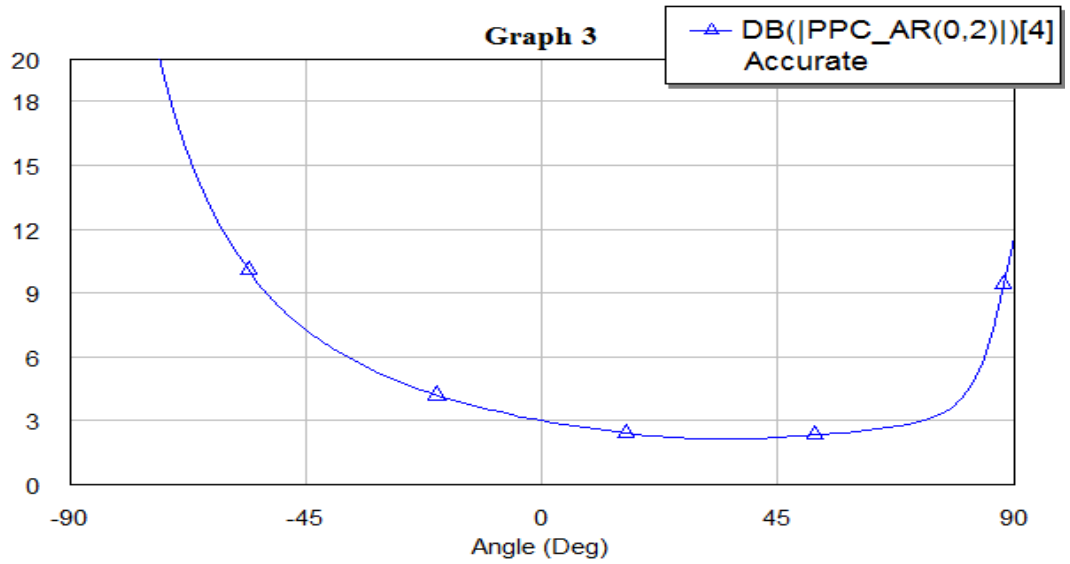

Figure 6.15 Axial Ratio

6.3.4 Measured results for Antennas with FR4 (0.8mm) Substrate

Return Loss

The return loss measured from the network analyzer is shown in the figure 6.16 below. It is quite similar to the simulation result. At 5.8 GHz a return loss of -14 dB is measured.

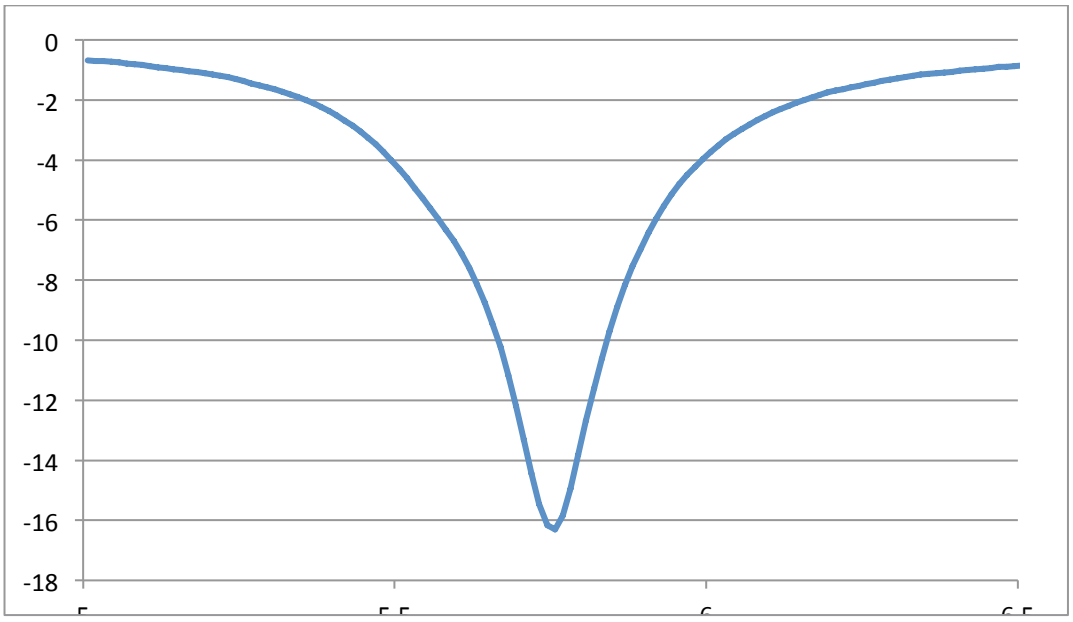

Figure 6.16 Return Loss

Gain

The gain curves for both azimuth and elevation plane were measured in the anechoic chamber however even with a good return loss the measured gain values were below the expectations. The gain curves for both azimuth and elevation planes are shown in the figure 6.17 below.

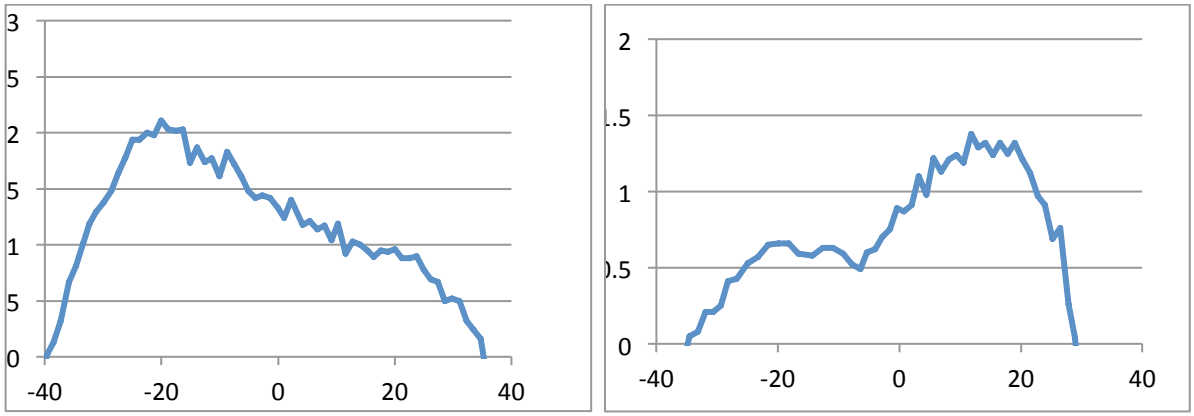

(a) (b)

Figure 6.17 Gain in both azimuth (a) and Elevation (b) plane

Cross Polarization

Measured results for cross polarization were also far from simulated values. The cross polarization curves for both azimuth and elevation plane are shown in the figure 6.18 below. Both curves show high cross polarization values.

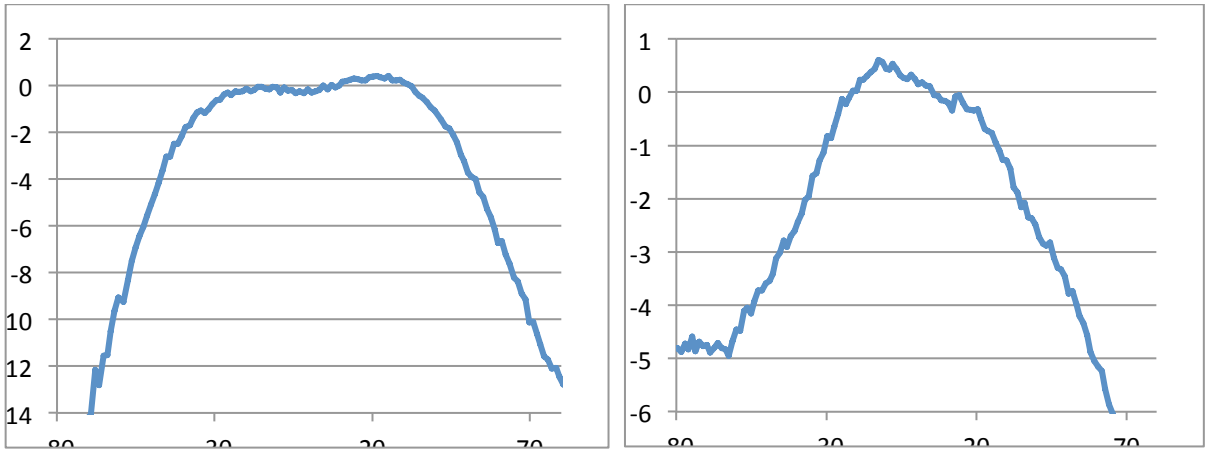

(a) (b)

Figure 6.18 Cross Polarization in both azimuth (a) and Elevation (b) plane

6.3.5 Simulated Results for Antennas with FR4 (1.6mm) Substrate

Two antennas with different feeding techniques were designed with this substrate simulation results of these antennas are shown below.

Return Loss

The return loss recorded in MWO for both the antennas are shown in the figure 6.19 below. A return loss of -12 dB for microstrip line feed antenna and -16 dB for the coaxial probe feed antenna is achieved.

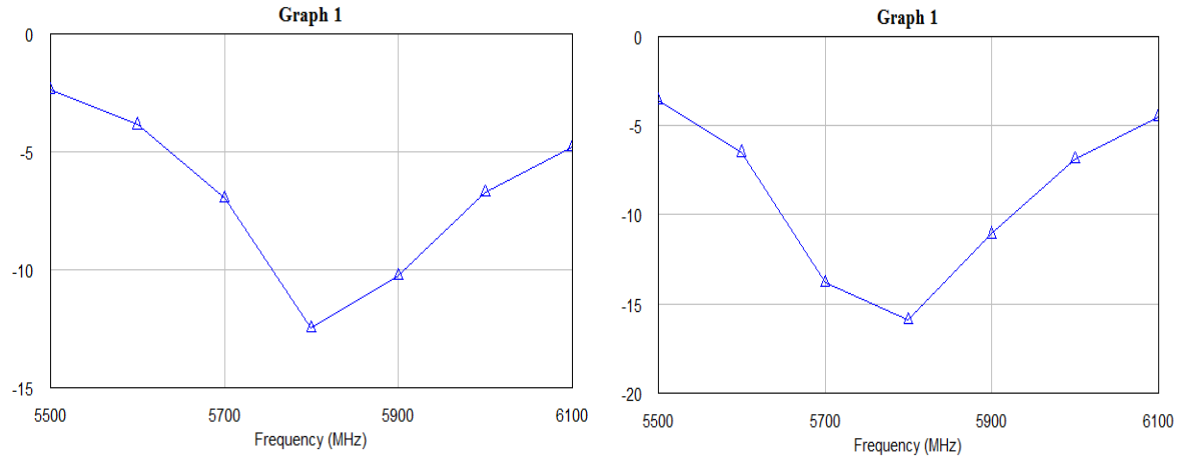

(a) (b)

Figure 6.19 The Return Loss of the antenna with Microstrip Line (a) and Coaxial (b) Feeding

Gain

Similarly the gain the curves are also shown in the figure 6.20 for both antennas.

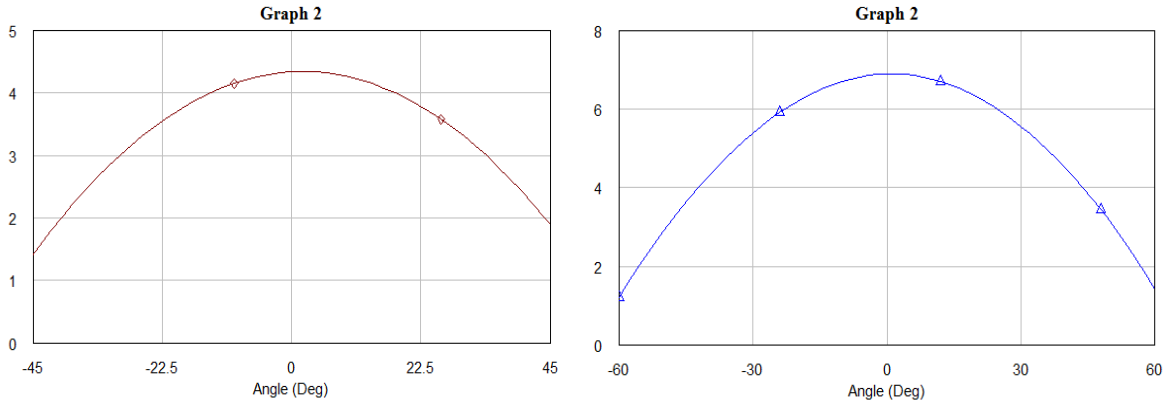

(a) (b)

Figure 6.20 Gain of the antenna with Microstrip Line (a) and Probe (b) feeding

It is however interesting to see that the antenna with the probe feeding is showing more gain than the antenna with microstrip line feeding.

Cross Polarization

Cross polarization is another parameter which should be as low as possible. Cross polarization curves for both the antennas are shown in the figure 6.21 below.

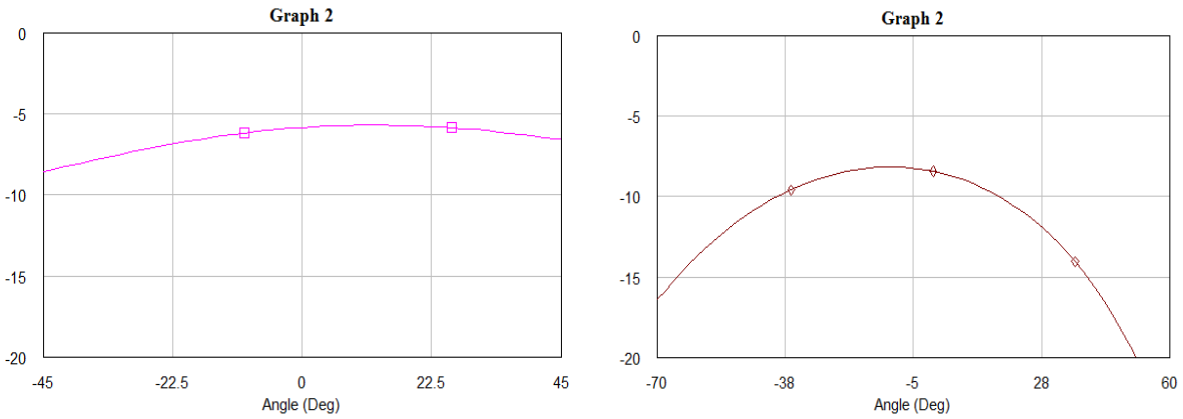

(a) (b)

Figure 6.21 Cross Polarization in both azimuth (a) and Elevation (b) plane

Both curves showed that the cross polarization level will be lower than -5 dB level.

Radiation Pattern

Radiation pattern gives a good idea that how much an antenna is radiating and in what direction. These plots are shown in the figure 6.22 below for both antennas

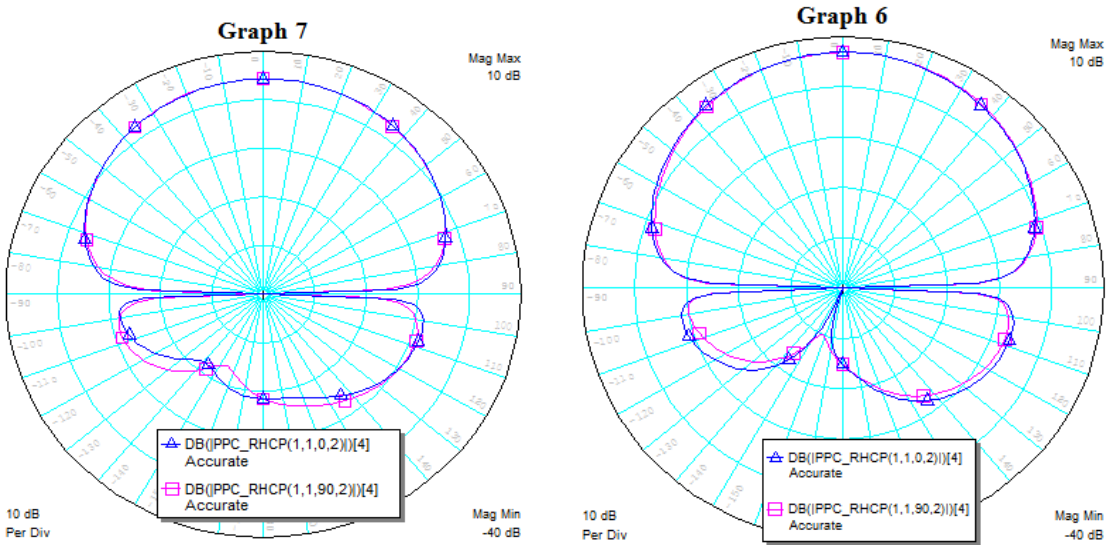

(a) (b)

Figure 6.22 Radiation Pattern of the antenna with Microstrip (a) and Probe (b) feeding

Axial Ratio

Axial ratio is another factor which gives the circular polarization status of an antenna. The axial ratio curves for both antennas are shown in the figure 6.23

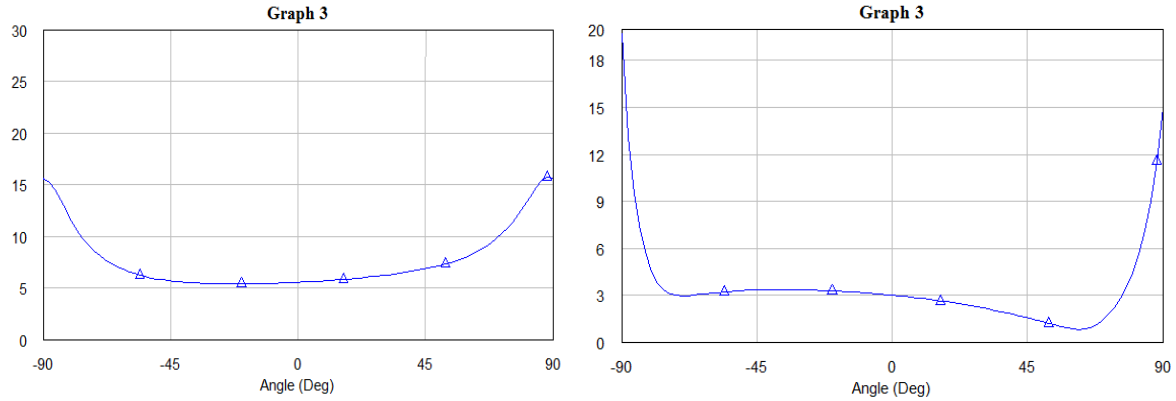

(a) (b)

Figure 6.23 Axial Ratio of the antenna with Microstrip feeding (a) and Probe feeding (b)

The axial ratio for the microstrip line fed antenna is slightly high however for the probe fed antenna it is in the desired region which is around 3 dB.

6.3.6 Measured Results for the Antennas with FR4 (1.6mm thick) Substrate

The measured results for these antennas are shown in this section

Return Loss

The return loss measured from the network analyzer for both the antennas are shown in the figure 6.24. The return loss for the microstrip line feed antenna is slightly high which is -9 dB however for the probe fed antenna the return loss is around -25 dB

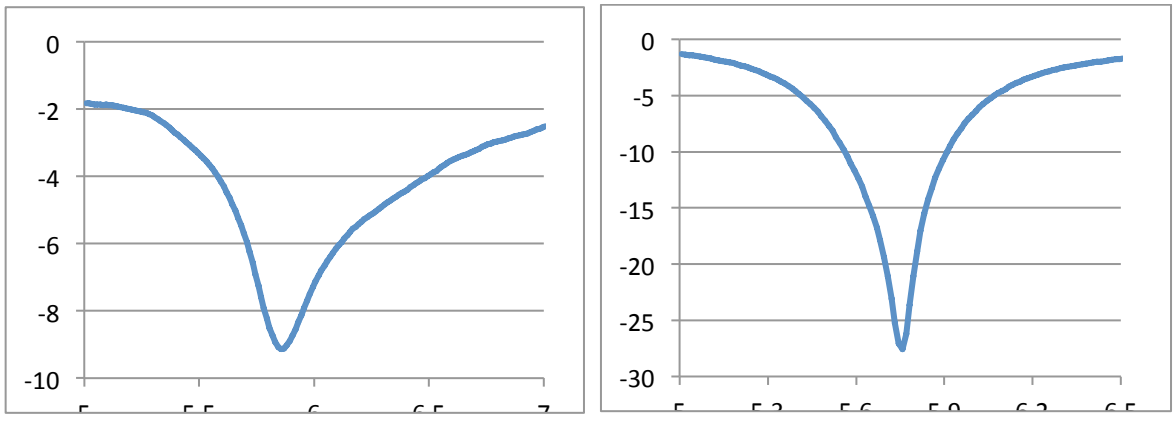

(a) (b)

Figure 6.24 The Return Loss of the antenna with Microstrip Line (a) and Probe (b) Feeding

Gain

The gain curves were measured in anechoic chamber for both azimuth and elevation plane. The gain curves for microstrip line fed antenna are shown in the figure 6.25 below.

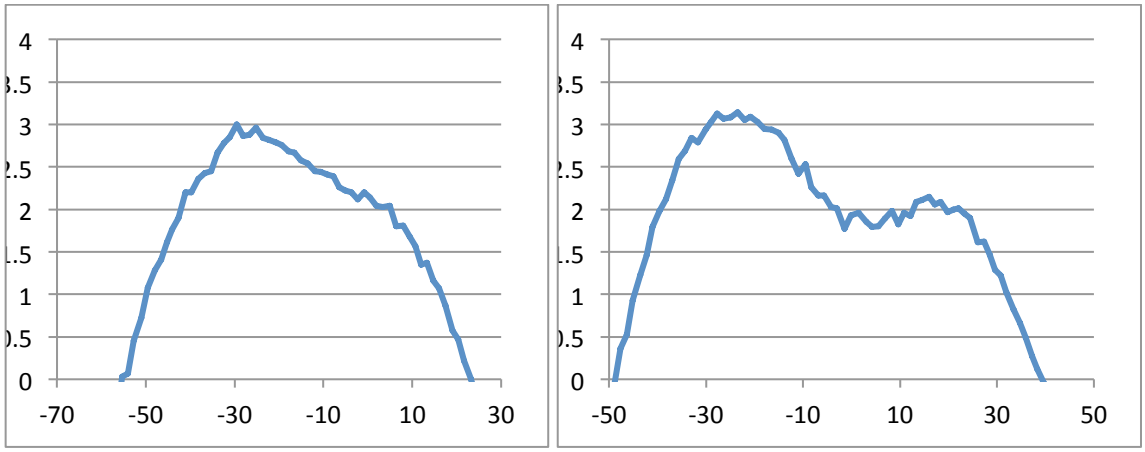

(a) (b)

Figure 6.25 Gain of the antenna with Microstrip Line (a) and Probe (b) feeding

A peak gain of 3 dB is achieved which is a little lower than the simulation result which showed a peak gain of 4.5 dB. Similarly the gain curves for the probe fed antenna are shown in the figure 6.26 for both azimuth and elevation planes

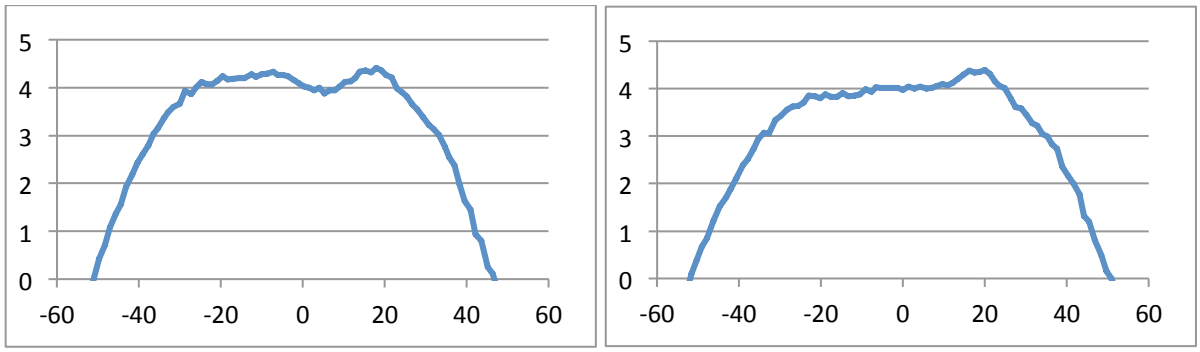

(a) (b)

Figure 6.26 Gain of the antenna with Microstrip Line (a) and Probe (b) feeding

A peak gain of 4.4 dB is achieved which is also at least 2 dB lower than the simulation results where a gain of almost 7 dB was recorded. However the beam width of the antenna is quite wide which will ensure a good gain value at ±35^{o} that is around 3.5 dB

Cross Polarization

The cross polarization curves are also shown in the figure 6.27 below for the microstrip line fed antenna. The figure shows a cross polarization for both azimuth and elevation planes.

The results are very identical to the simulation results and ensured good circular polarization.

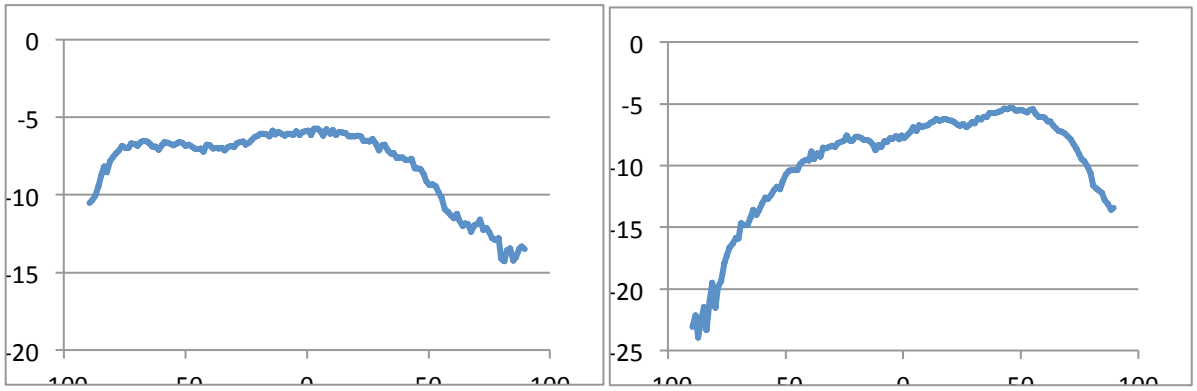

(a) (b)

Figure 6.27 Cross Polarization in both azimuth (a) and Elevation (b) plane

Similarly the cross polarization curves for probe fed antenna are shown in the figure 6.28

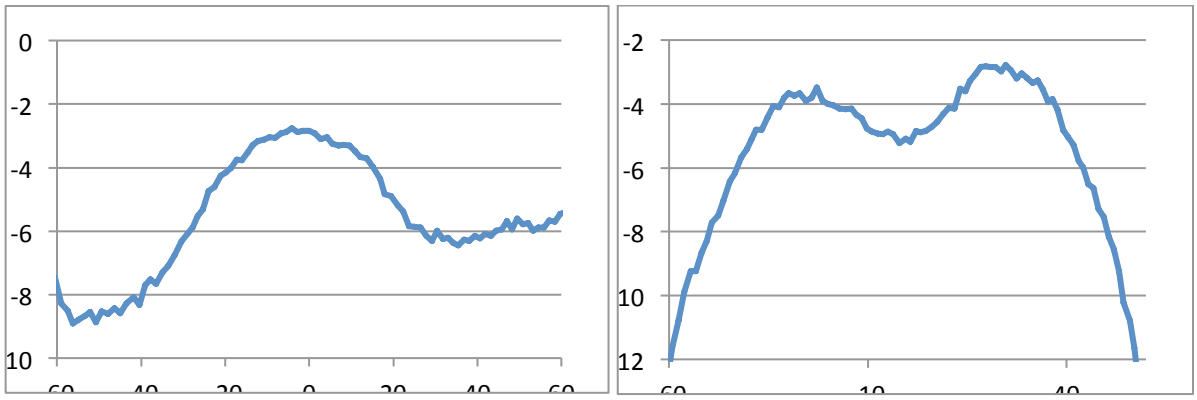

(a) (b)

Figure 6.28 Cross Polarization in both azimuth (a) and Elevation (b) plane

The cross polarization values are a bit high as compared to the simulation results.

6.4 Conclusion

These antennas did not show as good results as they should have. A vast difference between the simulated and measured results is visible. The gain is low and the cross polarization is also considerably high which shows that designing an antenna on a thin substrate can be very tricky.

Chapter 7

Other Antenna Designs

7.1 Introduction

Some other antennas were also designed and although they did yield good results but were not selected to manufacture due to the complexity and cost. These antenna designs will be discussed in this chapter. They were designed only in MWO and will not be explained in entire detail as they were not manufactured.

7.2 Parasitic Patch Antenna

This antenna design is shown in the figure below. It consists of a rectangular patch with two square slots. A circular parasitic patch is placed at an optimized distance from the normal patch. The spacing between ground and the patch is t_1 and the spacing between the normal patch and the parasitic patch is t_2. Both of these are air spacing which makes it expensive and at the same time hard to manufacture as it will need three layers.

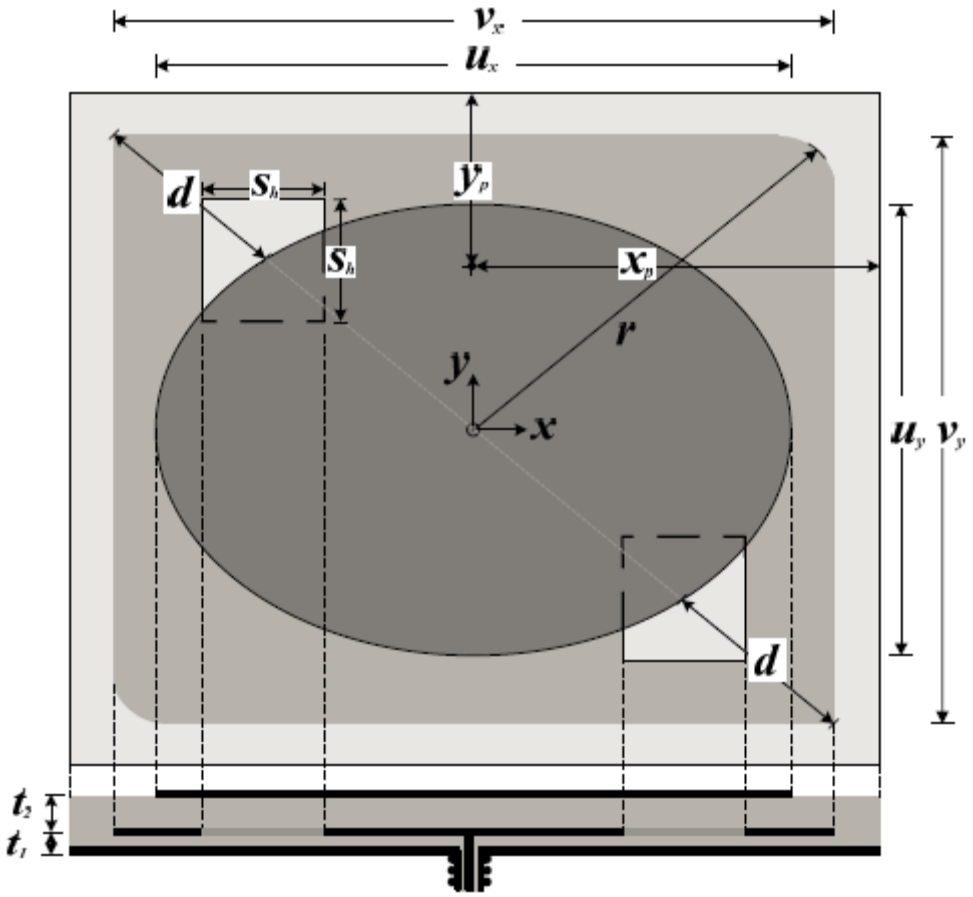

Figure 7.1 Parasitic Patch Antenna

Results

The simulation results of this antenna are shown below

Return Loss

The return loss of the antenna is shown in the figure below. An S11 of -12 dB is achieved at 5.8 GHz.

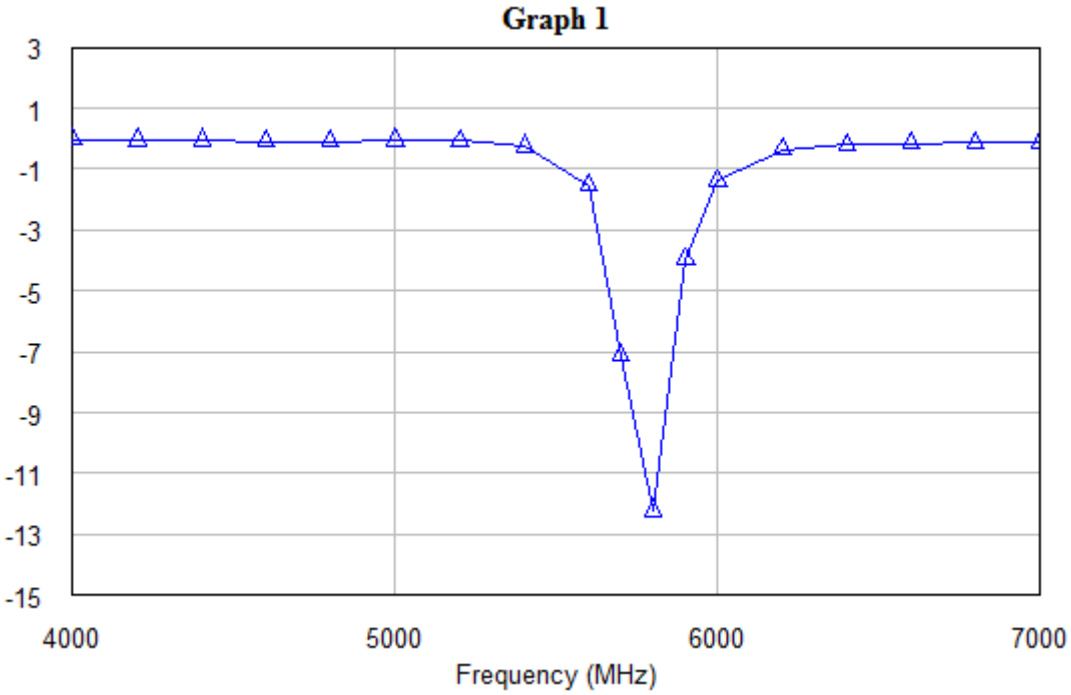

Figure 7.2 Return Loss

Radiation Pattern

The radiation pattern for $\phi=0^{o}$ and $\phi=90^{o}$ is shown in the figure below.

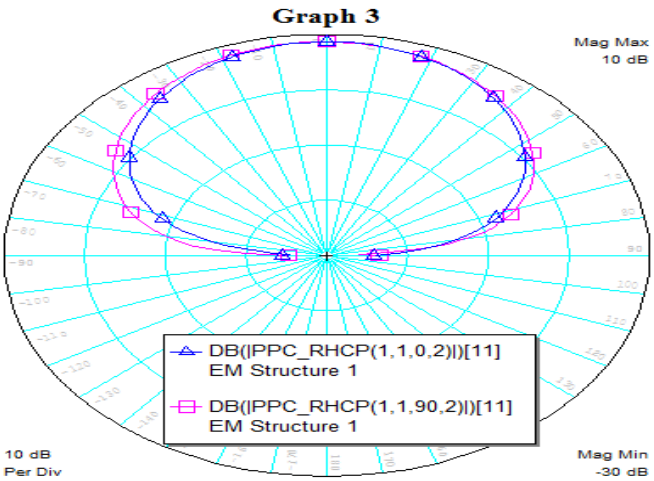

Figure 7.3 Radiation Pattern

Gain

The gain for (RHCP and LHCP) is also shown in the figure below. A peak gain of 8 dB is achieved and a gain of 5 dB at ±35^{o} which is really good. A good separation between co and cross polarization is also achieved.

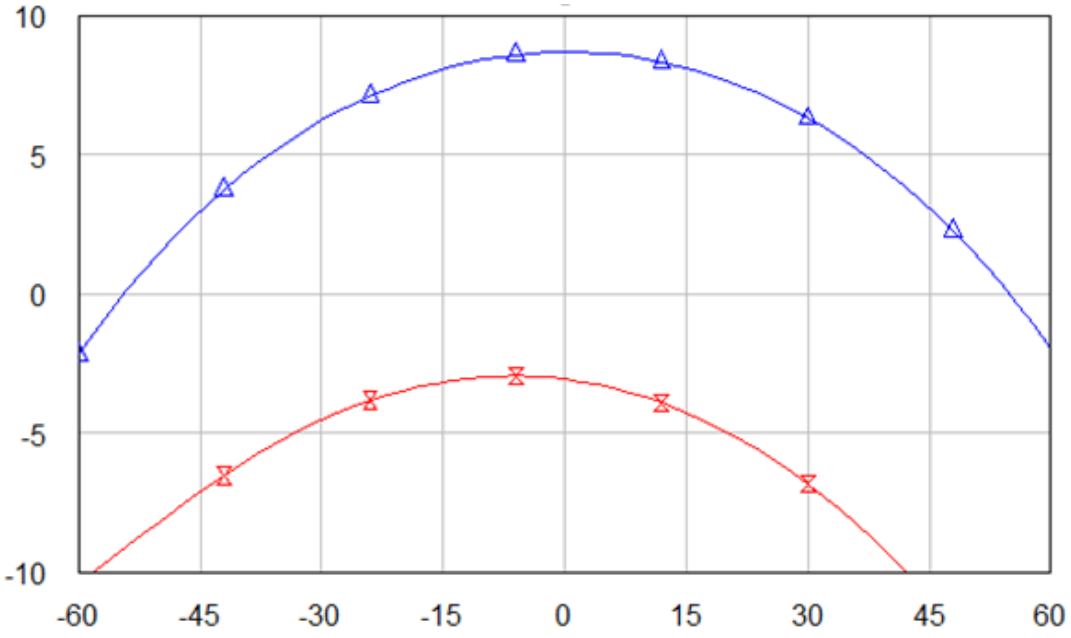

Figure 7.4 Gain(blue) and cross polarization(red)

Axial Ratio

The axial ratio of this antenna is shown in the figure below. An axial ratio of around 5 dB is achieved for ±35^{o}.

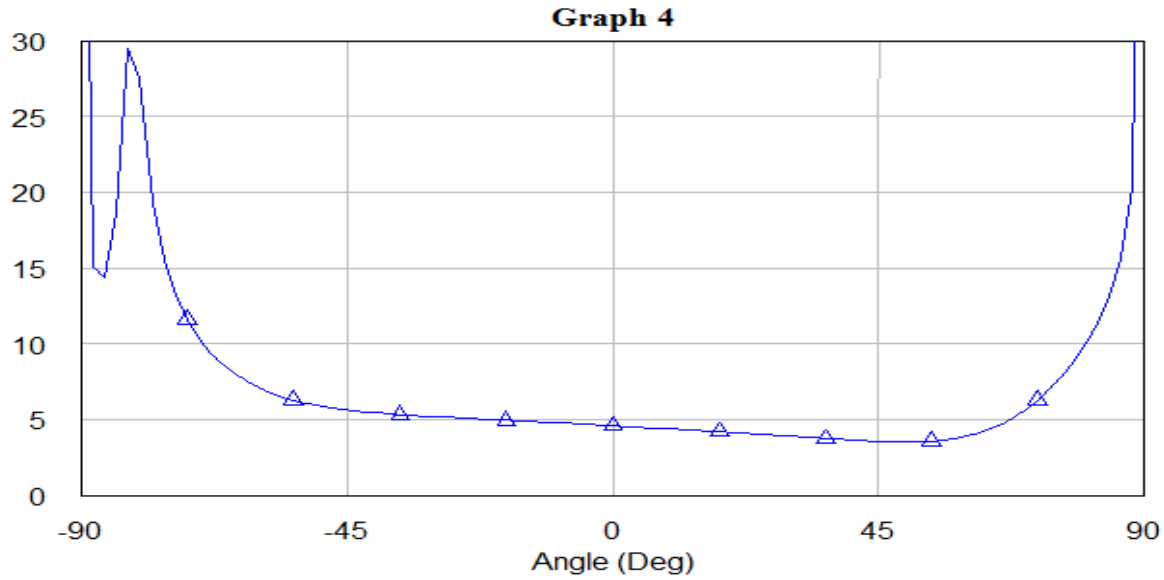

Figure 7.5 Axial Ratio

7.3 Spiral Antenna

A spiral antenna was also designed as shown in the figure. This antenna is without a ground plane and it radiates in both directions. A ground plane is needed at a distance of λ/4 from the antenna to make it radiate in only one direction and secondly it also needs a differential feeding mostly implemented with a balun. Due to those complexities this antenna was not manufactured although it was very small in size i.e. 15mm x 15mm.

Figure 7.6 A Spiral Antenna

Results

The simulation results of the spiral antenna are shown in the following section.

Return Loss

The return loss is shown in the figure below. At 5.8 GHz a return loss of -20 db is achieved

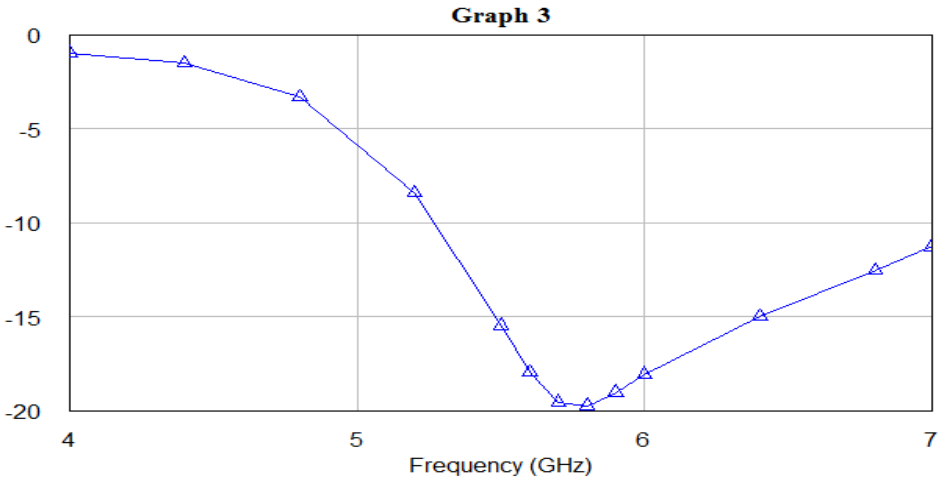

Figure 7.7 Return Loss

Radiation pattern

The radiation pattern is shown for $\phi=0^{o}$ and $\phi=90^{o}$ in the figure below

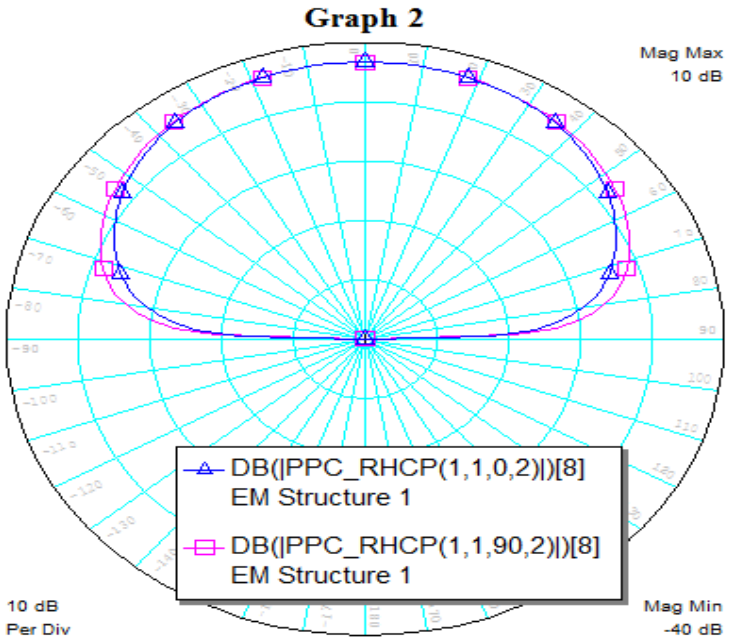

Figure 7.8 Radiation Pattern

Gain

A gain of 6.7 db is achieved at the center frequency as shown in the figure. The results show a very wide beam width and a gain or around 5 dB at ±35^{o}. However the cross polar level is a bit high which will affect the circular polarization.

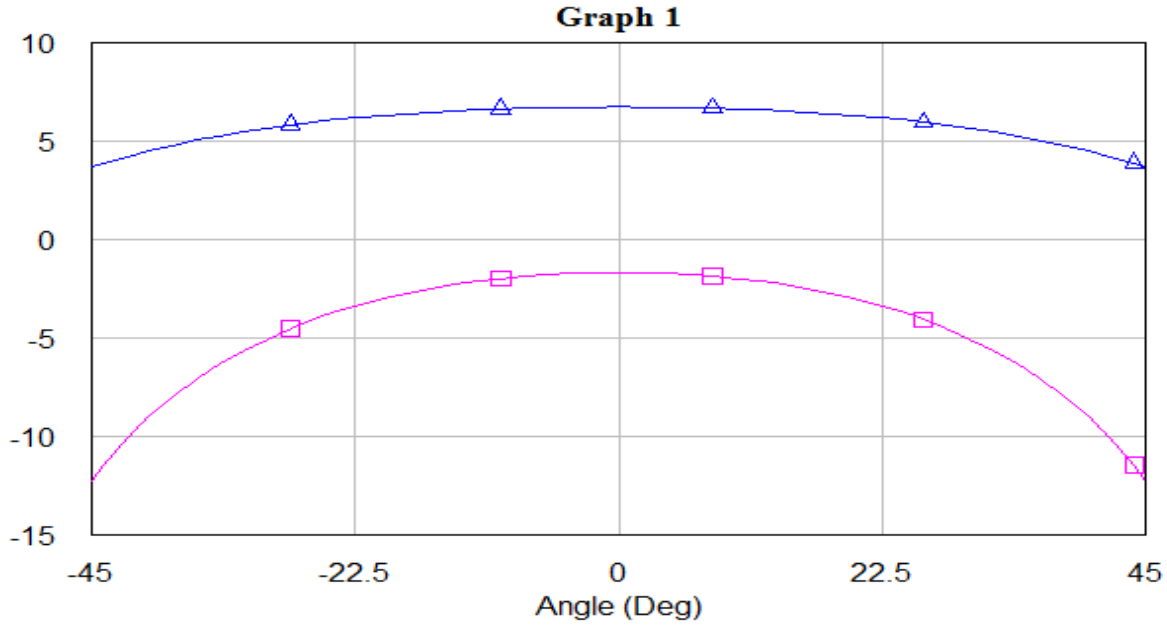

Figure 7.9 Gain(blue) and Cross Polarization(pink)

Axial Ratio

The axial ratio plot is shown in the figure below and is a little bit high due to the high cross polarization level.

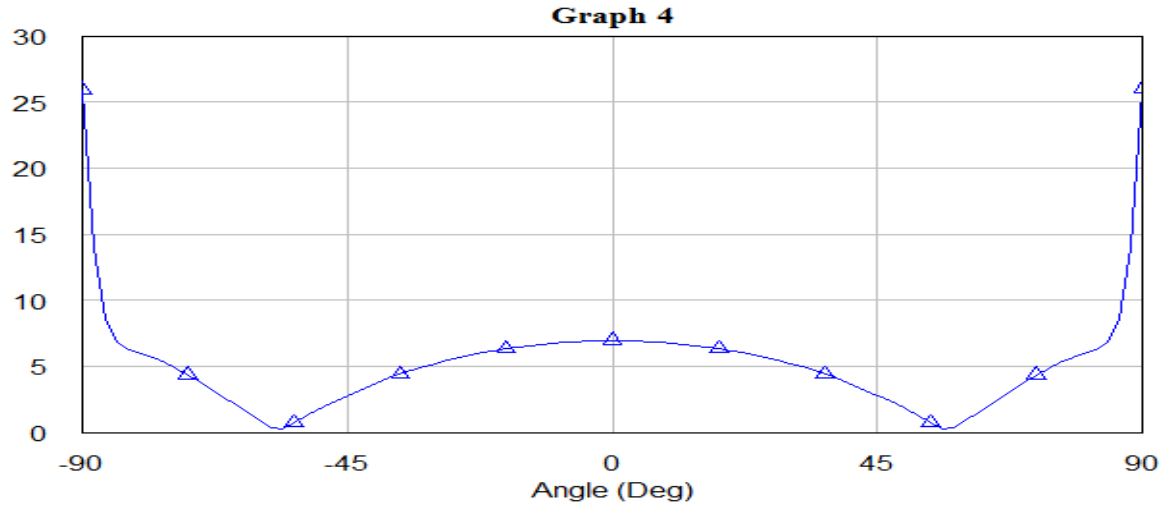

Figure 7.10 Axial Ratio

7.4 U Parasitic Antenna

The U parasitic Antenna is shown in the figure below. It consists of two u shaped parasitic patches and a rectangular patch in the center. The antenna used an FR4 substrate with a thickness of 4 mm which was one of the main reasons it was not manufactured. This antenna is linearly polarized, however a technique might have been used to excite the circular polarization however the substrate thickness of 4 mm made it a really expensive choice.

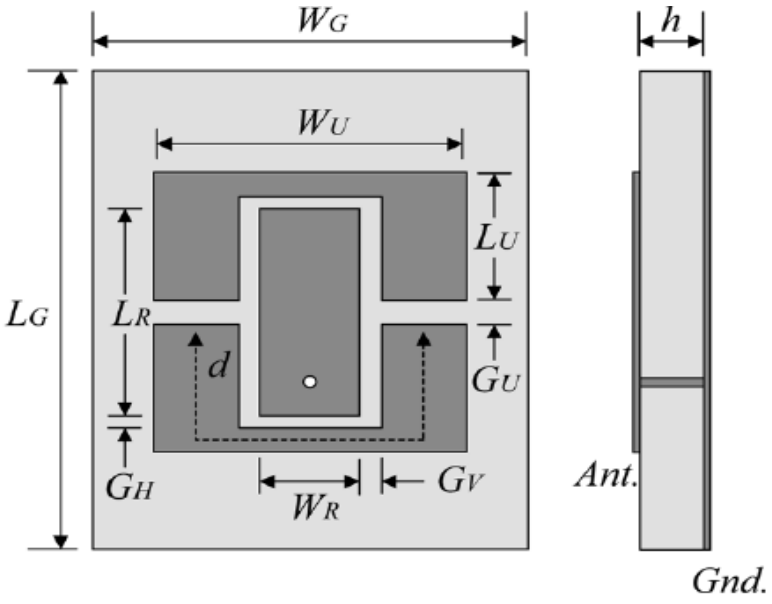

Figure 7.11 U Parasitic Antenna

Results

The results of this antenna are described in the following section. This antenna is designed at a frequency of 6 GHz in the research paper so the same parameters have been used to design this antenna here.

Return Loss

The return loss of this antenna is shown in the figure. At 6 GHz a return loss of -22 dB is achieved.

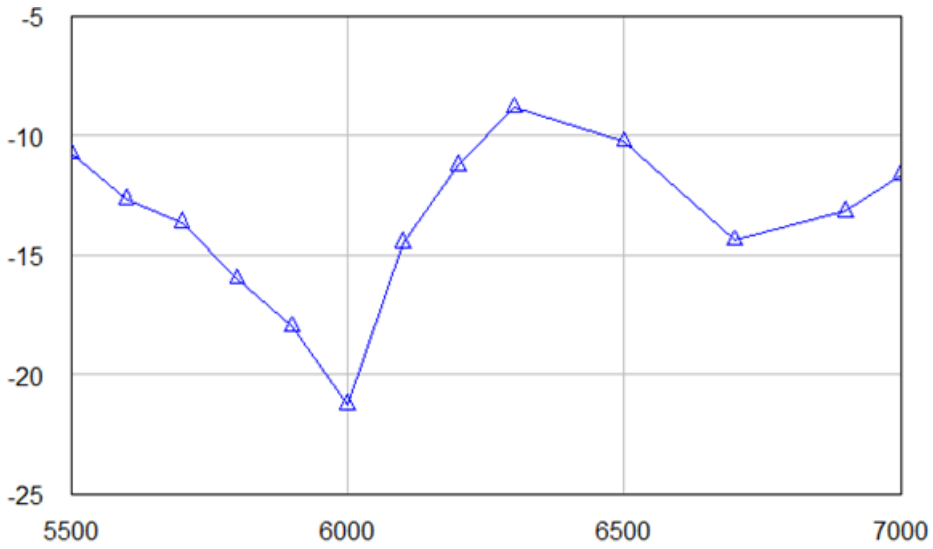

Figure 7.12 Return Loss

Gain

A peak gain of over 7 dB was achieved from this antenna with a gain of 5 dB at ±35^{o}.

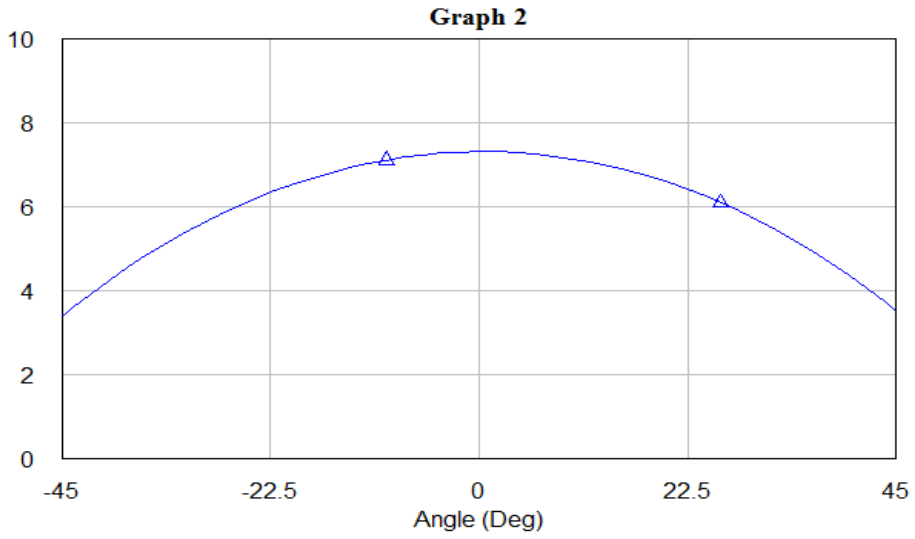

Figure 7.13 Antenna Gain

7.5 Conclusion

All three antennas discussed in this chapter showed good results however due to manufacturing cost and complexity they were not selected for the manufacturing process.

Chapter 8

Antennas Comparison

8.1 Introduction

In this chapter we will compare the measured antenna results with Microwave Office and HFSS to get a good idea about the accuracy of the simulators. Three antennas were designed both in HFSS and Microwave Office i.e. X Antenna, Circular Patch Antenna with aperture coupling and Patch antenna with probe feeding.

8.2 Results Comparison for X Antenna

In the following section the measured results of X Antenna are compared with HFSS and Microwave Office

Return Loss

The return loss from MWO and HFSS are shown in the figure below.

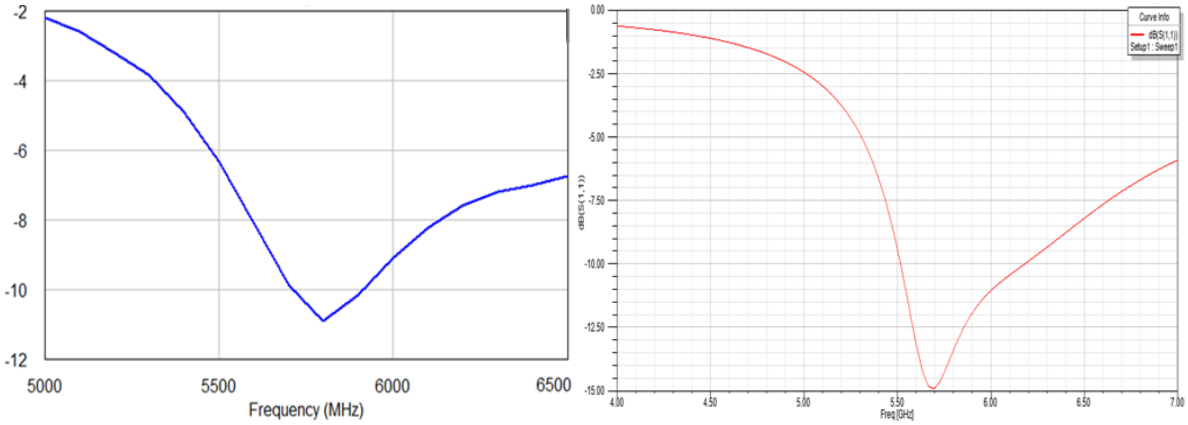

(a) (b)

Figure 8.1 Return Loss in MWO (a) and in HFSS (b)

Similarly the Return Loss measured in Network Analyzer is shown in the figure 8.2. So at 5.8 GHz from MWO the return loss achieved was -11 dB, from HFSS the return loss was found to be -13 dB and during the measurements the return loss was found to be -10 dB. Also the shape of the curves was very similar. Both simulators showed accurate results for the return loss.

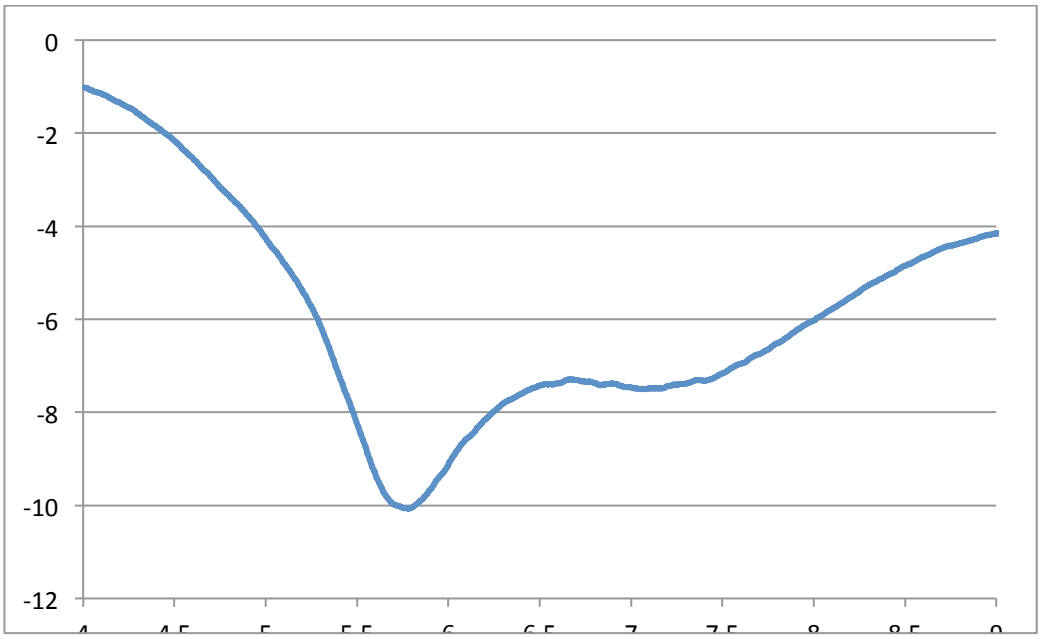

Figure 8.2 Measured Return Loss

Gain and Cross Polarization

Similarly the gain and cross polarization curves from MWO and HFSS are shown in the figure below.

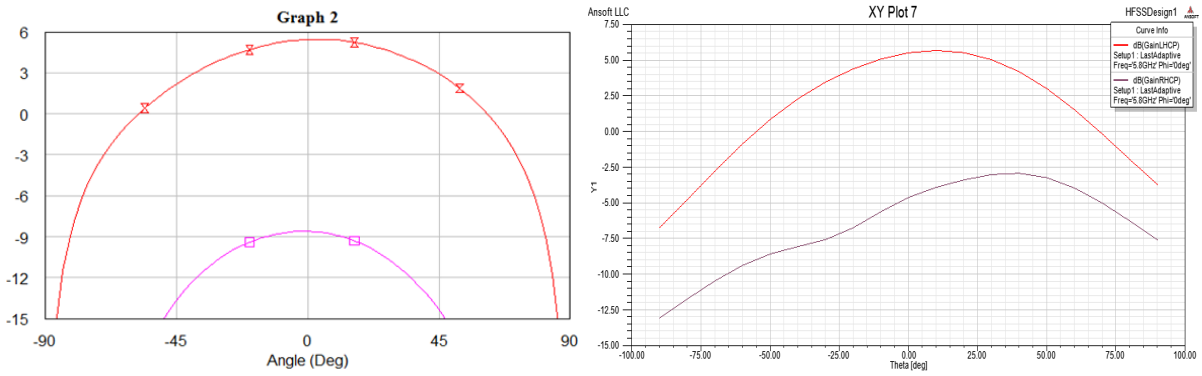

(a) (b)

Figure 8.3 Gain and Cross Polarization in MWO (a) and HFSS (b)

The measured values for Gain and Cross Polarization are shown in the figure 8.4. At 5.8 GHz the peak gain calculated from MWO was 5.5 dB and from HFSS was 5.7 dB. In the measured results the peak gain was 5.9 dB which is more than expectation so again both simulators have shown accurate results. Regarding shape of the curves there was a small deviation. The simulated curves were very symmetric but the measured curve was little asymmetric.

Coming to the cross polarization results, MWO showed a peak cross polarization value of -8.5 dB, HFSS showed a very high cross polarization value of -3 dB however the measured results showed a peak cross polarization value of -7.5 dB. Hence for the cross polarization results, MWO showed more accurate results. Regarding curve shapes the simulated and measured results showed big differences, the measured curve were more complex.

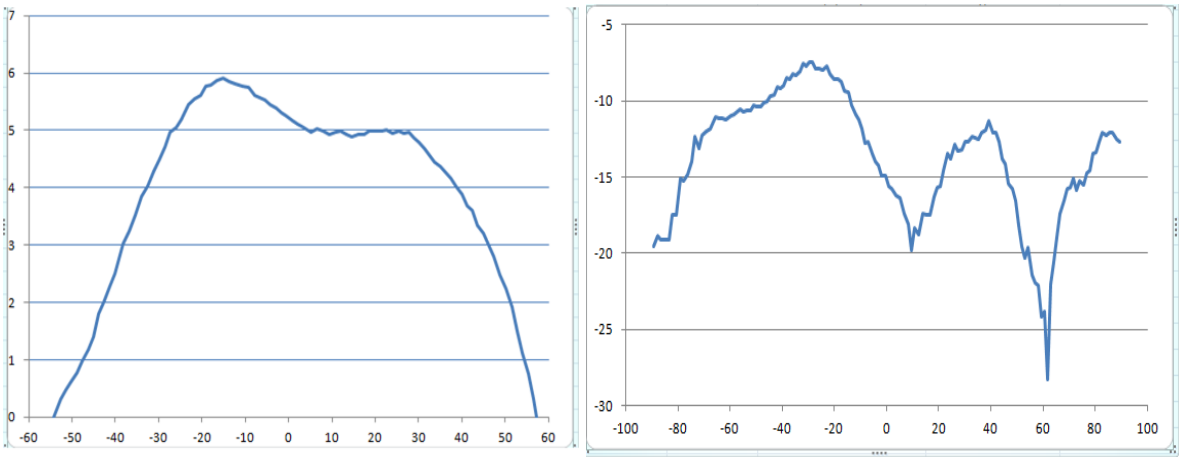

(a) (b)

Figure 8.4 Measured Gain (a) and Cross Polarization (b)

8.3 Results Comparison for Patch antenna with aperture coupling

In this section the measured results of Patch Antenna with aperture coupling are compared with HFSS and Microwave Office.

Return Loss

The return loss calculated by both MWO and HFSS are shown in the figure 8.5 (a) and 8.5 (b) below.

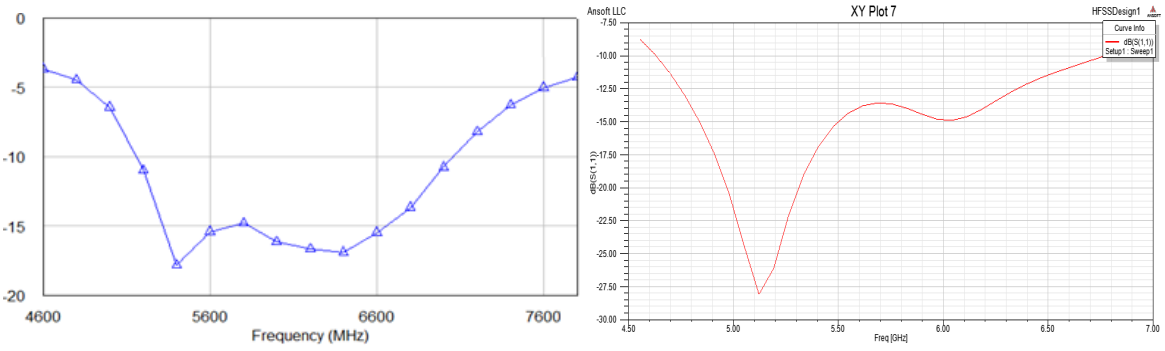

(a) (b)

Figure 8.5 Return Loss from MWO (a) and HFSS (b)

Similarly the return loss measured from the network analyzer is shown in the figure 4.3. So at 5.8 GHz the return loss recorded in MWO is -16 dB in HFSS -14 dB and in measurements it is found to be -15 dB. So again both simulators have shown similar and accurate results.

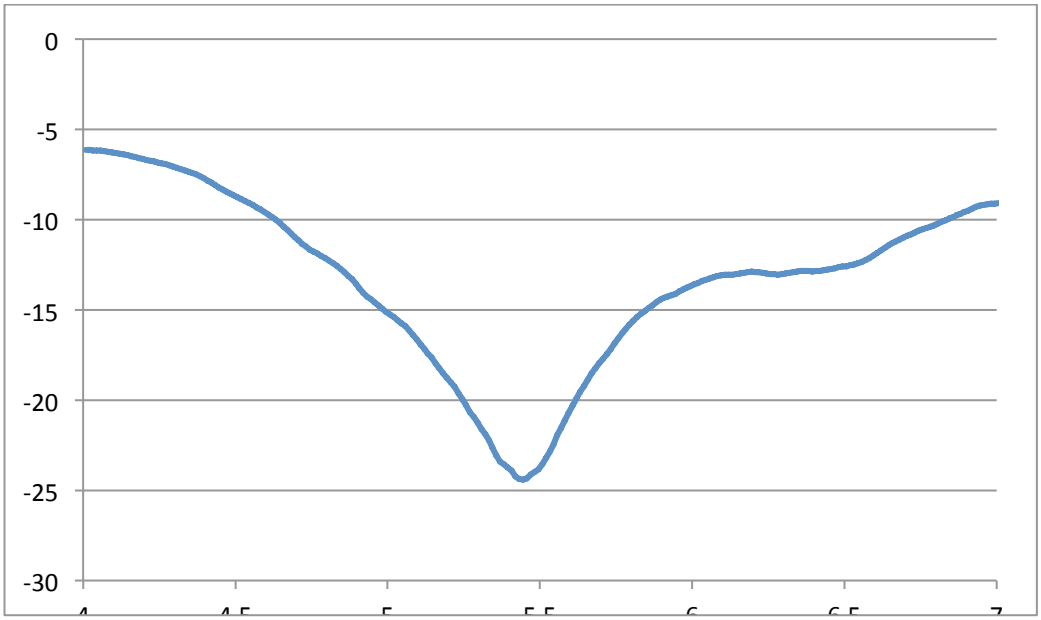

Figure 8.6 Measured Return Loss

Gain and Cross Polarization

Gain and cross polarization plots from MWO and HFSS are shown in the figure 4.4

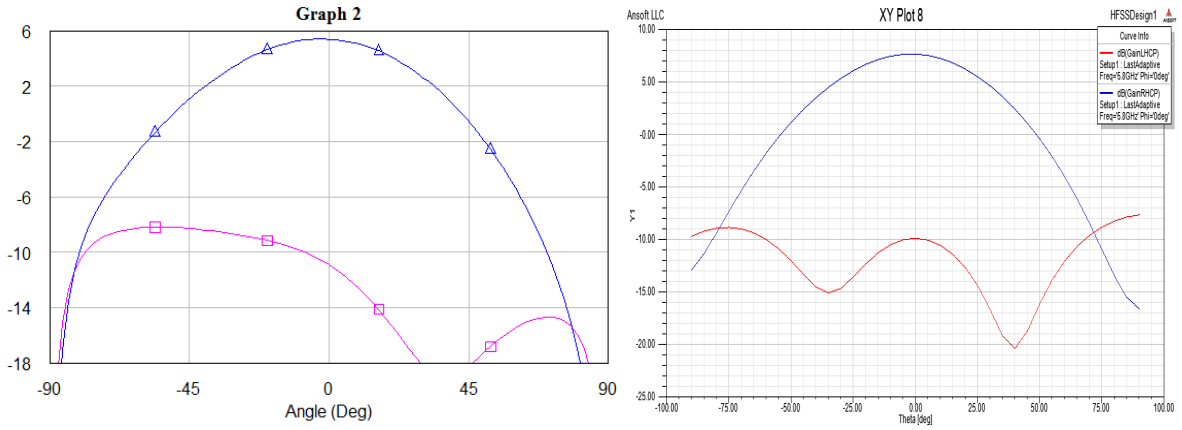

(a) (b)

Figure 8.7 Gain and Cross Polarization in MWO (a) and HFSS (b)

Similarly the measured gain and cross polarization plots from network analyzer are shown in the figure 8.4. The gain recorded in MWO is around 5.5 dB and that found in HFSS is 7.5 dB so there is a little difference between the two simulators. The measured result shows a gain of 7 dB which is more close to HFSS results. All curve shapes looks very similar.

Similarly for the cross polarization results, both simulators showed cross polarization in the range of -10 dB which is proved in the measurement results. Also very interesting is that the curve shape of HFSS and measured cross polarization looks similar, the similarity with the MWO is smaller.

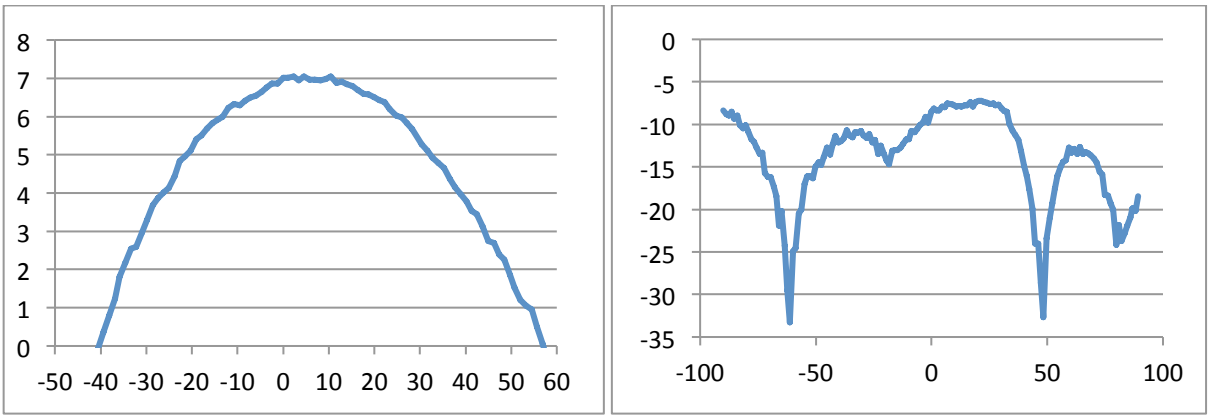

(a) (b)

Figure 8.8 Measured Gain (a) and Cross Polarization (b)

Chapter 9

Conclusion

Different Antennas were designed in this thesis work according to the requirements of different products. Some products needed a good peak gain and some needed good gain at ±35^{o}. In this chapter a final conclusion is shown about all the antennas which have been designed, manufactured and tested during this thesis work.

The first designed antenna was X antenna which was very small in size and still showed good results for all major requirements. Firstly it showed an acceptable return loss around -10 dB, secondly it showed nice gain and thirdly it proved to have an excellent circular polarization. Also the beam width of the antenna is very wide which helps to achieve good gain within ±35^{o}. The major question mark about this antenna is however that it uses a substrate thickness of 3.2mm which makes it a little expensive, however it is fabricated with a standard FR4 substrate which is significantly cheaper than substrates made especially for microwave applications.

The second antenna was a circular patch antenna which was fed through aperture coupling. The idea behind this antenna was to use air as a substrate and reduce the cost of the substrate. The overall performance of the antenna was good. It has a desired return loss, high peak gain and a good circular polarization. Size is also small, even if the ground plane is bigger than then the one with X antenna. However the gain drops considerably at ±35^{o} so it is not a very good choice for the products which need good gain within ±35^{o}.

The third designed antenna was a circular patch antenna which was fed through extended probes. Again the idea was to use air as a substrate and reduce the cost. This antenna also showed very nice results i.e. high peak gain, good return loss and circular polarization. Also the gain within ±35^{o} is very nice. The drawback is that the size is slightly large and also it is expensive to use probe feeding in volume production however it can be used for almost all products as it showed a high peak gain and also good gain within ±35^{o}.

The last antenna which was designed in this thesis work was truncated patch antenna. This antenna was designed with two feeding techniques and on three different substrates. It was the last antenna in this thesis work so due to shortage of time it was only designed in Microwave Office and not in HFSS. The antennas did not show results according to the expectations. A reasonable difference between the simulated and measured results is visible. The gain is low and the cross polarization is also considerably high. One reason that can be given for such results is that the antenna was not designed in HFSS so the optimizing techniques available in HFSS were not used. So some optimization is needed before this antenna is ready to be used.

Overall it can easily be said that the thesis work was a success. From the four antennas manufactured, three have shown nice results. These antennas might replace existing antennas in different products in future.

Appendix

X Antenna (with 1.6 mm Substrate)

An effort was made to design the X antenna with 1.6 mm substrate thickness. However it was not successful as both gain and cross polarization got worse. The substrate used was FR4. The antenna had similar dimensions as the previous X Antenna.

Results

The results for the X Antenna are shown in the following section. The results include both simulated and measured values.

Return Loss

Both simulated and measured values of return loss are shown in the figure below which are almost the same except that the frequency is slightly shifted.

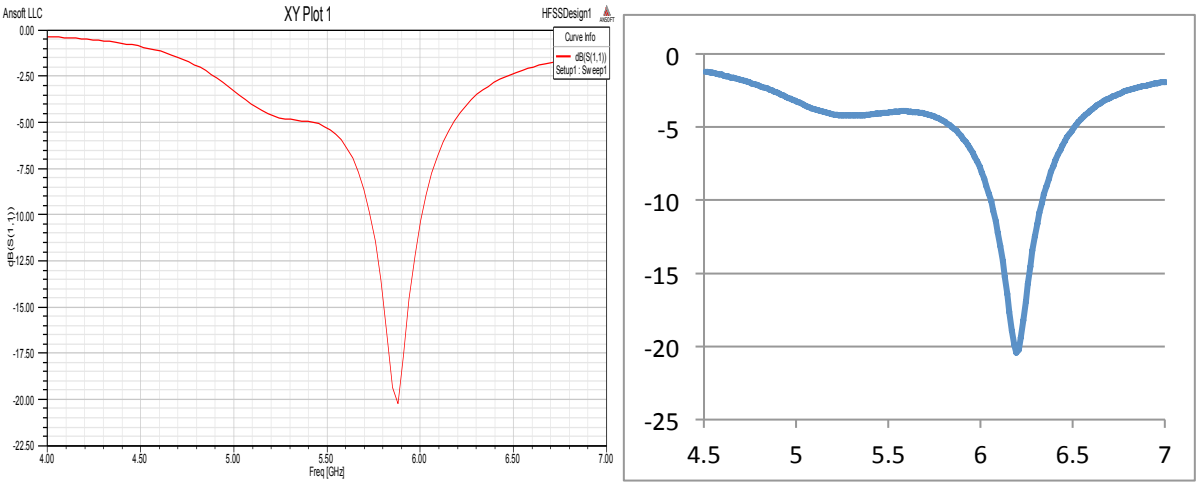

(a) (b)

Simulated (a) and Measured (b) Return Loss

Gain and Cross Polarization

The gain curves from both simulation and measurements are shown in the figure below. The measurement results are a little lower as compared to the simulation results.

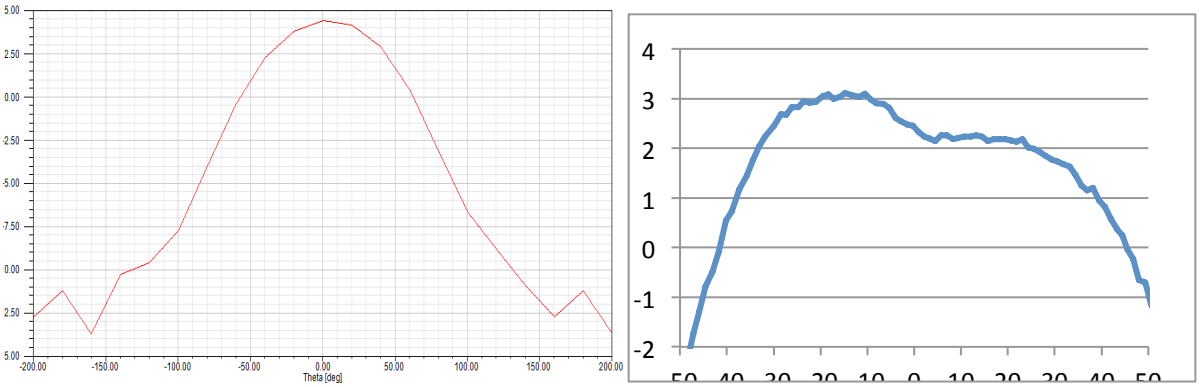

(a) (b)

Simulated (a) and Measured (b) Gain

Similarly the cross polarization curves are also shown in the figure below which also shows measured values higher than simulation results.

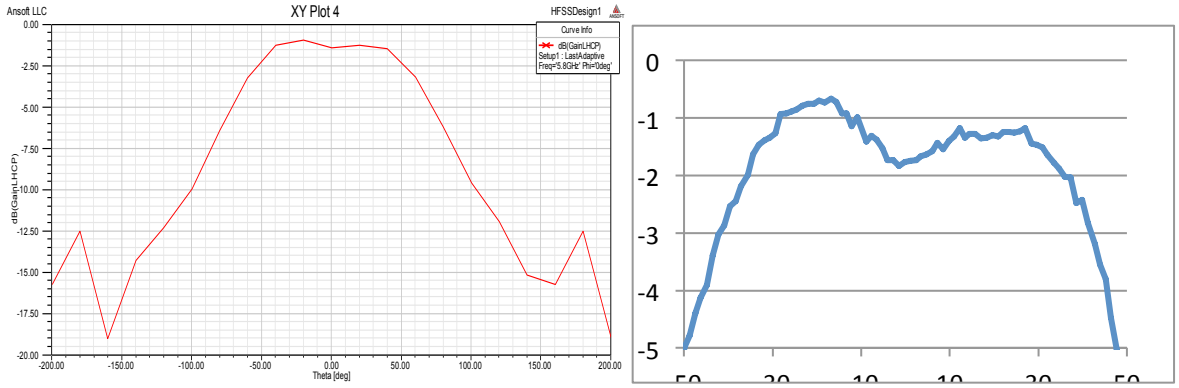

(a) (b)

Simulated (a) and Measured (b) Cross Polarization

Although the simulation results were not very strong either but at least the gain was around 5 dB and cross polarization -2 dB so it was decided that if it yields similar results may be it will be a possibility to work further on this design however it was not the case.

References

[1] Per-Simon Kildal. FOUNDATIONS of ANTENNAS A Unified Approach for Line-Of-Sight and Multipath. March 2009

[2] J. R. James and P. S. Hall, Handbook of Microstrip Antennas. Stevenage, U.K.: Peregrinus, 1989.

[3] Halim Boutayeb, Tarek Djerafi and Ke Wu. “Gain enhancement of a circularly polarized microstrip patch antenna surrounded by a circular mushroom-like substrate”. P*roceedings of the 3rd European Wireless Technology Conference*

[4] D. Bouchouicha, M. Latrach, F. Dupont, L. Ventura. “An experimental Evaluation of Surrounding RF Energy Harvesting Devices.” *Proceedings of the 40th European Microwave Conference*

[5] Rattapong Suwalak and Chuwong Phongcharoenpanich. “A Two-Square-Aperture Antenna Excited by a Probe on Rectangular Ground Plane with Elliptical Parasitic Patch for UHF-RFID Reader” *Proceedings of ECTI-CON 2008*

[6] D. Orban and G.J.K Moernaut, “The Basics of Patch Antenna.”

[7] Debatosh Guha, Sudipta Chattopadhyay, and Jawad Y.Siddiquf. “Estimation of Gain Enhancement Replacing PTFE by Air Substrate in a Microstrip Patch Antenna.” *IEEE Antennas and Propagation Magazine*, Vol. 52, No.3, June 2010

[8] Sang-Hyuk Wi, Yong-Shik Lee, and Jong-Gwan Yook. “Wideband Microstrip Patch Antenna With U-Shaped Parasitic Elements.” *IEEE Transactions on Antennas and Propagation,* Vol. 55, No. 4, APRIL 2007

[9] Ali K. Aswad , Lway Faisal Abdulrazak and Tharek Abd. Rahman. ” Design and development of high-gain wideband circularly polarized patch antenna” *IEEE International RF and Microwave Conference Proceedings*, 2008.

[10] Wen-Shyang Chen, “Inset-microstripline-fed circularly polarized microstrip antennas.”

[11] Jong Moon Lee, Nae Soo Kim, Cheol Sig Pyo. “A Circular Polarized Metallic Patch Antenna for RFID Reader” *Asia-Pacific Conference on Communications*,October 2005.

[12] Halim Boutayeb and Tayeb A. Denidni*, “*Gain Enhancement of a Microstrip Patch Antenna Using a Cylindrical Electromagnetic Crystal Substrate*”IEEE Transactions on Antennas and Propagation*, Vol. 55, No. 11, November 2007.

[13] A. F. A. Ayoub, "Analysis of Rectangular Microstrip Antennas with Air substrates," *Journal of Electromagnetic Waves and Applications*, 17,12,2003, pp. 1755-1766.

[14] Chih-Yu Huang, Jian-Yi Wu and Kin-Lu Wong, “High-gain compact circularly polarized microstrip antenna”

[15] http://www.kapsch.net

[16] http://www.antenna-theory.com/

[17] http://en.wikipedia.org/wiki/Microstrip_antenna

[18] http://ethesis.nitrkl.ac.in/1043/1/final_copy.pdf

[19] http://bada.hb.se/bitstream/2320/8167/1/Fatthi%20Alsager.pdf